Doctoral Thesis at the Medical University of Vienna for obtaining the Degree
"Doctor of Philosophy – PhD"

Interleukin-13 protects from atherosclerosis and modulates plaque composition by inducing a regression phenotype

Author

Larissa Cardilo dos Reis Weismann, M.Sc.

Supervisor

Univ. Prof. Christoph J. Binder, MD, PhD

KILM

Department of Laboratory Medicine

Ce-M-M-

Research Center for Molecular Medicine
of the Austrian Academy of Sciences

Medical University of Vienna
Lazarettgasse 14, AKH BT 25.2/6
A-1090 Vienna, Austria

Vienna, December 2012

This thesis is dedicated to
Naidê Cardilo dos Reis and
Vera Lúcia Goncalves Koatz
– two shiny stars!

« Rien ne se perd, rien ne se crée, tout se transforme. »

(Antoine Lavoisier)

TABLE OF CONTENTS

1. ABSTRACT

1.1. Abstract – English

Atherosclerotic lesions are characterized by the accumulation of oxidized LDL (OxLDL) and the infiltration of macrophages and T-cells. Cytokine expression in the microenvironment of evolving lesions can profoundly contribute to plaque development. While the pro-atherogenic effect of T helper (Th) 1 cytokines, such as Interferon (IFN)-γ is well established, the role of Th2 cytokines is less clear. For example, interleukin (IL)-5 has been shown to mediate atheroprotection, while IL-4 has been reported to have no or even pro-atherogenic properties. Therefore, we characterized the role of the Th2 cytokine IL-13 in murine atherosclerosis. Here we report that IL-13 administration favourably modulated the morphology of already established atherosclerotic lesions by increasing lesional collagen content and reducing vascular cell adhesion molecule-1 (VCAM-1)-dependent monocyte recruitment, resulting in decreased plaque macrophages. This was accompanied by the induction of alternatively activated (M2) macrophages, which exhibited increased clearance of OxLDL compared to IFN-γ-activated (M1) macrophages *in vitro*. Importantly, deficiency of IL-13 results in accelerated atherosclerosis in *LDLR*$^{-/-}$ mice without affecting plasma cholesterol levels. Thus, IL-13 protects from atherosclerosis and promotes favourable plaque morphology, in part through the induction of alternatively activated macrophages.

1.2. Kurzfassung – Deutsch

Arteriosklerotische Plaques sind durch die Ansammlung von oxidizertem LDL (OxLDL) sowie von Makrophagen und T-Zellen gekennzeichnet. Die Entwicklung der Läsionen wird zudem stark durch die lokale Expression von Zytokinen beeinflusst. Im Gegensatz zu den von T-Helfer (Th) 1 produzierten Zytokinen, wie zum Beispiel IFN-γ, deren pro- atherogener Effekt als gesichert gilt, ist die Rolle der Th2-Zytokine nach wie vor umstritten. In dieser Dissertation wird berichtet, dass ein Mangel an dem Th2-Zytokin IL-13 die Entwicklung von Arteriosklerose beschleunigt, ohne den Cholesterinspiegel im Plasma zu beeinflussen. Die Verabreichung von IL-13 verursachte

ein Ansteigen des Kollagengehalts in bereits etablierten Läsionen bei gleichzeitiger Reduktion der durch das vaskuläre Zelladhäsionsmolekül 1 (VCAM-1) hervorgerufenen Monozytenadhäsion. Letzteres führte einerseits zu einer geringeren Anzahl von Makrophagen in den Läsionen und andererseits zu einem vermehrten Auftreten von alternativ aktivierten (M2) Makrophagen, die OxLDL mit einer größeren Effizienz als IFN-γ aktivierte (M1) Makrophagen unschädlich machen. IL-13 schützt daher vor Arteriosklerose und verursacht, teilweise durch die Induktion von M2 Makrophagen, eine Regression atherosklerotischer Läsionen.

2. INTRODUCTION

Atherosclerosis is described as a chronic inflammatory disease of the vessel wall and this pathological process is the underlying cause of heart attacks and a majority of strokes. It was commonly believed that atherosclerosis was simply a passive accumulation of excess cholesterol in the artery wall. In the past decades, this view has changed and atherogenesis is considered to be more complex, with evidence that both innate and adaptive immune responses influence the development and progression of this disease. In face of these concepts, new potential therapeutic interventions in addition to established cholesterol lowering strategies are being developed (Hansson & Hermansson, 2011; Libby et al, 2011).

2.1. Immunity and Atherosclerosis

Atherosclerotic plaques are characterized by the accumulation of lipids together with the infiltration of activated monocyte/macrophages and T-cells in the intimal areas of arteries. Subsequently, increased cell death and cellular debris accumulation lead to the formation of necrotic core areas that are rich in cholesterol crystals. In addition, the induction of fibrosis by collagen production and proliferation of vascular smooth muscle cells creates a fibrous cap around the necrotic core areas defining the progression of lesion formation towards advanced atheroma plaques (Binder et al, 2002). Advanced lesions frequently cause clinical manifestations by either producing stenosis or by provoking thrombosis after disruption of plaques that can interrupt blood flow, which then results in tissue ischemia (Libby et al, 2011).

Based on experimental research in animal models, as well as clinical and epidemiological observations, high cholesterol levels in the blood (high LDL/low HDL) are considered to be initiators of atherogenesis. Apart from dyslipidemia, also hypertension and inflammation favour the activation of arterial endothelial cells to express adhesion molecules, which retain circulating leukocytes. In addition, changes in the vascular permeability and in the extracellular matrix composition underneath the endothelium allow the entrance and accumulation of cholesterol-rich LDL particles that, by interacting with matrix-proteoglycans, are trapped inside the subendothelial layer of

the artery, the intima, where they are prone to oxidation. Oxidative modifications of these particles further induce endothelial cell activation, chemokine production, and leukocyte recruitment (Hansson & Hermansson, 2011).

Thus, the initial lesions, called “fatty streaks”, are characterized by the accumulation of oxidized lipids and the recruitment of monocytes that undergo differentiation into macrophages, which are able to sense and engulf these modified particles through the expression of a variety of pattern-recognition and scavenger receptors, respectively. Fatty streaks develop into mature atherosclerotic plaques following additional recruitment of different inflammatory cells, such as T-cells, mast cells, dendritic cells, and neutrophils and the accumulation of extracellular lipids in core areas, which are covered by collagen-rich caps of smooth muscle cells (Figure 1) (Hansson & Hermansson, 2011; Weber et al, 2008).

Paralleling macrophage recruitment, T-cells enter the lesions by similar mechanisms involving chemokines and adhesion molecules. And although not as abundant as macrophages, with a ratio of approximately 1:4 in mice and 1:10 in humans, both $CD4^+$ and $CD8^+$ T-cells are prominent cellular components of the atherosclerotic plaque and also exhibit signs of activation, including the expression of cytokines and pro-inflammatory mediators (Ait-Oufella et al, 2011; Hansson & Hermansson, 2011). Indeed, lipid-laden macrophages and dendritic cells, present within the atherosclerotic plaque, interact with recruited T-cells and by presenting antigens stimulate T-cell-mediated responses, which are predominantly of the Th1 type in early lesion formation and further contribute to the progression of atherosclerosis. On the other hand, the presence and participation of Th2-cells and regulatory T-cells indicate additional and potentially opposing functions for adaptive immune-cells subsets in atherogenesis (Hansson & Hermansson, 2011).

Taken together, these observations suggest that innate and adaptive immune mechanisms have central roles in atherosclerosis and that their interaction can determine the fate of this disease.

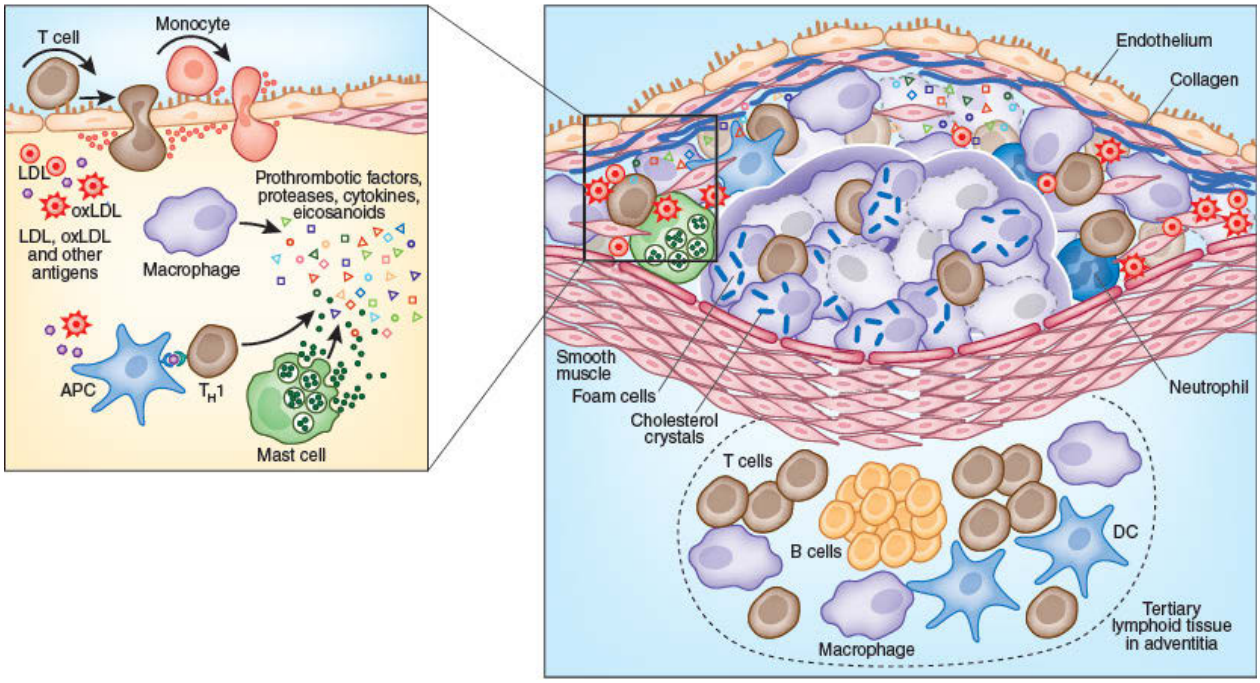

Fig 1: The atherosclerotic plaque composition. The atherosclerotic lesions are constituted by a core of living cells, accumulated lipids and necrotic areas, which are formed by excess of cholesterol crystals, necrotic and apoptotic cells. All surrounded by a fibrous cap made of smooth muscle cells and collagen. Many immune cell types, including macrophages, T-cells, mast cells and dendritic cells are recruited to the atheromatous plaque in response to excess oxidized plasma lipoproteins and endothelial cell activation. These cells can accumulate outside advanced plaques and potentially form tertiary lymphoid structures important in the atherosclerosis development. APC, antigen-presenting cell. DC, dentritic cell. Extracted from (Hansson & Hermansson, 2011).

2.2. The Th1-Th2 balance in Atherosclerosis

By definition, cytokines are a group of proteins with low-molecular-weight produced by a broad range of different cells in the body. They act as mediators and/or regulators between neighbouring cells, are involved in many physiological and pathophysiological responses, and have therapeutic potential (Balkwill & Burke, 1989; Tedgui & Mallat, 2006). All cells present within the atherosclerotic plaque and adventitia are able to produce and respond to cytokines. Moreover, a plethora of cytokines are expressed in human atherosclerotic lesions, i.e. IFN-γ, TNF-α, IL-12, IL-10, and TGF-β (Ait-Oufella et al, 2011).

$CD4^+$T-cells are functionally subcategorized according to the different types of cytokines they can produce. Th1-cells mainly secrete IFN-γ and activate macrophages

and dendritic cells; whereas Th2-cells secrete IL-4, IL-5, and IL-13, down-regulate Th1-mediated responses, stimulate antibody production by B-cells, and alternatively activate macrophages. Th17-cells are a newly defined lineage differing from Th1 and Th2. They produce IL-17, IL-21, and IL-22 and are associated with defence against extracellular bacteria and fungi. Finally, regulatory T (Treg)-cells secrete IL-10 and TGF-β and exert suppressive functions, thereby mediating autoimmunity prevention and maintenance of self-tolerance (Ait-Oufella et al, 2011).

Substantial evidence supports that Th1-driven responses, mainly characterized by IFN-γ production are detrimental to the disease and correlate with progression of atherosclerosis (Buono et al, 2005; Buono et al, 2003; Gupta et al, 1997; Tellides et al, 2000). The pro-atherogenic properties include increased recruitment of T-cells and macrophages to lesions, enhanced activation of antigen-presenting cells, and augmenting the production of Th1-derived cytokines, which further propagates the inflammatory process. Exogenous injections of recombinant IFN-γ lead to enhanced lesion formation in mice (Whitman et al, 2000). In contrast, blocking INF-γ response by gene transfer of a soluble mutant of IFN-γ receptor in *ApoE*$^{-/-}$ mice abrogated the progression of established atherosclerotic plaques that remodelled towards a more stable and less inflammatory phenotype (Koga et al, 2007).

These pro-atherogenic responses have been shown to be dampened by the presence of specific Treg-cells, which secrete the anti-atherogenic cytokines TGF-β and IL-10 (Ait-Oufella et al, 2006; Ait-Oufella et al, 2011). Indeed, IL-10 secreted by T-cells decreases atherogenesis in mice (Mallat et al, 1999a; Pinderski Oslund et al, 1999). In addition, recently it has been demonstrated that IL-17, produced by Th17-cells or related cells, was also able to inhibit the development of Th1-cells by activation of IL-17 receptors on these cells and by inhibiting the expression of T-bet and IL-12 receptor (O'Connor et al, 2009). Based on this report, one would assume that Th17-cells and/or IL-17 may be atheroprotective. However, its precise function in atherogenesis is still contradictory (Taleb et al, 2010). While one report showed that promoting Th17-responses ameliorates the development of atherosclerosis in *LDLR*$^{-/-}$ mice (Taleb et al, 2009), others have shown a pro-atherogenic effect of IL-17 (Erbel et al, 2009; Smith et al, 2010).

Studies have shown that under conditions of extreme and persistent hyperlipidaemia, the Th-cell balance shifts from a Th1- to a Th2- type of response in

murine atherosclerotic plaques; suggesting that the equilibrium between these two subsets of T-cells may undergo dynamic changes during atherogenesis (Binder et al, 2004; Buono et al, 2005; Zhou et al, 1998). In a relatively atherosclerosis resistant mouse model, Balb/c, a Th2-biased response demonstrated protection against early fatty streak formation (Huber et al, 2001) and the inhibition of Th1-cell differentiation by a chemical compound reduced atherogenesis *in vivo* (Laurat et al, 2001). IL-4 is the prototypic Th2-related cytokine with an important function in promoting Th2-cell differentiation and Th1-suppression (Amsen et al, 2009; Seder & Paul, 1994). Its role in atherogenesis has been investigated in many different mouse models in which early studies reported a pro-atherogenic role for IL-4 (Davenport & Tipping, 2003; King et al, 2002), while a later report found no effect of IL-4 in lesion development (King et al, 2007). These divergent results might reflect the complex array of IL-4 biological activities, including on the non-lymphoid compartment of the body. Indeed, IL-4 can activate endothelial cells, enhancing leukocyte adhesion and attraction (Hickey et al, 1999; Walch et al, 2006), and mast cells, leading to increased production of proteases, promote apoptosis of smooth muscles cells, and reduced collagen production (Leskinen et al, 2003). Thus, IL-4 may have both anti- and pro-atherogenic effects.

On the other hand, it has been shown previously that the atheroprotective immunization of *LDLR*$^{-/-}$ mice with malondialdehyde-modified LDL (MDA-LDL) induces a Th2-biased immune response that was characterized by antigen-specific production of IL-5 and IL-13 but only small amounts of IL-4 and IFN-γ. In the same study, the capacity of IL-5 to stimulate natural atheroprotective IgM specific for OxLDL and its ability to protect from atherosclerosis has been demonstrated (Binder et al, 2004). Consistently, Sampi *et al* also found that plasma IL-5 levels are related to plasma levels of IgM antibodies binding to OxLDL and to decreased subclinical atherosclerosis in humans (Sampi et al, 2008). Moreover, IL-33, a Th2-inducing cytokine, has been shown to prevent atherosclerosis development in *ApoE*$^{-/-}$ mice in part by the induction of IL-5 and OxLDL antibodies (Miller et al, 2008). Thus, IL-5 is a Th2-related cytokine with anti-atherogenic properties.

Taken together, the role of Th2 responses in atherosclerosis is complex, as different Th2 cytokines have been found to contribute differently to the atherogenic process. Thus, only the individual analyses of specific cytokines will identify their role in atherosclerotic lesion formation. Nevertheless, it has been assumed that IL-13 affects atherosclerosis in the same way as IL-4 due to fact that both bind the IL-4 receptor.

However, no studies are currently available to support this notion (Robertson & Hansson, 2006; Tedgui & Mallat, 2006).

2.3. Interleukin-13: an effector Th2-type cytokine

Two decades ago, IL-13 has been described as a new cytokine produced by activated Th2-cells (Brown et al, 1989; McKenzie et al, 1993; Minty et al, 1993). To date, this view has expanded and it is known that IL-13 is exclusively produced by hematopoietic cells, including dendritic cells, NKT-cells, activated mast cells, basophils, eosinophils, Th2-cells, and a recently discovered innate lymphoid cells, termed nuocytes (Barlow & McKenzie, 2011; Oliphant et al, 2011; Wynn, 2003). IL-13 is an essential immune regulator and an indispensable mediator of type 2 immune responses, which are associated with the control and expulsion of parasitic helminth infections, the induction of some inflammatory states (i.e. asthma and allergies), but also the suppression of inflammation related to bacterial and viral infections, as well as the promotion of tissue fibrosis (Hershey, 2003; Wynn, 2003).

IL-13 possesses a broad range of functions due to the variety of cells that can respond to this cytokine in the body (Figure 2). More specifically, IL-13 has been involved in the regulation of IgE synthesis by human B-cells (Punnonen et al, 1993), the maturation and activation of lung epithelial cells and mucus production (Zhu et al, 1999), the activation of monocytes/macrophages (Doherty et al, 1993), the induction of airway hyperreactivity (Wills-Karp et al, 1998), the recruitment and activation of eosinophils (Horie et al, 1997; Luttmann et al, 1996; Pope et al, 2001), the synthesis of extracellular matrix proteins, and the enhancement of tissue remodeling and fibrosis (Liu et al, 2012; Wynn, 2011).

Most of these actions are mediated by a complex receptor system that comprises the IL-4 receptor α (IL-4Rα) chain and at least two other IL-13 binding proteins IL-13Rα1 and IL-13Rα2 (Figure 3). The Type II receptor (IL-4Rα/IL-13Rα1) is expressed on both hematopoietic and non-hematopoietic cells and it is hypothesized to be the main receptor used by IL-13 signalling (Hershey, 2003), although a previous report showed IL-13 effects in the lung independently of IL-4Rα (Mattes et al, 2001). Furthermore, IL-13 has been shown to bind the IL-13Rα2 with higher affinity compared to IL-13Rα1, but

failed to induce signaling leading to speculation that this receptor acts as a decoy receptor (Donaldson et al, 1998; Kawakami et al, 2001). This notion is further supported by the finding that this receptor exists in soluble form *in vivo* (Zhang et al, 1997) and its overexpression might counteract IL-13 functions (Mentink-Kane & Wynn, 2004; Wood et al, 2003). However, the importance of IL-13Rα2 in IL-13 signalling is still not clear, as later studies demonstrated IL-13 induction of TGF-β through usage of this receptor in a STAT6-independent way (Fichtner-Feigl et al, 2007; Fichtner-Feigl et al, 2006). Because IL-4 and IL-13 shares approximately 25% homology at the amino acid level and engage a common receptor signalling pathway (IL4Rα/IL-13Rα1/STAT6), similar cellular activities for both cytokines have been described (Chomarat & Banchereau, 1998; Kuperman & Schleimer, 2008). However, IL-13 also possesses exclusive functions that differ from those of IL-4, for example, in promoting eosinophil accumulation, mucus production, and airway and liver fibrosis (Chiaramonte et al, 1999b; Kumar et al, 2002; Liang et al, 2011; McKenzie et al, 1998b; Oriente et al, 2000). In addition, several animal models demonstrated a preferential role of IL-13 over IL-4 in promoting asthma (Grunig et al, 1998). Importantly, in contrast to IL-4, up to date no direct effect of IL-13 on T-cells (in humans and mice) has been described, as these cells do not express an IL-13 receptor (IL-13Rα1), suggesting that this cytokine may not participate in the initial differentiation of naive $CD4^+$T-cells into Th2-cells (Zurawski & de Vries, 1994).

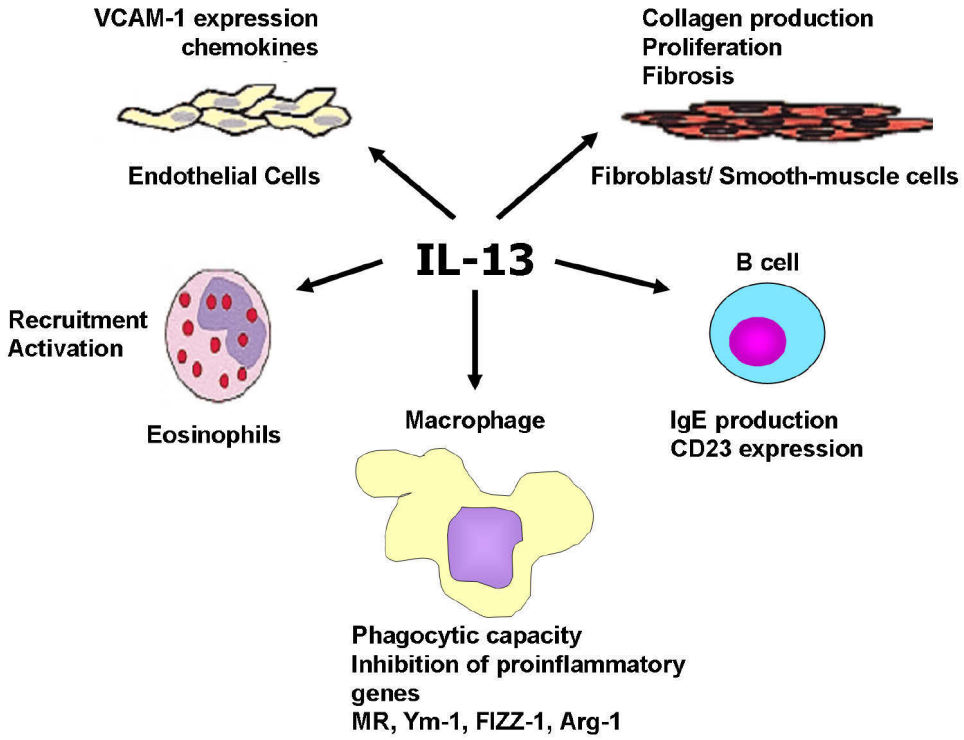

Fig 2: Diverse actions of IL-13 in the hematopoietic and non-hematopoietic compartments of the body. Modified from (Hershey, 2003)

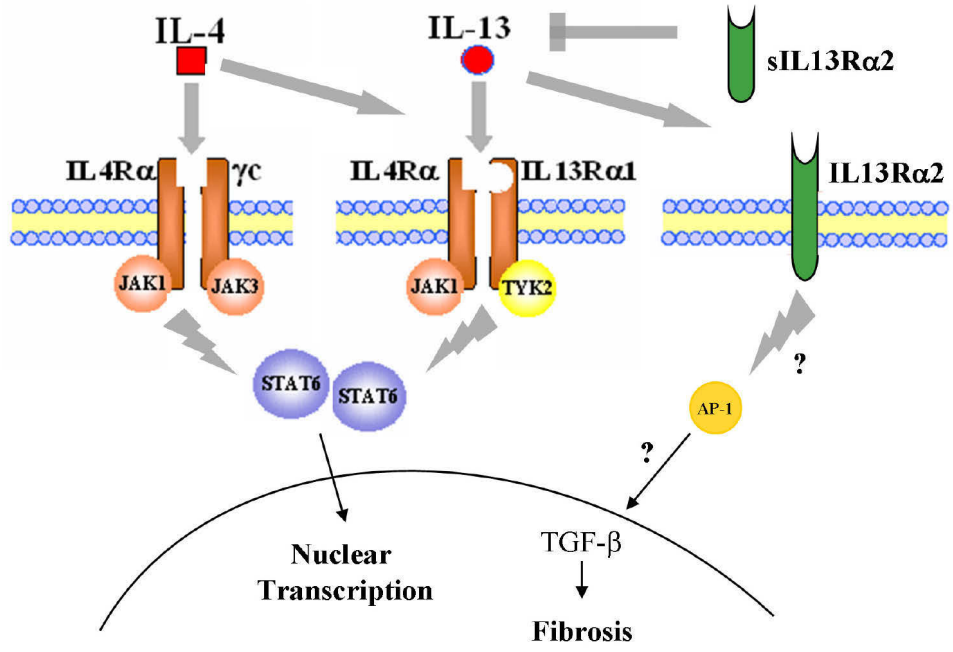

Fig 3: The complex receptor system of IL-13 and IL-4. IL-13 and IL-4 can share the Type II receptor complex IL-4Rα/IL-13Rα1 for cell signalling. The signalling cascade is dependent on recruitment and activation of signal transducer and activator of transcription (STAT) 6 leading to its phosphorylation and translocation to the nucleus. IL-4 posses a second heterodimeric IL-4

receptor mainly in hematopoietic cells (Type I) containing the IL-4Rα/γ common chain, which stimulation also results in STAT6 activation. On the other hand, IL-13 also has a second receptor IL-13Rα2 that can be found in a soluble or cell surface form. Still few are known about the exact signal and importance of this second receptor in the IL-13 biology. Modified from (Kasaian & Miller, 2008)

The strong correlation of Th2 cytokines, principally IL-13, with allergic diseases has promoted a large interest in targeting this cytokine and/or its receptors for therapeutic intervention (Brightling et al, 2010; Hansbro et al, 2011; Mitchell et al, 2010; Townley et al, 2011). In particular, IL-13 up-regulation is associated with development of severe asthma conditions in humans (Arima et al, 2002) and genetic polymorphisms in the IL-13 gene are shown to be linked with allergic phenotypes in different ethnical populations (Bottema et al, 2010; Heinzmann et al, 2000). Pharmaceutical companies developed several strategies to block the IL-13 response, including the development of antibodies directly against IL-13 (Corren et al, 2011; Gauvreau et al, 2011; Singh et al, 2010) or against its common receptor IL-4Rα (Antoniu, 2010; Corren et al, 2010; Wenzel et al, 2007). Most of these studies and clinical trials have shown efficacy in controlling chronic asthma, but additional repression of eosinophilic recruitment may be required (Hansbro et al, 2011). Furthermore, no studies are currently available regarding the use of these compounds outside pulmonary disorders.

As collagen content of atherosclerotic lesions is a critical aspect of atherosclerosis and determines the vulnerability for plaque rupture causing the clinical events of myocardial infarction and stroke, the specific function of IL-13 to promote tissue remodelling may be highly relevant to atherogenesis. In fact, IL-13 is considered to be the actual effector cytokine of Th2-driven fibrotic responses (Liu et al, 2012; Wynn, 2004; Wynn, 2008). By definition, fibrosis is a multistage, progressive scarring process characterized by the proliferation/activation of fibroblast and the excessive deposition of extracellular matrix components, such as collagen (Wynn, 2008). Previous studies demonstrated the non-redundant capacity of IL-13 to induce collagen production (Liu et al, 2012; Wynn, 2004; Wynn, 2008; Wynn, 2011). For example, in a chronic murine model of schistosomiasis, IL-13 blockade led to a substantial decrease in collagen deposition, while IL-4 production remained unchanged. Importantly, the inflammatory response generated by the eggs was unaltered in the absence of IL-13 (Chiaramonte et al, 2001; Chiaramonte et al, 1999a; Fallon et al, 2000). During liver fibrogenesis, IL-13

directly induces expression of collagen I and other important fibrosis-associated genes (i.e. α-smooth muscle actin and connective tissue growth factor) in hepatic stellate cells (Liu et al, 2012). In addition, overexpression of IL-13 in murine lungs alone contributed significantly to the development of fibrosis in the airways (Zhu et al, 1999), whereas treatment with IL-13-specific antibodies clearly diminished collagen deposition in challenged lungs (Belperio et al, 2002; Blease et al, 2001). Moreover, IL-13, through the engagement of IL-13 receptor α2, can induce TGF-β1 production in macrophages leading to collagen deposition *in vivo* (Fichtner-Feigl et al, 2006). In this regard, there is great evidence of cooperation between TGF-β and IL-13 in promoting fibrogenesis. Many cell types secrete and respond to TGF-β (Letterio & Roberts, 1998). The isoform TGF-β1 is considered the most relevant isoform in tissue fibrosis and is produced primarily by circulating monocytes and tissue macrophages (Wynn, 2004). TGF-β1 is stored inside the macrophage in an inactive form associated to an inhibitory protein called latency-associated protein (LAP). Binding to its receptors requires dissociation of the LAP (Wynn, 2004). In this context, IL-13 can also indirectly activate the release of produced TGF-β1 by inducing the expression of metalloproteinase that are able to cleave the LAP/TGF-β1 complex (Lanone et al, 2002; Lee et al, 2001). The diverse possibilities of IL-13 induction of collagen are exemplified in Figure 4.

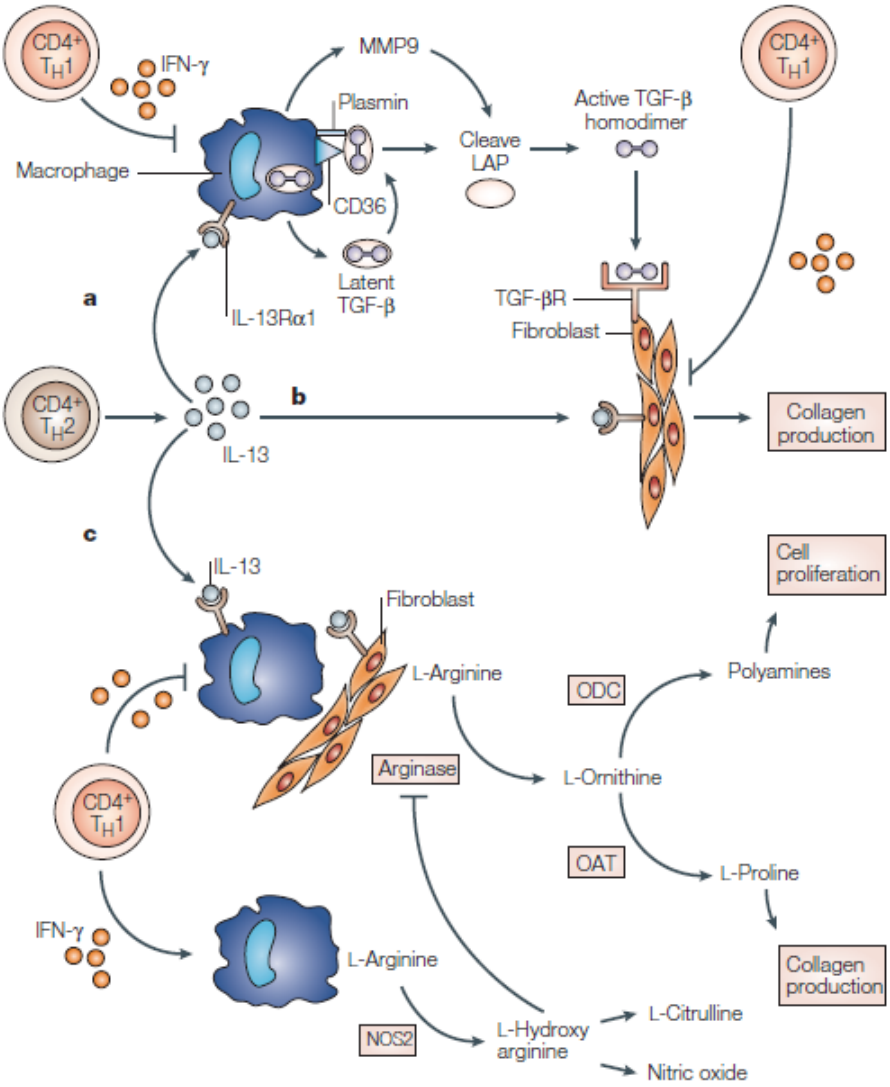

Fig 4: Some mechanisms of IL-13 induction of collagen production. **a** IL-13 is produced by Th2-cells and stimulates directly the production of latent TGF-β by macrophages. The latent TGF-β is secreted and its activation might be mediated by plasmin/serine protease- and/or matrix metalloproteinase 9 (MMP9)-dependent mechanisms. **b** Fibroblasts also express IL-13 receptors (IL-13Rs) and IL-13 can also directly activate the collagen-producing machinery in fibroblasts (Oriente et al, 2000). **c** IL-13 by promoting the alternative activation of macrophages and/or fibroblasts, upregulates arginase activity in these cells resulting in fibroblast proliferation, collagen production and ultimately, fibrosis (Hesse et al, 2001). IFN-γ produced by Th1-cells seems to antagonize all these pathways. OAT- ornithine amino transferase; ODC- ornithine decarboxylase. Extracted from (Wynn, 2004).

In addition, IL-13 also plays an important role in activation of macrophages into the so called alternatively activated macrophages (M2), which have potent anti-inflammatory and tissue repair capacities (Gordon & Martinez, 2010). Lately, the specific role of macrophage polarization in atherosclerosis development has gained attention (Butcher & Galkina, 2012; Hoeksema et al, 2012; Shalhoub et al, 2011).

2.4. Macrophage polarization

A potentially important function of cytokines in atherogenesis is their capacity to modulate the activation state of macrophages, which are hallmark cells of all stages of atherosclerosis. Indeed, continuous recruitment of monocytes into lesions has been shown to be related to plaque progression (Gautier et al, 2009; Swirski et al, 2006). In this context, the heterogeneity of lesional macrophage and their functions as well as their inducible mechanisms are being more and more investigated in face of disease development and/or disease regression (Butcher & Galkina, 2012; Ley et al, 2011; Saha et al, 2009).

Initially, a simple dual model for macrophage activation was proposed to classify pro-inflammatory (M1) versus anti-inflammatory macrophages (M2) (Gordon & Taylor, 2005). Derived from *in vitro* experiments, macrophages could be ascribed as classically activated macrophages, which were induced by IFN-γ and/or lipopolysaccharides (LPS) and were mainly associated with high microbicidal activity, pro-inflammatory cytokine production (i.e. TNF-α, IL-12, and IL-1β), and cellular immunity; or as alternatively activated macrophages, which resulted from IL-4 and/or IL-13 induction and were related with tissue repair and humoral immunity (Gordon & Taylor, 2005). The specific role of the latter macrophages in host defence remains unclear, although there is direct evidence that they can contribute to the clearance of helminths and nematodes (Anthony et al, 2006; Zhao et al, 2008).

More specifically, macrophages activated with IL-13 fail to present antigens to T-cells (Edwards et al, 2006), produce minimal (or no) amounts of pro-inflammatory cytokines (i.e. IL-1, IL-6, IL-8, TNF-α, and IL-12) (de Vries, 1998; Edwards et al, 2006), reactive oxygen, and nitrogen intermediates, (Doherty et al, 1993), through a mechanism that involves suppression of nuclear factor κB (Lentsch et al, 1997). In addition, alternatively activated macrophages enhance the expression of several adhesion molecules, including CD11b, CD11c, CD18 (Zurawski & de Vries, 1994), membrane receptors such as mannose receptor (Coste et al, 2003) and dectin-1 (Gales et al, 2010), and soluble proteins, for example, chitinase-like proteins (Ym-1/2) (Raes et al, 2002b; Welch et al, 2002) and resistin-like secreted proteins (FIZZ-1) (Nair et al, 2003; Raes et al, 2002a). Importantly, IL-13 can induce the expression of arginase-1

(Arg-1) in macrophages which counteracts the activity of nitric oxide synthase by competing for the same substrate – L-arginine (Hesse et al, 2001; Munder et al, 1999). Furthermore, Arg-1 is believed to participate in promoting collagen production and tissue fibrosis (Hesse et al, 2001; Wynn, 2004). Most of these markers have been used to help the identification and characterization of these subtypes of macrophages *in vitro* and *in vivo* during various disease states (Table I) (Wolfs et al, 2011).

The capacity of completely differentiated macrophages to alter their phenotype and functions in response to outside stimuli is broadly termed *macrophage polarization*. In the context of atherosclerosis the basic M1/M2 model of macrophage polarization may oversimplify the reality, as the plaque microenvironment is very heterogeneous and could promote various stages of polarization (Mantovani et al, 2009). Indeed, besides the common M1 and M2 macrophages, also mixed M1/M2 profiles, and two other clearly divergent macrophage phenotypes have recently been demonstrated in atherosclerotic lesions of humans and mice (Figure 5) (Wolfs et al, 2011).

Bouhlel *et al* were the first to show the presence of M2 macrophages in human carotid atherosclerotic lesions. They identified these cells through the expression of the mannose receptor (MR) and observed that MR^+M2 cells distributed differently from foam cells (Oil Red O^+ cells) and M1 macrophages, which were identified as MCP-1^+cells, thus supporting the presence of different macrophage subtypes in atherosclerotic plaques (Bouhlel et al, 2007). Later, the same group observed that MR^+ macrophages were mostly found in the vicinity of stable cell-rich areas and co-localized with IL-4 expression (Chinetti-Gbaguidi et al, 2011). In the same study, these MR^+M2 plaque macrophages showed enhanced phagocytic capacity in vitro in contrast to an apparently lower lipid handling capability, suggesting a potential function for these subtype of macrophages in scavenging of dead cells and debris from the lesions (Chinetti-Gbaguidi et al, 2011).

Table I: Some known markers of macrophage subsets.

	Priming factors	
	Classically activated (M1)	Alternatively activated (M2a)
Inducers	IFNγ	IL-4/IL-13
Expression profile		
Signalling pathways	STAT1	STAT6
Transcription factors	NF-κB p65/p50	NF-κB p50/p50
	IRF5	IRF4
		PPARγ
Effectors and cytokines upon activation	RNS, ROS	Arg-1
	IL-10^{low}	IL-10^{high}
	TNF	
	IL-1β	
Surface molecules	MHCII	MMR
	CD86	SR
	CD80	
Others		Ym-1
		FIZZ-1

Modified from (Wolfs et al, 2011).

Recently, Khallou-Laschet *et al* showed that lesion-infiltrating macrophages of young *ApoE*$^{-/-}$ mice exhibit predominantly the M2 phenotype, while M1 macrophages were dominant in more advanced lesions of aged mice. Moreover, the prevalence of M1 macrophages over M2 was correlated with disease progression. Interestingly, they also demonstrated that M2 macrophages favoured the proliferation of smooth-muscle cells *in vitro*, suggesting a reparative function of this macrophage in early lesion development. Using the differential expression of two subtypes of arginase as markers to specifically indentify M1 (Arg-2^{+}cells) and M2 (Arg-1^{+}cells) macrophages in murine lesions, this report demonstrated for the first time changes from M2 to M1 polarization in the course of plaque development (Khallou-Laschet et al, 2010).

In addition to the classically and alternatively activated macrophages, Kadl *et al* described a newly distinct type of murine lesional macrophages, called Mox, which were

generated by activation with oxidized phospholipids and represent a completely separate population (around 30% of all macrophages) in advanced atherosclerotic plaques. The Mox macrophages were characterized by a clear upregulation of an anti-oxidant response through the overexpression of the transcription factor nuclear factor erythroid 2-like 2 (NRF2). In comparison to the other macrophage phenotypes (i.e. M1 and M2), Mox exhibit lower phagocytotic and chemotactic capacity as well as a different gene expression profile (Kadl et al, 2010).

Along the same line, two groups analyzed the capacity of human monocytes to differentiate into distinct macrophage phenotypes upon stimulation with certain factors present within the atherosclerotic lesion (Gleissner et al, 2010; Waldo et al, 2008). In the first study, monocytes were differentiated with macrophage colony-stimulating factor (M-CSF) or granulocyte-macrophage colony-stimulating factor (GM-CSF) and they observed that compared to M-CSF–differentiated macrophages, GM-CSF–differentiated macrophages displayed increased expression of genes that promote macrophage emigration (i.e. CCR7) and reverse cholesterol transport, such as peroxisome proliferator activated receptor gamma (PPAR-γ), liver X receptor alpha (LXR-α), and ATP binding cassette, subfamily G, member 1 (ABCG1). Furthermore, they demonstrated that both differentiated macrophages were capable to accumulate lipids, but they were differentially distributed in vascular lesions (Waldo et al, 2008). A more recent report classified human monocytes differentiated with CXCL-4 as M4 macrophages, given that these cells displayed a diverse transcriptome compared to the traditionally characterized M1 and M2 macrophages (Gleissner et al, 2010). M4 macrophages showed lower expression of scavenger receptors and increased levels of cholesterol efflux transporters. Furthermore, CXCL-4 expression was found inside atherosclerotic lesions, supporting a role for this new subtype of macrophages in disease development (Gleissner, 2012; Gleissner et al, 2010).

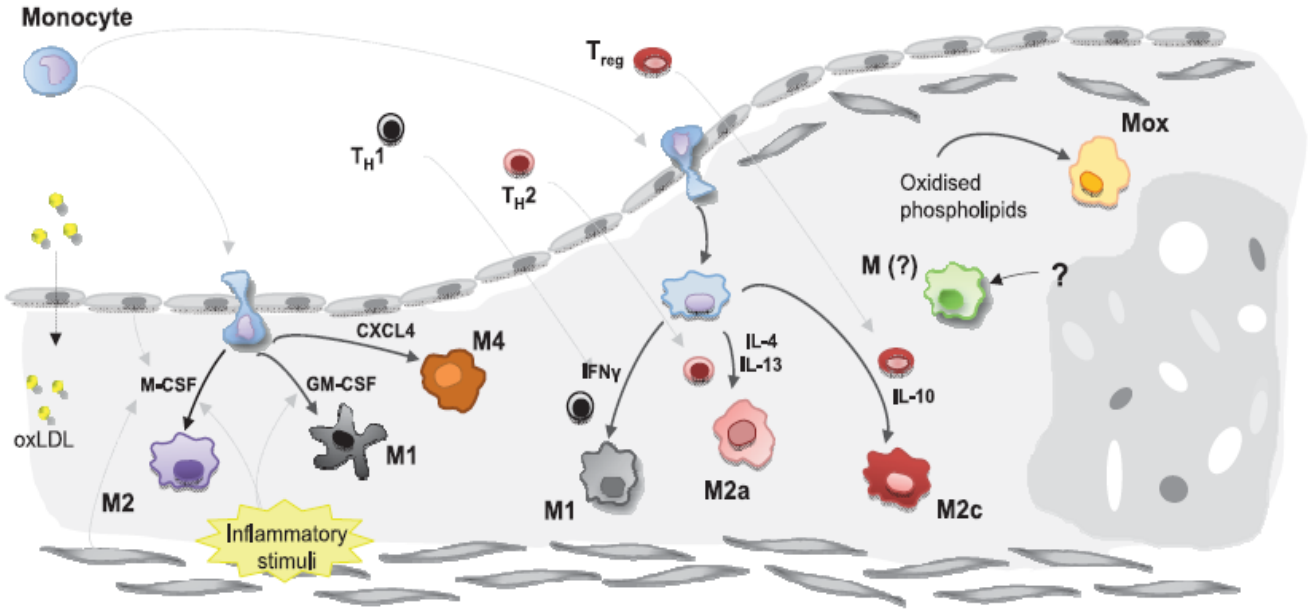

Fig 5: Model of macrophage polarization in atherosclerosis. The atherosclerotic plaque microenvironment offers a broad range of stimulus, such as growth factors (M-CSF and GM-CSF), cytokines (IFN-g, IL-4, IL-13, IL-10), chemokines (CXCL4) and other factors (Oxidised phospholipids and unknown factors ?). All together influence and coordinate the macrophage polarization, resulting in the co-existence of many subtypes of macrophages. Modified from (Wolfs et al, 2011).

In summary, the cytokine profile of the local microenvironment present in atherosclerotic lesions can profoundly affect the activation state of macrophages and their function, e.g. foam cell formation and lipid metabolism. Polarization of plaque macrophages has been shown to occur inside atherosclerotic lesions and seems to be more complex than the initial M1/M2 dichotomy (Butcher & Galkina, 2012; Ley et al, 2011; Wolfs et al, 2011). Besides the later mentioned macrophage subtypes, new phenotypes of macrophages are being discovered and characterized regarding their surface markers and functional activity, and many others, still unidentified, may co-exist in atherosclerotic plaques. Thus, it is important to define the molecular basis of such activation states and the role of these macrophage subtypes in disease progression. Furthermore, the retained plasticity of macrophages to polarize back and forward opens potentially new targets for therapeutic interventions in atherosclerosis (Hoeksema et al, 2012; Saha et al, 2009).

2.5. Atherosclerosis regression

Atherosclerosis is a slow, silent and progressive disease, and most patients typically enter in a clinical setting already with established and advanced lesions. Thus, there is a real need to develop new therapies that are able to halt and/or even reverse plaque formation (Feig et al, 2009; Williams et al, 2008). To date, the use of statins to reduce serum LDL levels has been the main intervention applied to delay disease progression (LaRosa et al, 2005), but these drugs have been shown to present limitations regarding plaque burden and risk (Collins et al, 2003; Nissen, 2005a; Nissen, 2005b; Nissen et al, 2006).

Although a variety of mouse models have provided important and helpful information about atherosclerosis progression and its mechanisms, comparatively little is known about the cellular and molecular pathways underlying lesion regression. Fisher and colleagues developed a transplantation-based mouse model in which atherosclerotic plaques are allowed to form in *ApoE*-deficient mice and then some segments of the diseased aorta are transplanted into recipient mice with a normolipidemic plasma environment. In this model, plaque regression rapidly ensues and it is defined by a significant reduction in the monocyte/macrophage-derived cell population and its replacement with collagenous matrix (Reis et al, 2001; Trogan et al, 2004). Subsequent studies performed using this mouse model revealed that LXR, high HDL levels rather than low LDL levels, and the induction of macrophage emigration via a CCR7-dependent manner are possible factors implicated in plaque regression (Feig et al, 2010; Feig et al, 2011b; Trogan et al, 2006).

In the past years, the concept that migratory egress from plaques is the main aspect of the observed loss of plaque macrophages during atherosclerosis regression has been strengthened (Feig et al, 2011a; Feig et al, 2010; Feig et al, 2011b; Feig et al, 2011c; Llodra et al, 2004; Trogan et al, 2006). It has been demonstrated to be dependent on CCR7 expression and that a possible link between lipid lowering and decreased macrophage content can be explained by the structure of the mouse and human CCR7 promoters. Both likely contain sterol response elements (SREs), which are functional *in vitro* and can promote chemotaxis of macrophages in response to the CCR7 ligands, such as CCL19 or CCL21 (Feig et al, 2011c). However, recent data from Potteaux *et al* showed that after restoring ApoE expression in atherosclerotic *ApoE*$^{-/-}$ mice, the significant reduction in macrophages did not involve CCR7-mediated

egression from plaques. In contrast, a clear suppression of monocyte recruitment together with a stable rate of apoptosis was shown to be responsible for this reduction (Potteaux et al, 2011). Thus, the exact mechanism underlying the macrophage removal during lipid-lowering is still to be further determined.

Importantly, a number of studies demonstrated that the experimental regression of atherosclerotic lesions is associated with a switch towards alternatively activated macrophages, as demonstrated by the up-regulation of M2-specific genes, such as Arg-1 and mannose receptor (Feig et al, 2011a; Feig et al, 2011b; Feig et al, 2012; Rayner et al, 2011a). These data together with the anti-inflammatory properties of M2 macrophages suggest a potentially protective role of this subtype of macrophages in atherosclerotic lesion formation and may indicate that M2 polarization is a hallmark of regressing lesions.

Based on the prominent functions of IL-13 in inducing fibrosis and alternative macrophage activation described above, I hypothesized that IL-13 may have an atheroprotective role by modulating plaque composition. Therefore, I tested the role of IL-13 in atherosclerotic lesion formation.

Here, I demonstrate that macrophages, which were alternatively activated with IL-13, have an increased capacity of clearing OxLDL *in vitro*. Moreover, I show that *LDLR*$^{-/-}$ mice that were reconstituted with bone marrow of *IL-13*-deficient mice develop accelerated atherosclerosis. In addition, exogenous administration of IL-13 to cholesterol-fed *LDLR*$^{-/-}$ mice promotes collagen formation and reduces lesional macrophage content of existing lesions by decreasing VCAM-1-dependent monocyte recruitment, while having no effect on serum cholesterol levels.

3. AIM OF THE STUDY

The central hypothesis of this thesis is that IL-13 mediates atheroprotective effects by modulating the macrophage phenotype within atherosclerotic lesions resulting in a more stable plaque. Insights gained from this project will not only further delineate the role of Th2 cytokines in atherosclerosis, but contribute significantly to the understanding of macrophage polarization in plaque stability – an aspect with high clinical relevance.

The specific aims of this study were:

1) To test the role of IL-13 in atherosclerosis *in vivo* and *in vitro* by analyzing:

a) The effect of IL-13 administration on established atherosclerosis in *LDLR*$^{-/-}$ mice

b) The effect of IL-13-deficiency in hematopoietic cells on the development of atherosclerosis

c) The role of IL-13-induced (M2) macrophages in foam cell formation and cholesterol metabolism.

4. METHODS

4.1. Animals and intervention studies

LDL receptor-deficient mice (*LDLR*$^{-/-}$) and C57BL/6J were from The Jackson Laboratories (Bar Harbor, Maine, USA); *IL-13*$^{-/-}$ mice were a kind gift of Dr. Thomas Wynn (NIAID/NIH, Bethesda, USA). All mice were on a C57BL/6J background and were bred in-house. All experimental protocols were approved by the institutional animal experimentation committee and the Austrian Ministry of Science.

Bone marrow transplantation (BMT) studies were performed as previously described (Binder et al, 2004). Briefly, a single dose of 9-Gy lethal total body irradiation were given to *LDLR*$^{-/-}$ mice (n=30, 8-week-old, male) and subsequently, irradiated mice were injected intravenously with 2x10^6 bone marrow cells harvested from either *IL-13*$^{-/-}$ (n=15) or *IL-13*$^{+/+}$ (n=15) mice. Following the next 4 weeks, mice were fed regular chow diet to allow for bone marrow reconstitution and then switched to an atherogenic diet containing 21% fat and 0.2% cholesterol (TD88137, Ssniff Spezialdiäten GmbH, Soest, Germany) for an additional 16 weeks to induce lesion formation. Three mice (one in the *IL-13*$^{-/-}$ and two in control group) were *a priori* excluded from final analyses because they developed skin lesions and lost weight, or due to technical problems of tissue collection. One mouse from the control group was excluded as statistical outlier, which however did not alter the statistical significance of the results.

For the atherosclerosis intervention study, *LDLR*$^{-/-}$ mice (n=24, 12 week-old, female) were fed an atherogenic diet (Ssniff) for a total of 16 weeks to induce lesion formation. At week 11, mice were divided randomly into two groups and injected intraperitoneally with PBS (n=11) or IL-13 (50 ng/mouse R&D systems, Minneapolis, Minnesota, USA; n=13) twice per week for the following remaining 5 weeks.

4.2. Evaluation of atherosclerosis

Total size of the atherosclerotic lesion was quantified in *en face* preparations of the whole descending aorta, and in cross sections through the aortic origin as previously described (Binder et al, 2004; Schiller et al, 2001). Briefly, at time of sacrifice, animals

were perfused by gravital force with PBS and formalin (4% paraformaldehyde in PBS, pH 7.4). Subsequently, the mouse aorta was dissected from the heart to the iliac bifurcation. Under the microscope, the entire aorta was cleaned from surrounding fat tissue, opened longitudinally, pinned, stained with Sudan IV, and photographed with a digital camera. Total aortic area and aortic lesion area were calculated using Adobe Photoshop CS3 (Adobe Systems, San Jose, California, USA) and ImageJ 1.41 software. Results are reported as percentage of lesion area per total aortic surface area. Cross-sections of the aortic origin were also quantified for lesion size and phenotype. Serial sections (5 μm in thickness) were cut through a 400 μm segment of the aortic root, starting with the appearance of all 3 valve leaflets. For each mouse, 8 sections separated by 50 μm were examined. Each section was stained with H&E and photographed using the AxioVison software (Carl Zeiss AG, Jena, Germany). Total lesion area was quantified using Adobe Photoshop CS3 and ImageJ 1.41 softwares.

4.3. Immunohistochemistry and phenotypic analysis of lesions.

Lesion phenotype was determined by the content of collagen, size of necrotic core area, and the presence of macrophages, smooth-muscle cells, T-cells, classical activated (M1) macrophages, alternatively activated (M2) macrophages, ABCA1 expressing cells, and CCR7 expression in lesions of equal size. For the collagen content, sections were stained with Sirius Red, and for the assessment of necrotic cores, sections were stained with a modified elastic-trichrome stain. The photographed images were analyzed using ImageJ 1.41 software to determine the percentage of collagen and necrotic core area, respectively. For the presence of macrophages, smooth-muscle cells, T-cells, M1 macrophages and M2 macrophages immunohistochemistry was performed using antibodies against mouse Mac-3 (1:50 rat anti-mouse, clone M3/84, BD-Biosciences Pharmingen, San Diego, California, USA), smooth-muscle cell actin (1:10,000 polyclonal rabbit anti-mouse, Sigma-Aldrich), CD3 (1:800 polyclonal rabbit anti-human/mouse, DAKO, Glostrup, Denmark), iNOS (1:500 polyclonal rabbit anti-human/rat/mouse, ABCAM, Cambridge, UK), CD206 (1:20 rat anti-mouse, clone MR5D3, BioLegend, San Diego, California, USA) and Ym1/2 (1:1,000 polyclonal rabbit anti-mouse, a kind gift of Dr. Shioko Kimura, NIH/NCI, Bethesda, USA). For the evaluation of CCR7 and ABCA1 expression, immunohistochemistry was

performed using antibodies against mouse CCR7 (1:700 monoclonal rabbit anti-human/rat/mouse, clone Y59, ABCAM) and mouse ABCA1 (1:1,000 polyclonal rabbit anti-mouse, Novus Biological, Littleton, Colorado, USA). Briefly, sections were incubated with the primary antibody overnight at 4°C, blocked for endogenous peroxidase with 3%H_2O_2 and following several washes incubated with a secondary biotinylated anti-rat (1:100 rabbit anti-rat IgG, DAKO) or anti-rabbit (1:500 goat anti-rabbit IgG, Vector Laboratories, Burlingame, California, USA) antibody for 30 min at room temperature. Then, sections were incubated with streptavidin-HRP Ultrasensitive (1:1,000 Sigma-Aldrich, St. Louis, Missouri, USA) for 30 min at room temperature in the dark, and subsequently developed with DAB (Liquid DAB + Substrate chromogen System, DAKO). The sections were photographed and the stained area was quantified using ImageJ 1.41 software or positive cells were counted.

4.4. Serum Total Cholesterol and Triglycerides

At time of sacrifice, blood samples were collected from the vena cava of all mice. Total serum cholesterol and triglycerides were measured by enzymatic methods using an automated analyzer AU5400 – Chemistry System (Beckman Coulter, Brea, California, USA).

4.5. Lipoprotein isolation and modification

Human LDL and HDL were isolated from EDTA-plasma of healthy donors after overnight fasting by differential density ultracentrifugation on OTD Combi (Sorvall, Thermo Fisher Scientific, Waltham, Massachusetts, USA) over the density range of d 1.019 to 1.063 and 1.21 g/ml, respectively as described (Binder et al, 2003). The quality of LDL-preparations was checked by lipoprotein electrophoresis. LDL was sterile filtered and stored at 4°C. CuOx-LDL and MDA-LDL were prepared as described previously (Binder et al, 2003). Protein concentrations were determined by Lowry or BCA-method (Pierce, Thermo Fisher Scientific). All lipoprotein preparations used for cell culture were tested for endotoxin levels by chromogenic Limulus amoebocyte assay (QCL-1000;

BioWhittaker Inc, Wakersville, Maryland, USA) and contained less than 1 ng lipopolysaccharides/mg protein.

4.6. Macrophage foam cell assays

Isolation of peritoneal macrophages. For all *in vitro* experiments, C57BL/6J mice, 12-16 weeks of age, were injected intraperitoneally with 2 ml of 3% thioglycollate (Difco, Thermo Fischer Scientific). After 3 days, thioglycollate-elicited macrophages were harvested and plated in full culture medium (RPMI 1640 media, 100 U/ml penicillin, 100 µg/ml streptomycin and 50 µg/ml gentamicin; all Invitrogen, Carlsbad, California, USA) containing 10% heat-inactivated fetal calf serum (FCS) at a density of $3x10^5$ cells/well in 48-well plate; $5x10^5$ cells/well in 24-well plate; $1.5x10^6$ cells/well in 12-well plate or $3.5x10^6$ cells/well in 6-well plate for lipid uptake, cholesterol efflux, RNA/protein isolation and cellular cholesterol quantification experiments, respectively.

Macrophage differentiation and generation of foam cells. Macrophages were differentiated into classical activated macrophages (M1) with 100 ng/ml IFN-γ (R&D systems) or alternatively activated macrophages (M2) with 5 ng/ml IL-13 (R&D systems) in full culture medium containing 10% FCS for 16 hours at 37°C. Following differentiation, cells were washed once with PBS and stimulated with 50 µg/ml CuOx-LDL in full culture medium containing 1% mouse serum for 24 hours at 37°C.

Lipid uptake – Oil Red O staining. After foam cell generation, cells were washed once with PBS and fixed with a solution of formalin-sucrose (4% paraformaldehyde, 4% sucrose in PBS) for 20 min at room temperature. Following a wash with 60% isopropanol, cells were stained with Oil Red O (Sigma-Aldrich) diluted 6:4 parts in dH_2O for 20-30 min at room temperature. After washing several times with dH_2O, 3 random-fields were counted for positive and negative stained cells under the microscope. The data are expressed as percentage of Oil Red O positive cells per total cells.

Cellular cholesterol content. Foam cells were lysed with a solution of 0.1M NaOH, and cellular lipids were extracted by hexane/isopropanol (3:2). Total cholesterol content was determined using the Amplex Red Cholesterol Assay kit (Invitrogen). Values are related to total protein content of each sample.

Cholesterol efflux assay. Following macrophage differentiation, cells were stimulated with 50 µg/ml CuOx-LDL plus 1 µCi [H^3]-cholesterol (Perkin Elmer, Waltham, Massachusetts, USA) in full culture medium for 24 hours at 37°C (Fig 12A) or macrophages were loaded with 50 µg/ml CuOx-LDL plus 1 µCi [H^3]-cholesterol in full culture medium for 24 hours at 37°C prior to macrophage differentiation with either 100 ng/ml IFNγ or 5 ng/ml IL-13, respectively in full culture medium for further 16 hours (Fig 12B). Thereafter, cells were equilibrated in serum free-full culture medium for 2h at 37°C. After equilibration, cells were incubated with or without 10 µg/ml HDL plus 50 µg/ml CuOx-LDL in serum free-full culture medium for 6 hours at 37°C. Supernatants were collected and spun down (at 3,000 rpm for 10 min) to remove cellular debris, and the radioactivity in the supernatants was measured using a liquid scintillation counter (β-counter 2000 CA; TRI-CARB Liquid Scintillation Analyzer, Packard). Cells were lysed in 0.1M NaOH and the cell-associated radioactivity was measured as described above. All measured counts were corrected for total cellular protein content as determined by the Bradford method (Bio-Rad Protein Assay, Bradford Laboratories, Hercules, California, USA). The percent efflux was calculated as (media dpm)/(cell+media dpm) x 100 and the HDL dependent-efflux was calculated as (mean % efflux with HDL)-(mean % efflux w/o HDL).

RNA/protein isolation. Following foam cell generation, total RNA was isolated using the RNeasy Mini Kit (PeqLab, Vienna, Austria) and 500 ng of total RNA was reverse-transcribed using the High Capacity cDNA Reverse Transcription kit (Applied Biosystems, Carlsbad, California, USA). Quantitative real-time PCR was performed using iTaq SYBR Green Supermix with ROX Dye (Bio-Rad Laboratories, Hercules, California, USA) in a CFX96 Real-time System (Bio-Rad Laboratories). All data were normalized to Cyclin B (CycB) and expressed as fold change over control (untreated cells). Primer sequences are available in Table II. For protein detection, cells were incubated for 10 min at room temperature with a lysis buffer containing 62.5mM Tris, 8M Urea, 20mM EDTA, 20mM EGTA, 10% glycerol, 1% SDS (pH6.8), and lysates were sonicated for 2 seconds and stored at -20°C for further analyses.

4.7. Immunoblotting

Samples were separated by SDS-PAGE and blotted on nitrocellulose-membranes (Trans-Blot® Transfer Medium, Bio-Rad Laboratories). Membranes were blocked in 5% non-fat dry milk in TBS containing 0.1% Tween 20 for 60 min at room temperature. Following 3 washing steps, blots were probed using anti-ABCA1 (rabbit IgG anti-mouse, 1:500, Novus Biological) or anti-ABCG-1 (rabbit IgG anti-mouse, 1:2,000, Novus Biological) or anti-β-actin (mouse IgG2a anti-mouse, 1:5,000, Sigma-Aldrich) antibodies overnight in washing buffer (TBS + 0.1% Tween 20) containing 3 % BSA at 4°C. After 3 washing steps, blots were incubated with a secondary HRP-labeled goat anti-rabbit (1:10,000, Sigma-Aldrich) or goat anti-mouse IgG (1:10,000, Bio-Rad Laboratories) in washing buffer containing 5% non-fat dry milk for 60 min at room temperature. After further washing, membranes were developed using a 1:1 solution of Luminol/Enhancer and Stable Peroxidase (Super Signal® West Dura Extended Duration Chemiluminescent Substrate, Pierce Biotechnology, Rockford, Illinois, USA), and chemiluminescence was detected using a CCD camera (FUSION FX7, PEQLAB Biotechnologie GmbH, Erlangen, Germany). AlphaEase FC software (Alpha Innotech Corporation, San Leandro, California, USA) was used for quantification.

4.8. Splenocyte cytokine release assay

To induce maximal activation of T-cells, splenocytes from individual mice were stimulated with a combination of anti-mouse CD3/CD28 over 3 days and the supernatants analyzed for cytokine production as previously described (Binder et al, 2004). Briefly, total splenocytes (0.25×10^5) were plated in full culture medium containing 10% FCS (96-well round-bottom plates in a final volume of 100 µl, quadruplicates) and incubated for 72 hours at 37°C/5% CO_2 either alone or in the presence of 10 µg/ml plate-bound anti-mouse CD3 (clone 145-2C11, BD Biosciences — Pharmingen) and 10 µg/ml soluble anti-mouse CD28 (clone 37.51, BD Biosciences — Pharmingen). The amounts of INF-γ, IL-4, IL-5, IL-10 and IL-13 were determined by a fluorescent bead immunoassay in undiluted supernatants (FlowCytomix 5-plex kit, eBioscience, Vienna, Austria).

4.9. Flow Cytometry

At time of sacrifice, peritoneal exudate cells (PEC) were harvested by peritoneal lavage using HBSS supplemented with 2% FCS. Total white blood cells were isolated from blood collected in EDTA-tubes via the vena cava. Blood was diluted 1:1 in a solution of PBS containing 2% Dextran (Sigma-Aldrich) and incubated for 40 min at 37°C to separate the red blood cells. All cells were washed and incubated with an anti-Fcγ receptor blocking antibody (anti-mouse CD16/CD32, clone 93, 1:200, eBioscience) for 30 min at 4°C. T-cells, B-cells and macrophages in PEC were assessed using FITC-labeled anti-CD23 (clone B3B4, 1:800, BD Biosciences – Pharmingen), phycoerythrin (PE)-labeled anti-CD5 (clone 53-7.3, 1:100, eBioscience), PercP-labeled anti-CD19 (clone 1D3, 1:200, BD Biosciences – Pharmingen), and APC-labeled anti-CD11b/Mac-1 (clone M1/70, 1:800, eBioscience); macrophage subpopulations were determined using FITC-labeled anti-CD206 (clone MR5D3, 1:200, BioLegend), PE-labeled anti-CD80 (clone 16-10A1, 1:200, BD Bioscience – Pharmingen) and APC-labeled anti-F4/80 (clone BM8, 1:200, Invitrogen). Peripheral blood cells were analysed for the presence of resident monocytes, inflammatory monocytes, neutrophils and B-cells using FITC-labeled anti-Ly6C (clone HK1.4, 1:200, BioLegend), PE-labeled anti-Ly6G (clone 1A8, 1:2000, BioLegend), PercP-labeled anti-CD19 (clone 1D3, 1:200, BD Biosciences – Pharmingen) and APC-labeled anti-CD11b/Mac-1 (clone M1/70, 1:800, eBioscience). All stains were performed in 100 µL of FACS buffer (PBS + 2% FCS) for 30 min at 4°C in darkness, followed by two washes. Stained cell populations were analyzed by multiparameter flow cytometry using a BD FACSCalibur (BD Bioscience, Franklin Lakes, New Jersey, USA). More than 10^5 cells were acquired per sample, with dead cells excluded by forward and side scatter properties and data were analyzed using FlowJo 7.6.4 software (Tree Star, Inc., Oregon Corporation, Ashland, Oregon, USA).

4.10. Immunoassays

Antibody titers to MDA-LDL were determined by chemiluminescent ELISA as previously described (Binder et al, 2003). Total isotype levels were determined by a chemiluminescent-based sandwich ELISA using matched pairs of specific antibodies for capture and detection, followed by incubation steps with AP-conjugated NeutrAvidin

(1:10,000 in TBS-BSA, Perkin Elmer) at room temperature and Lumiphos Plus (P-701, 30% solution in water, Lumigen, South Field, Michigan, USA). Chemiluminescence was detected using a luminescence reader (BioTek Synergy 2, BioTek, Winooski, Vermont, USA). The following antibodies were paired with appropriated AP-conjugated or biotinylated detecting antibodies, respectively: anti-mouse IgM (coated at 2 μg/ml, Sigma-Aldrich) and AP-conjugated goat anti-mouse IgM (1:20,000 in TBS-BSA, Sigma-Aldrich), anti-mouse IgG1 (coated at 2 μg/ml, BioLegend) and biotinylated anti-mouse IgG1 (at 0.5 μg/ml in TBS-BSA, BD Bioscience), anti-mouse IgG2c (coated at 1 μg/ml, AbDSerotec, Oxford, United Kingdom) and biotinylated goat anti-mouse IgG2c (1:4,000 in TBS-BSA, Jackson ImmunoResearch Laboratories, West Grove, Pennsylvania, USA). Isotype levels were measured at following three serum dilutions: 1:10,000, 1:30,000 and 1:90,000 for IgM, 1:50,000, 1:150,000, 1:450,000 for IgG1 and 1:250,000, 1:500,000, 1:1,000,000 for IgG2c. Results were calculated on a standard curve, which was generated using respective purified isotypes obtained from Biolegend (IgM and IgG1) or Southern Biotech (IgG2c, SouthernBiotech, Birmingham, Alabama, USA).

4.11. Monocyte labeling and macrophage egression assessment

Macrophage emigration from atherosclerotic lesions were analyzed by a fluorescent labelled-bead tracking technique previously described (Potteaux et al, 2011). Twenty-two male, 8 weeks old, *ApoE* $^{-/-}$ mice (C57BL/6J background) were fed a standard western diet containing 21% fat and 0.2% cholesterol (Altromin Spezialfutter GmbH & Co.KG, Lage, Germany) for 6 weeks to induce lesion formation. At week 3, circulating classical Ly6C^{hi} monocytes were labeled by intravenous (i.v) injection of 1 μm Fluoresbrite green fluorescent (YG) plain microspheres (Polysciences Inc., Warrington, Pennsylvania, USA) diluted 1:4 in sterile PBS, 24 hours after an i.v. injection of 250 μl clodronate-loaded liposomes to deplete monocytes. Mice were not manipulated for the following week to allow latex-beads^{+}monocytes to accumulate within atherosclerotic plaques. At week 4, mice were divided into three groups randomly. One group was sacrificed for the quantification of bead and macrophage (mac-2^{+}cells) content (baseline, n=7); the remaining two groups received biweekly intraperitoneal injections of either PBS (n=7) or IL-13 (50 ng/mouse, R&D systems n=8) for the remaining 2 weeks. All animal experiments were approved by the local ethical committee (Regierung von

Oberbayern). At the end of week 6, numbers of beads per plaque area in the aortic root and mac-2^+cells per total $DAPI^+$cells were quantified in cross-sections of atherosclerotic lesions of PBS- and IL-13-treated mice. Macrophage egress was assessed by the number of beads present within the plaque area at the end of the experimental approach compared to baseline (week 4).

4.12. Intravital microscopy

Leukocyte endothelial interactions and expression of endothelial adhesion molecules were analyzed by intravital microscopy of the left carotid artery. Sixteen male, 8 weeks old, *Cx$_3$cr1*$^{gfp/wt}$ *ApoE* $^{-/-}$ mice (C57BL/6J background, for leukocyte endothelial interactions) and sixteen male, 8 weeks old, *ApoE* $^{-/-}$ mice (C57BL/6J background, for endothelial adhesion molecules expression) were fed a standard western diet containing 21% fat and 0.2% cholesterol (Altromin) for 6 weeks to induce lesion formation. At week 4, they were divided into two groups randomly and injected intraperitoneally with PBS (n=8) or IL-13 (50 ng/mouse, R&D systems n=8) twice per week for the remaining 2 weeks. At the end of this period, mice were anaesthetized with ketamine/xylazine and the left carotid artery was exposed as described previously (Drechsler et al, 2010). All animal experiments were approved by the local ethical committee (Regierung von Oberbayern). Circulating leukocytes were labeled by injection of a PE-labeled anti-mouse Gr1 antibody (clone RB6-8C5, 5µg, eBioscience) via an intravenous catheter 5 min prior to recording. Intravital microscopy was performed using an Olympus BX51 microscope (Olympus, Hamburg, Germany) equipped with a beam splitter to enable synchronized dual-channel recording, a Hamamatsu 9100-02 EMCCD camera (Hamamatsu Photonics, Hamamatsu City, Japan), and a 10x saline-immersion objective. For image acquisition and analysis Olympus Cell^r software was used. Adherent monocytes (GFP) and neutrophils (GFP^-/PE^+) were recorded at the bifurcation. For luminal detection of VCAM-1 or CCL-2 presented on the endothelium, 50 µl of Protein G Fluoresbrite YG Microspheres (Polysciences Inc., Warrington, Pennsylvania, USA) were coupled to 50 µg of polyclonal antibodies against mouse VCAM-1 (eBioscience) or mouse CCL2 (eBioscience) as described recently (Engel et al, 2011). Antibody/bead complexes were injected intravenous and allowed to circulate for 15 min.

Complexes immobilized along the carotid artery were detected by intravital microscopy as described above.

4.13. Statistical analysis

Statistical analyses were performed using GraphPadPrism 4.03 software (GraphPad Software, Inc., La Jolla, California, USA). Results were analyzed by one-way analysis of variance (ANOVA) with the post-test Bonferroni's multiple comparison tests for all the *in vitro* data. Student's unpaired *t*-test was used for results of *in vivo* studies (unless indicated differentially). Data are presented as mean ± SEM and $P < 0.05$ was considered significant.

Table II: Primer sequences for quantitative RT-PCR.

Gene	Forward	Reverse
CycB	CAGCAAGTTCCATCGTGTCATCAAGG	GGAAGCGCTCACCATAGATGCTC
CD11b	CAAGTGCCTGTCACACTGAGC	TGCAACAGAGCAGTTCAGCAC
CD68	TGGCGCAGAATTCATCTCTTC	GGTCAAGGTGAACAGCTGGAG
Arg-1	GTGAAGAACCCACGGTCTGT	CTGGTTGTCAGGGGAGTGTT
Ym-1	GGGCATACCTTTATCCTGAG	CCACTGAAGTCATCCATGTC
CCL9	TACTGCCCTCTCCTTCCTCA	TTGAAAGCCCATGTGAAACA
iNOS	AATCTTGGAGCGAGTTGTGG	CAGGAAGTAGGTGAGGGCTTG
CD86	CACGAGCTTTGACAGGAACA	TTAGGTTTCGGGTGACCTTG
CXCL10	GGTCTGAGTGGGACTCAAGG	GTGGCAATGATCTCAACACG
ABCA-1	GAGCAAAGCCAAGCATCTTC	AGCAGGGACCACATAATTGC
ABCG-1	TTCCGGAAGGTCTCCTGCTAC	ATCATGGCCTCCTGAACAGTG
LOX-1	GATGTTAGCCCAGCAGAAGG	GTCCAGCTTCCGGGTGAT
LXRα	GGATAGGGTTGGAGTCAGCA	GCTCAGCACGTTGTAATGGA
LXRβ	CTTCGGGCTTCCACTACAAC	CTTCCGAATCTGCTCCTCAG
CD36	GGAGCAACTGGTGGATGGTT	TTGAGACTCTGAAAGGATCAGCA
SRA-1	GAACAAGCGCACGTGGAAC	CCTTCAGTCTGAGGTCGTTGG

5. RESULTS

5.1. IL-13 administration modulates established atherosclerosis.

To study the capacity of IL-13 to influence existing atherosclerosis, I performed an intervention study in which IL-13 was administered exogenously to mice with established atherosclerotic lesions.

LDLR$^{-/-}$ mice were fed an atherogenic diet for 16 weeks and received biweekly intraperitoneal injections of IL-13 or PBS during the last 5 weeks of diet. Based on my observation that atherosclerotic *LDLR*$^{-/-}$ mice have IL-13 serum levels of approximately 2.5 ng/ml, I decided to administer 50 ng of IL-13 per *LDLR*$^{-/-}$ mouse twice per week, which corresponds to only three fold higher amounts of systemic IL-13 per day.

At time of sacrifice, mice were not different with respect to body weight, total plasma cholesterol, (TC), triglycerides, (TG) or levels of total IgG1 or IgG2c antibodies (Table III). Furthermore, there were no differences in the frequencies of splenic T- or B-cells (Table III). Stimulated splenocytes from atherosclerotic *LDLR*$^{-/-}$ mice treated with PBS or IL-13 produced similar amounts of Th2 (IL-4, IL-5, IL-10 and IL-13) and Th1 (INF-γ) cytokines, indicating that IL-13 administration at this dose did not alter the overall Th1/Th2 balance (Figure 6). In addition, no induction of liver or lung fibrosis due to the continuous IL-13 injection was observed (data not shown).

Table III: Overview of experimental data of the IL-13 administration study.

	LDLR $^{-/-}$ inj → PBS (n=11)	*LDLR* $^{-/-}$ inj → IL-13 (n=13)
Atherosclerosis		
Aortic origin (10^4 µm^2/sect.)	48.16 ± 3.66	47.15 ± 1.22
En face (% of aorta)	6.63 ± 0.94	6.22 ± 0.66
Metabolic parameters		
Weight (g)	23.6 ± 0.7	22.5 ± 0.5
TC (mg/dl)	1493 ± 49	1362 ± 93
TG (mg/dl)	863 ± 85	777 ± 81
Serum antibody titers		
Total IgM (mg/ml)	0.97 ± 0.11	0.85 ± 0.11
Total IgG1 (mg/ml)	1.11 ± 0.10	0.97 ± 0.11
Total IgG2c (mg/ml)	1.84 ± 0.16	1.58 ± 0.16
Serum chemokines		
CCL2/MCP-1 (pg/ml)	59.1 ± 8.3	69.3 ± 8.1
CXCL1/KC (pg/ml)	1709 ± 247	1535 ± 181
Characterization of PEC[a]		
Total Peritoneal cells (x10^6)	3.38 ± 0.52	2.22 ± 0.29
CD5$^+$ T-cells (% of total)	20.40 ± 3.74	15.25 ± 2.71
CD11b$^+$ Mac cells (% of total)	13.96 ± 2.16	18.78 ± 2.32
CD19$^+$ B-cells (% of total)	53.25 ± 3.43	51.84 ± 3.29
CD11b$^+$CD5$^+$ B1a-cells (% of B-cells)	27.24 ± 2.71	24.56 ± 3.29
CD11b$^+$CD5$^-$ B1b-cells (% of B-cells)	16.95 ± 1.35	19.37 ± 1.47
CD19$^+$CD23$^+$ B2-cells (% of B-cells)	28.43 ± 3.39	32.69 ± 3.68
Characterization of PBC[b]		
Total White blood cells/ml (x10^6)	1.40 ± 0.18	1.59 ± 0.25
CD11b$^+$ Ly6C^{lo} monocytes (% of total)	4.11 ± 0.34	4.96 ± 0.43
CD11b$^+$ Ly6C^{hi} monocytes (% of total)	2.59 ± 0.36	2.15 ± 0.36
CD11b$^+$ Ly6G$^+$ neutrophils (% of total)	3.97 ± 0.46	4.51 ± 0.65
Characterization of splenocytes[c]		
Total Spleen cells (x10^6)	67.3 ± 11.3	62.3 ± 9.4
CD43$^+$ T-cells (% of total)	24.83 ± 2.26	23.39 ± 1.42
B220$^+$ B-cells (% of total)	45.35 ± 3.32	46.67 ± 1.92
CD43$^+$IgM$^+$ B1-cells (% of B-cells)	16.29 ± 1.27	17.16 ± 1.22
CD43$^-$IgM$^+$ B2-cells (% of B-cells)	81.76 ± 1.21	80.97 ± 1.19

Atherosclerosis in the aortic origin was analyzed by cross-sections through the aortic origin and values represent the average µm^2/section. *En face* measurements are given in percent lesion area of the entire aorta. TC, total serum cholesterol; TG, serum triglycerides; PEC, peritoneal exudate cells; PBC, peripheral blood cells. Cellular populations in [a]PEC, [b]PBC and [c]Splenocytes were analyzed by flow cytometry. Data are mean ± SEM.

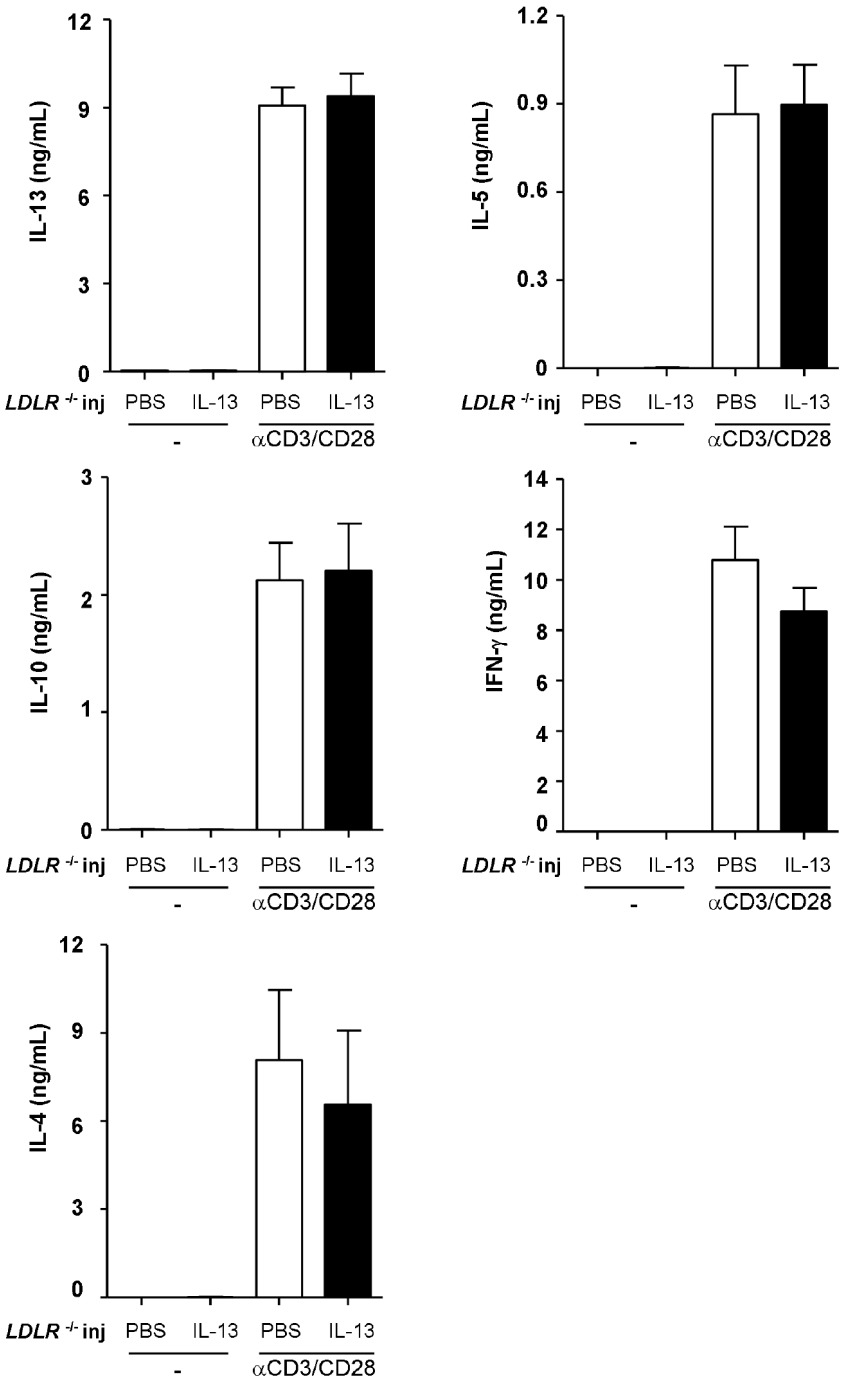

Fig 6: IL-13 administration does not alter cytokine production by splenic T-cells. *LDLR*$^{-/-}$ mice were fed an atherogenic diet for 16 weeks and received biweekly intraperitoneal injections with PBS (n=11) or IL-13 (n=13) during the last 5 weeks. At time of sacrifice spleens were collected from all mice and splenocytes stimulated with or without anti-CD3/CD28 *in vitro*. *LDLR*$^{-/-}$ mice from both groups show similar production of Th2 (IL-13, IL-5, IL-4 and IL-10) and Th1 (IFN-γ) cytokines. Data are presented as mean ± SEM ng/ml individual cytokines of splenocyte cultures of all mice of each group.

As expected with the relatively short time of administration only during the last 5 weeks of a 16-week feeding period, there were no differences in the extent of atherosclerosis in the cross-sectional analyses of the aortic origin or in the entire aorta by *en face* analyses between atherosclerotic *LDLR*$^{-/-}$ mice treated with PBS or IL-13, respectively (Figure 7A and Table III).

As lesion size was similar between the two groups, I was able to directly compare lesion composition. Morphological analyses of the cross-sectional lesions showed no significant differences in the necrotic core area, suggesting that both groups of mice had the same stage of lesion development (Figure 7B). In contrast, the collagen content was significantly higher in atherosclerotic *LDLR*$^{-/-}$ mice treated with IL-13 compared to PBS treated mice (Figure 7C), while the smooth-muscle cells content remained unchanged between the groups (Figure 7D). These results suggest that IL-13 injections stimulated the production of collagen by either macrophages or smooth-muscle cell rather than the proliferation of these cells, consistent with the pro-fibrotic function of IL-13.

Remarkably, immunohistological analyses of mac-3^{+} macrophages uncovered a significant reduction in lesional macrophages in the IL-13 treated mice (Figure 7E). These differences in macrophage content were not due to changes in circulating blood cell counts, as total numbers of white blood cells, monocytes (both classical Ly6C^{hi} and nonclassical Ly6C^{lo}) or neutrophils in the peripheral blood of mice were similar (Table III). Moreover, the plasma levels of CCL2/MCP-1 and CXCL1/KC, the two major chemokines involved in monocyte recruitment, were not reduced in IL-13 injected mice (Table III). In addition, the numbers of lesional T-cells were not different between the two groups (Figure 7F).

Taken together, our data showed that IL-13 modulates established atherosclerotic lesions by inducing a more stable plaque composition with higher collagen content and fewer macrophages.

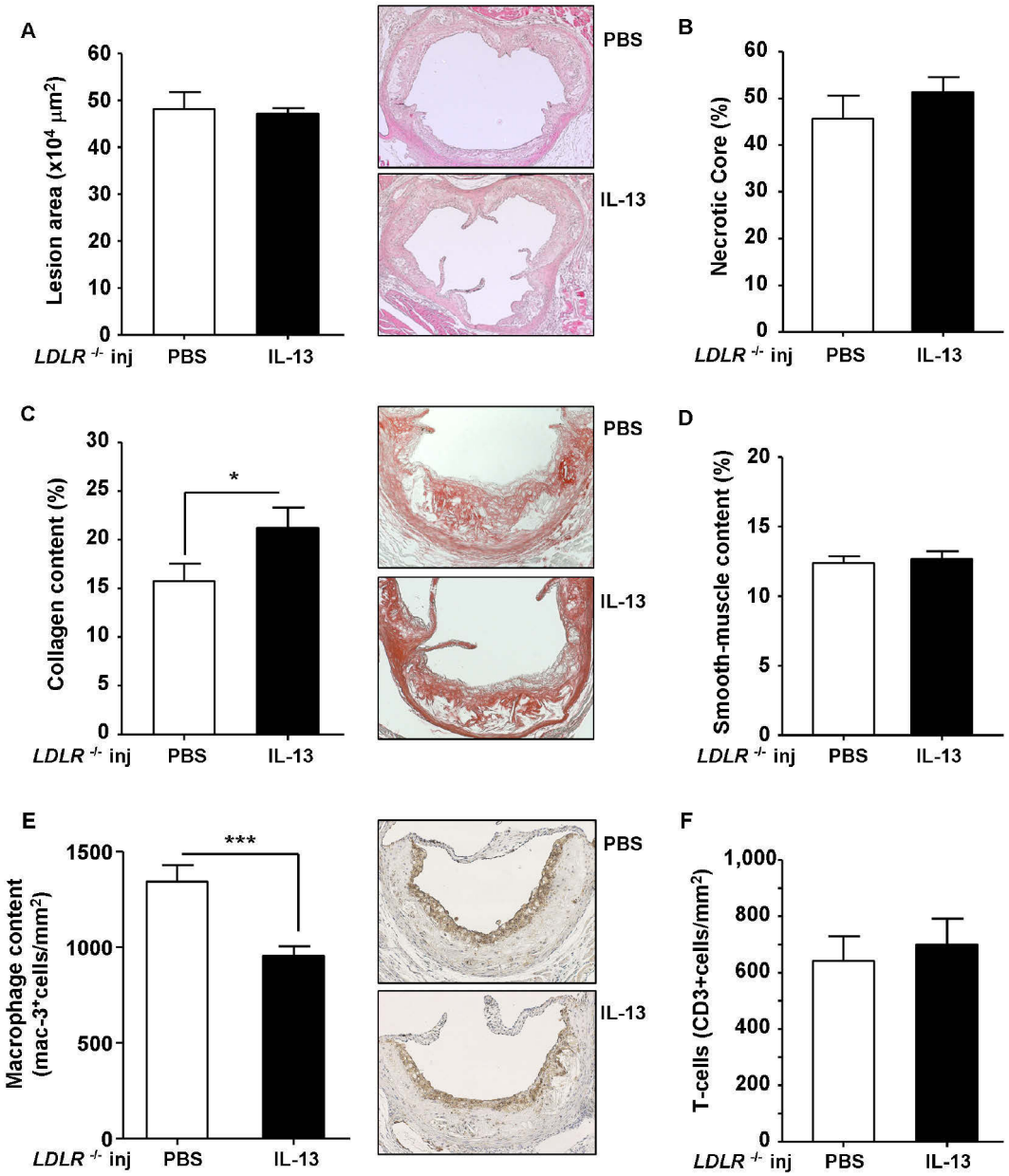

Fig 7: IL-13 administration alters the plaque phenotype of established atherosclerotic lesions. *LDLR*$^{-/-}$ mice were fed an atherogenic diet for 16 weeks and received biweekly intraperitoneal injections with PBS (n=11) or IL-13 (n=13) during the last 5 weeks. **(A)** Equal extent of atherosclerotic lesion size in cross-sections of the aortic origin in injected *LDLR*$^{-/-}$ mice. Values represent the average µm^2/section. **(B)** Equal necrotic core area in lesions of injected *LDLR*$^{-/-}$ mice. Values represent percentages of necrotic core area/total lesion area. **(C)** Increased collagen content in lesions of *LDLR*$^{-/-}$ mice injected with IL-13. Sections were stained with Sirius Red for the presence of collagen, and values represent the percentages of Sirius Red$^+$ area/total lesion area (*p<0.05). **(D)** Equal smooth-muscle cell content in lesions of injected *LDLR*$^{-/-}$ mice. Sections were stained with an anti-smooth-muscle cells actin specific antibody, and values represent the percentages of smooth-muscle actin$^+$ area/total lesion area. **(E)** Decreased macrophage content in lesions of *LDLR*$^{-/-}$ mice injected with IL-13. Sections were stained with the macrophage specific anti-mac-3 antibody and values represent the numbers of mac-3$^+$ cells/mm^2 of total lesion area (***p<0.001). **(F)**. Equal numbers of T-cells in the lesions of injected *LDLR*$^{-/-}$ mice. Sections were stained with a T-cell specific anti-CD3 antibody, and values

represent the numbers of $CD3^+$ cells/mm^2 of total lesion area. All data are mean ± SEM values of all mice of each group. Images show representative examples of the respective stainings. Original magnification: 50x (A), 100x (C, E).

5.2. IL-13 administration reduces macrophage content in lesions of atherosclerotic *ApoE*$^{-/-}$ mice, independent of macrophage egress.

The observed morphological changes of atherosclerotic lesions following IL-13 administration suggested the possibility of macrophage egression.

Because CCR7 has been implicated as a key chemokine receptor in this process, I first evaluated CCR7 expression in lesions of the cholesterol-fed *LDLR*$^{-/-}$ mice that were treated with either IL-13 or PBS, respectively. There was no significant difference in the percentage of $CCR7^+$ lesion area between the two groups, suggesting no major contribution of CCR7-mediated emigration (Figure 8).

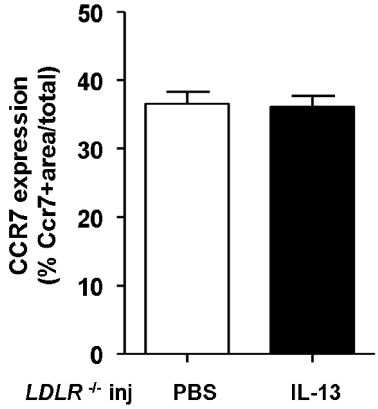

Fig 8: Equal expression of CCR7 in atherosclerotic lesions of injected *LDLR*$^{-/-}$ mice. *LDLR*$^{-/-}$ mice were fed an atherogenic diet for 16 weeks and received biweekly intraperitoneal injections with PBS (n=11) or IL-13 (n=13) during the last 5 weeks. CCR7 expression was assessed in lesions of injected *LDLR*$^{-/-}$ mice by immunohistochemistry. Values represent the percentages of $CCR7^+$ area/total lesion area. All data are mean ± SEM values of all mice of each group.

We then directly evaluated the ability of IL-13 to induce macrophage egress from existing lesions using a method that is based on the tracking of fluorescent bead-labeled monocyte/macrophages in *ApoE*$^{-/-}$ mice (Potteaux et al, 2011). To achieve comparable

lesion development in these mice, they were fed an atherogenic diet for a total of 6 weeks and received PBS or IL-13 during the last 2 weeks of diet. Following depletion of monocyte/macrophages by clodronate-liposome injection 20 days after initiation of the atherogenic diet, circulating monocytes were labeled with latex-beads to monitor lesional macrophage migration. At day 28, one third of mice were sacrificed to obtain a baseline number of beads per plaque area in the aortic root. The other mice were divided into two groups and received biweekly injections of either IL-13 or PBS, respectively, for the remaining two weeks (Figure 9A).

At time of sacrifice, cross-sections of the aortic origin were analyzed for the presence of fluorescent beads as well as mac-2^+ cells. The numbers of beads per plaque area at week 6 were not different between PBS- and IL-13-injected animals and comparable to the numbers at baseline (week 4), indicating that IL-13 had no effect on macrophage egression (Figure 9B). Nevertheless, macrophage content of the same lesions was significantly lower in IL-13-injected mice compared to PBS-injected mice, thereby confirming our initial observation in a different atherosclerosis-prone mouse strain (Figure 9C).

Thus, IL-13 limits lesional macrophage content by a mechanism other than macrophage emigration.

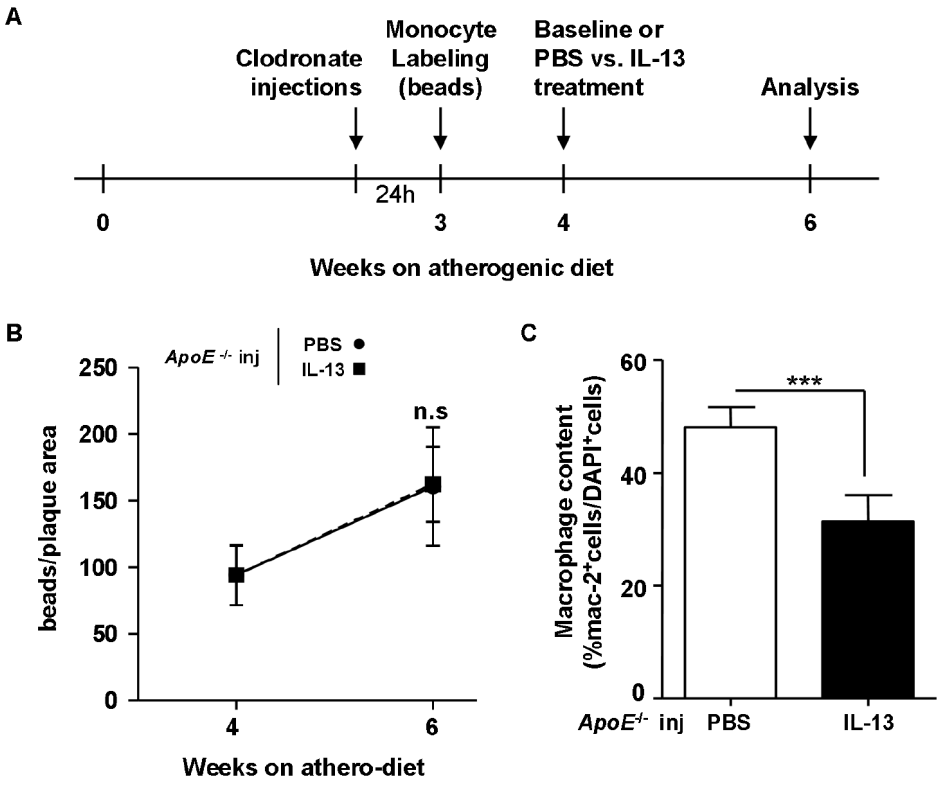

Fig 9: IL-13 administration has no effect on macrophage egress from established atherosclerotic lesions. *ApoE*$^{-/-}$ mice were fed an atherogenic diet for 4 weeks (baseline) or 6 weeks (PBS and IL-13, respectively). After 3 weeks, circulating monocytes of all mice were labeled with fluorescent-latex beads following clodronate-liposome depletion 24h before. One week later, one group of mice was sacrificed for baseline (n=7) measurements of bead and macrophage content and the remaining mice received biweekly intraperitoneal injections with either PBS (n=7) or IL-13 (n=8) until sacrifice. **(A)** Diagram of experimental design. **(B)** Similar content of fluorescent beads per plaque area in the aortic root of PBS and IL-13 administration respectively compared to baseline. **(C)** Decreased macrophage content in lesions of *ApoE*$^{-/-}$ mice injected with IL-13. Sections were stained with the macrophage specific anti-mac-2 antibody and values represent the percentages of mac-2^{+} cells/total DAPI^{+} cells (***$p<0.001$). All data are mean ± SEM values of all mice of each group.

5.3. IL-13 administration results in decreased monocyte adhesion and VCAM-1 expression in lesions of atherosclerotic ApoE$^{-/-}$ mice in vivo.

To explain the decreased numbers of macrophages in atherosclerotic lesions despite unchanged peripheral blood monocyte counts, similar plasma levels of important chemokines, and no effect on macrophage egression, I hypothesized that IL-13 reduced the recruitment and monocyte adhesion to the atherosclerotic wall.

To elucidate this directly, we assessed the adhesion of different leukocyte populations by intravital microscopy of carotid arteries of *Cx$_3$cr1*$^{gfp/wt}$ mice that were available on an *ApoE*$^{-/-}$ background. Mice were fed an atherogenic diet for a total of 6 weeks and received PBS or IL-13 during the last 2 weeks of diet. Following injection of a fluorescent antibody to GR1 (Ly6C/G), this animal model enabled us to differentiate, at the same time, between the adhesion of two subtypes of circulating monocytes (nonclassical Gr1$^-$ Cx$_3$cr1^{higfp} and classical Gr1$^+$ Cx$_3$cr1^{logfp}) and neutrophils (Gr1$^+$ gfp$^-$).

Indeed, the adhesion of circulating monocytes to carotid arteries was significantly decreased in atherosclerotic mice injected with IL-13 compared to PBS treated mice (Fig 5), whereas adhesion of circulating neutrophils was similar (Figure 10). In addition, the adhesion of the two monocyte subsets was equally reduced (data not shown), suggesting that IL-13 administration reduces monocyte recruitment through a common pathway.

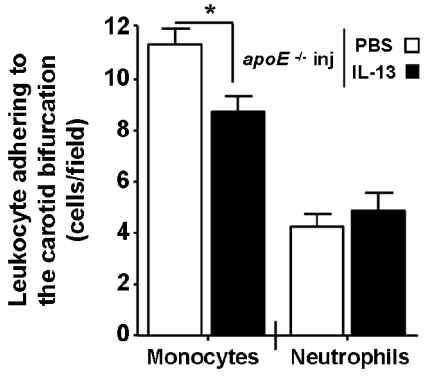

Fig 10: IL-13 administration reduces monocyte adhesion in established atherosclerotic lesions. *Cx3cr1*$^{gfp/wt}$ *ApoE*$^{-/-}$ mice were fed an atherogenic diet for 6 weeks and received biweekly intraperitoneal injections with PBS (n=8) or IL-13 (n=8) during the last 2 weeks. At time of sacrifice, PE-conjugated anti-GR1 antibodies were injected intravenously and the number of monocytes (GFP cells) and neutrophils (PE+ cells) adhering to the carotid bifurcation was

assessed by intravital microscopy. Values represent the numbers of cells/optical field (*p<0.05). All data are mean ± SEM values of all mice of each group

Thus, I hypothesized that IL-13-induced changes may result in decreased endothelial cell activation. To test this, we performed intravital microscopy of carotid arteries of *ApoE*$^{-/-}$ mice that were fed an atherogenic diet for a total of 6 weeks and received PBS or IL-13 during the last 2 weeks of diet, followed by the injection of fluorescently labeled beads coupled with anti-VCAM-1 antibody or anti-CCL2 antibody to analyze the carotid endothelial activation state in these mice. VCAM-1 expression was significantly decreased in IL-13 treated mice (Figure 11A), whereas the expression of CCL2 was similar in both groups (Figure 11B).

These data strongly suggest that the decrease in lesional macrophage content observed in IL-13-treated mice is caused by a reduction in the VCAM-1-dependent monocyte recruitment.

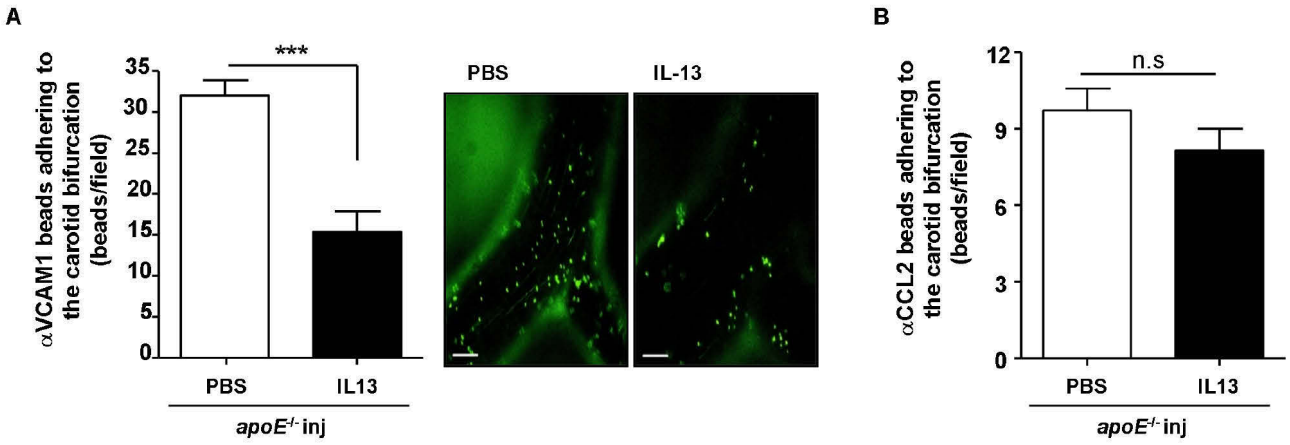

Fig 11: IL-13 administration reduces VCAM-1 expression, but not CCL2 in established atherosclerotic lesions. *ApoE*$^{-/-}$ mice were fed an atherogenic diet for 6 weeks and received biweekly intraperitoneal injections with PBS (n=8) or IL-13 (n=8) during the last 2 weeks. At time of sacrifice, fluorescent anti-VCAM-1 beads **(A)** or fluorescent anti-CCL2 beads **(B)** were injected intravenously and the number of beads adhering to the carotid bifurcation was assessed by intravital microscopy. Values represent the numbers of beads/optical field (***p<0.001). All data are mean ± SEM values of all mice of each group. **(A)** Representative microscopy images are shown. Bar: 100 µm.

5.4. IL-13 administration skews macrophage phenotype towards alternatively activated macrophages (M2) in vivo.

Because IL-13 is known to induce alternative macrophage differentiation, I investigated whether IL-13 administration had the capacity to generate M2 macrophages *in vivo*.

Indeed, I observed a shift within the macrophage population towards more $CD206^+$ macrophages (M2) and less $CD80^+$ macrophages (M1) in the peritoneal cavities of IL-13 treated-mice, as assessed by flow cytometry (Figure 12A) and further confirmed by quantitative PCR, demonstrating a significant up-regulation of common M2-related genes, including Arginase-1 (Arg-1), chitinase 3-like 3 protein (Chi3l3/Ym-1) and CCL9, and a concomitant down-regulation of M1-related genes such as inducible nitric oxide synthase (iNOS), CD86 and CXCL10 (Figure 12B). The total numbers of peritoneal macrophages, T- and B-cells (including B1- and B2-cells) were not different between the two groups (Table III).

Importantly, in analogy to the activation state of peritoneal macrophages, immunostaining of lesional macrophages for the expression of iNOS demonstrated fewer M1 macrophages in lesions of IL-13 injected mice (Figure 13A). Moreover, immunostaining for the expression of two different M2 markers, Ym-1 and mannose receptor (MR, CD206), demonstrated significantly higher numbers of M2 macrophages in lesions of IL-13 injected mice, despite an overall decreased macrophage content (Figure 13B and 13C, respectively).

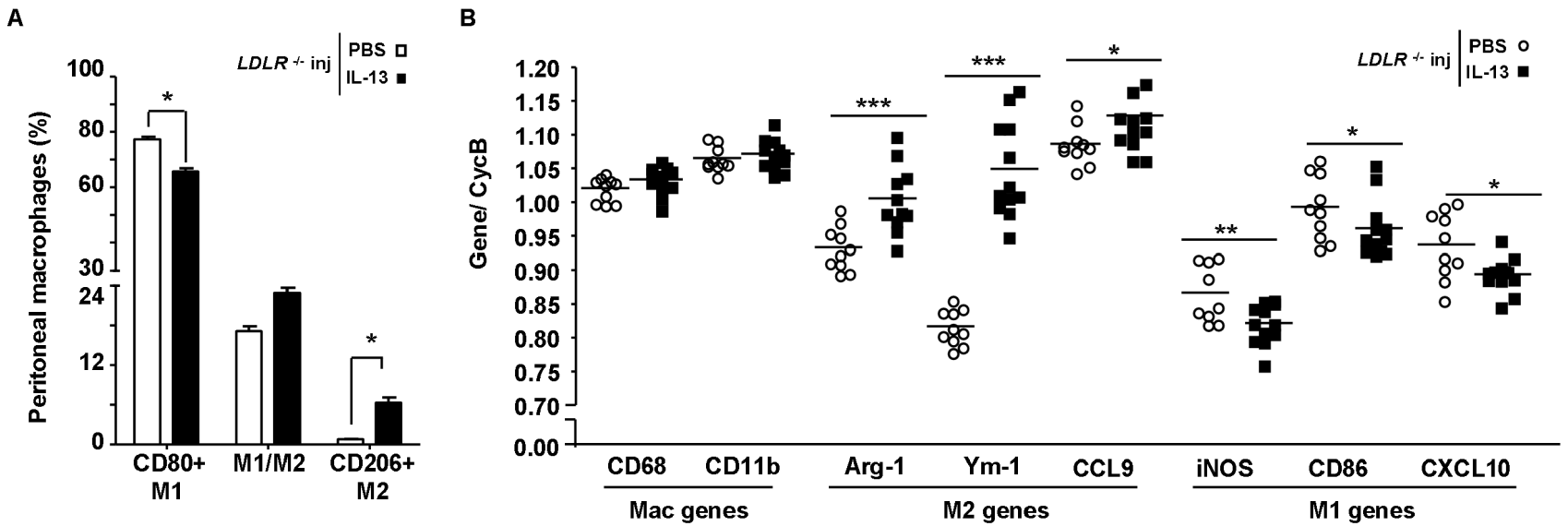

Fig 12: IL-13 administration skews peritoneal macrophage phenotype towards alternatively activated (M2) macrophages *in vivo*. *LDLR*$^{-/-}$ mice were fed an atherogenic diet for 16 weeks and received biweekly intraperitoneal injections with PBS (n=11) or IL-13 (n=13) during the last 5 weeks. **(A)** Increased frequencies of M2 macrophages and decreased frequencies of M1 macrophages in the peritoneal cavity of *LDLR*$^{-/-}$ mice injected with IL-13. Peritoneal cells were stained with antibodies against CD80 and CD206 and identified by flow cytometry as M1 and M2 macrophages, respectively. CD80/CD206 double positive cells were classified as M1/M2 macrophages. Values represent the percentages of individual macrophage subtypes/total macrophages (*$p<0.05$). All data are mean ± SEM values of all mice of each group. **(B)** Increased expression of M2 genes and decreased expression of M1 genes in the peritoneal cavity of *LDLR*$^{-/-}$ mice injected with IL-13. The expression of indicated genes was assessed in total peritoneal cells by quantitative RT-PCR. Data were normalized to CycB expression. Symbols indicate the normalized expression levels of individual mice, and horizontal bars indicate means of each group (*$p<0.05$, **$p<0.01$, ***$p<0.001$).

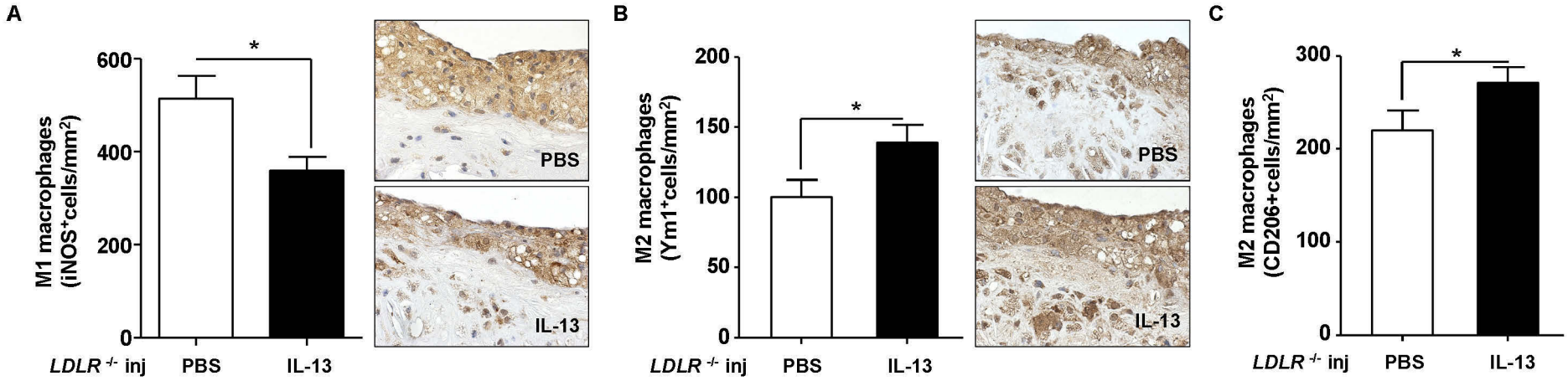

Fig 13: IL-13 administration skews lesional macrophage phenotype towards alternatively activated (M2) macrophages *in vivo*. *LDLR*$^{-/-}$ mice were fed an atherogenic diet for 16 weeks and received biweekly intraperitoneal injections with PBS (n=11) or IL-13 (n=13) during the last 5 weeks. **(A)** Decreased M1 macrophages in lesions of *LDLR*$^{-/-}$ mice injected with IL-13. Sections were stained with an antibody against iNOS, which is specifically expressed by M1 macrophages and values represent the numbers of iNOS^{+} cells/mm^{2} of total lesion area (*p<0.05). **(B-C)** Increased M2 macrophages in lesions of *LDLR*$^{-/-}$ mice injected with IL-13. Sections were stained with an antibody against Ym-1 **(B)** and CD206 **(C)**, which are specifically expressed by M2 macrophages. Values represent the numbers of M2^{+} cells/mm^{2} of total lesion area (*p<0.05). All data are mean ± SEM values of all mice of each group. Images show representative examples of iNOS **(A)** and Ym-1 **(B)** staining. Original magnification: 400x.

These changes in macrophage activation states resulted in a significantly increased M2:M1 ratio in lesions of IL-13-treated mice (Figure 14A). Of note, the changed M2:M1 ratio seems to be mainly a result of an absolute and relative increased induction of M2 macrophages (Figure 14B), as the relative ratio of M1 macrophages to total macrophages did not change (Figure 14C).

In summary, I showed for the first time that exogenous administration of IL-13 induces alternatively activation of lesional macrophages during the course of atherosclerosis development and furthermore I could demonstrate that the decreased lesional macrophage content was paralleled by the induction of M2 macrophages and concomitantly the reduction of M1 macrophages in atherosclerotic lesions.

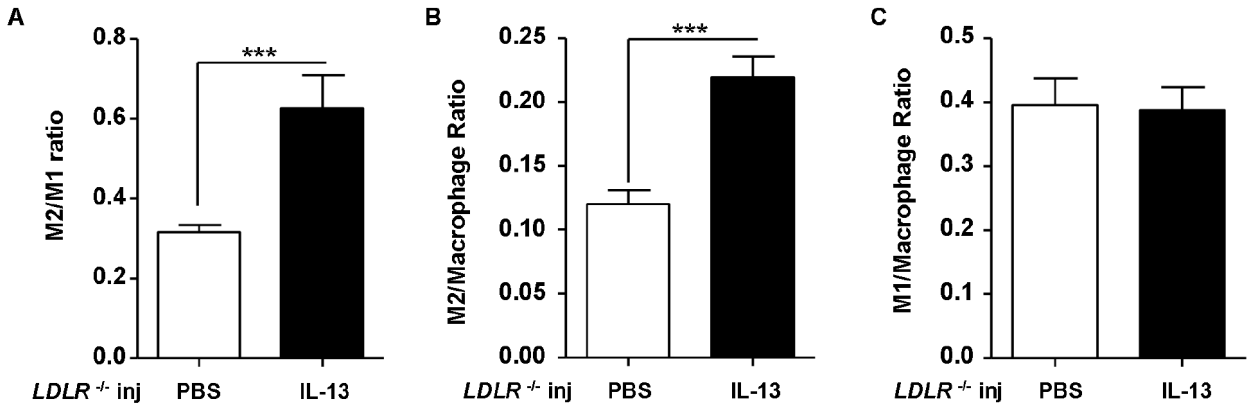

Fig 14: Increased ratio towards alternatively activated (M2) macrophages in lesions of *LDLR*$^{-/-}$ mice injected with IL-13. *LDLR*$^{-/-}$ mice were fed an atherogenic diet for 16 weeks and received biweekly intraperitoneal injections with PBS (n=11) or IL-13 (n=13) during the last 5 weeks. The ratio between M2:M1 macrophages **(A)**, M2:total macrophages **(B)**, and M1:total macrophages **(C)** was assessed in lesions of injected *LDLR*$^{-/-}$ mice. All data are mean ± SEM values of all mice of each group (***$p<0.001$).

5.5. Alternatively activated macrophages by IL-13 show higher clearance of OxLDL in vitro.

To study potential effects of differentially activated macrophages in atherogenesis, I evaluated the ability of IFN-γ and IL-13 to modulate macrophage foam cell formation by promoting either classical (M1) or alternative (M2) macrophage activation, respectively.

Thioglycollate-elicited macrophages were stimulated with either IFN-γ or IL-13, and successful differentiation into M1 or M2 macrophages was confirmed by the expression of iNOS (M1) and Arg-1 (M2), respectively (Figure 15).

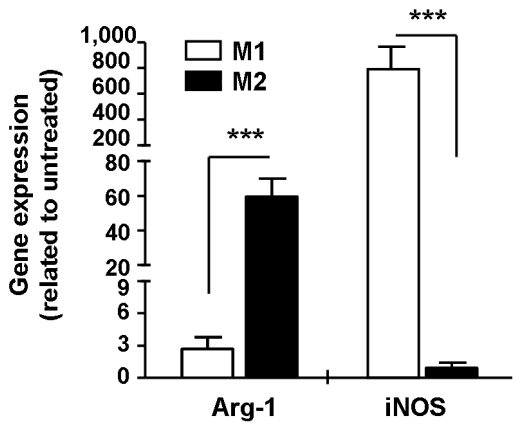

Fig 15: Differentially activated macrophages *in vitro*. Thioglycollate-elicited macrophages were differentiated with IFN-γ or IL-13 into classically (M1) or alternatively (M2), respectively. The expression of Arginase-1 (Arg-1) and iNOS was analyzed by quantitative RT-PCR. Data were normalized to CycB expression and values represent fold increased expression over untreated cells. Data are mean ± SEM of two independent experiments performed in triplicates (***$p<0.001$).

Differentially activated macrophages were then incubated with copper-oxidized LDL (CuOx-LDL) to induce foam cell formation. Subsequent analyses of these cells revealed an increase of total cellular cholesterol content in foam cell cultures derived from IFN-γ stimulated macrophages and to a significantly greater extent in macrophages stimulated with IL-13 (Figure 16A). An increased uptake of CuOx-LDL was further confirmed by Oil Red O (ORO) staining, which revealed a higher percentage of ORO^+ cells in IL-13-activated macrophages compared to IFN-γ-activated macrophages (Figure 16B). Consistent with that, IL-13 stimulation resulted in increased expression of the scavenger receptor CD36, which was further induced after CuOx-LDL loading (Figure 16C). The expression of scavenger receptor A-1 (SRA-1) and LOX-1 was not different between the two differentially activated macrophage foam cells (Figure 16D and 16E). Addition of high density lipoproteins (HDL) to the foam cell cultures significantly reduced the increased cellular cholesterol only in IL-13-activated macrophage cultures, thereby abrogating the increased foam cell formation (Figure 16A). These data suggested a

higher cholesterol efflux capacity of IL-13-activated compared to IFN-γ-activated foam cells.

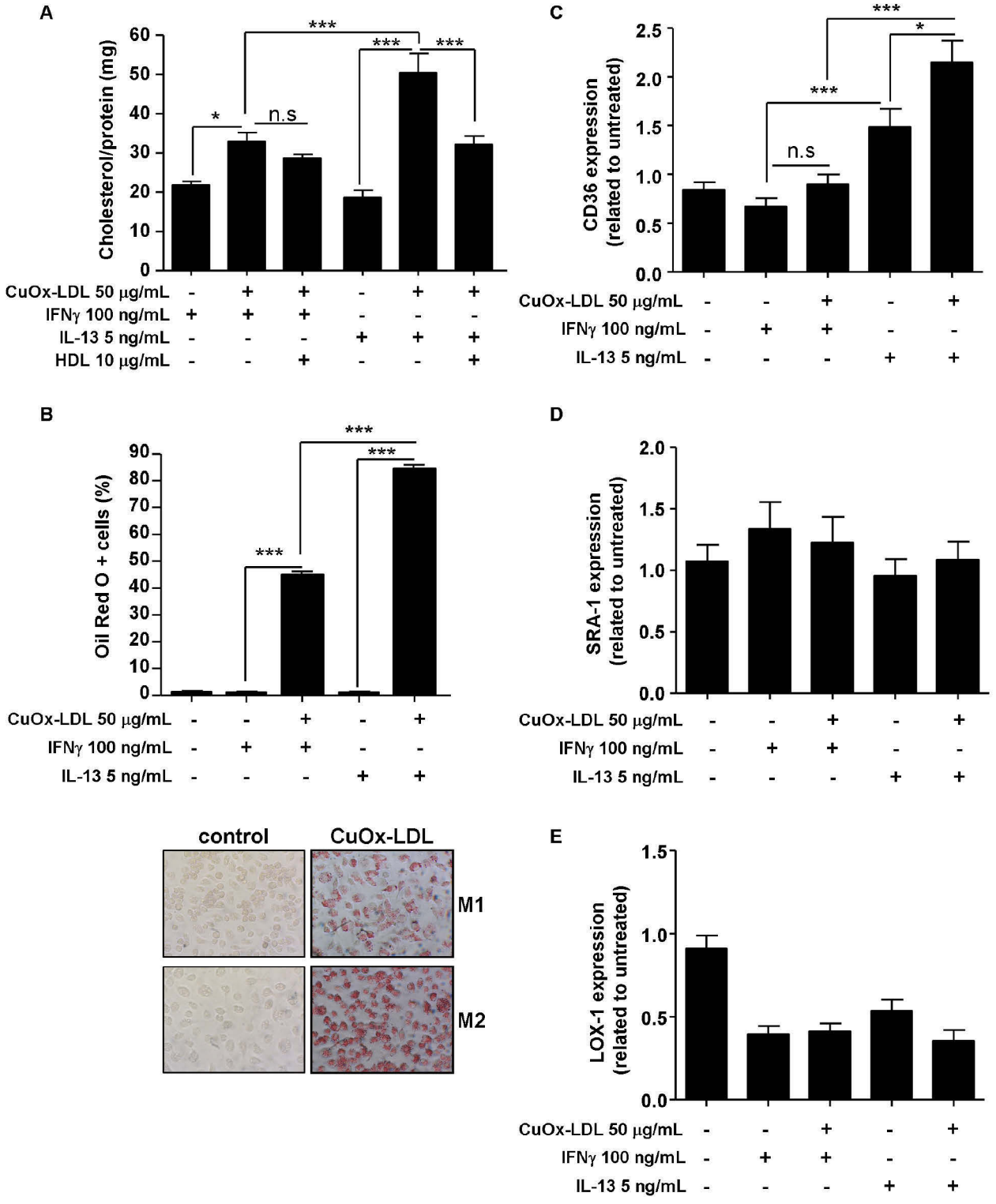

Fig 16: Increased foam cell formation in alternatively activated macrophages (M2) *in vitro*. Thioglycollate-elicited macrophages were differentiated with IFN-γ or IL-13 into classically (M1) or alternatively (M2), respectively, and then incubated with CuOx-LDL for 24h to generate

foam cells. **(A)** Increased cellular cholesterol levels in M2-derived foam cells are reduced in the presence of HDL. M1 and M2 macrophages were incubated with CuOx-LDL in the absence or presence of HDL 10 μg/ml. Lipids were extracted from cell lysates and total cholesterol and protein were measured. Data are mean ± SEM values of two independent experiments performed in quadruplicates and represent mg cholesterol/mg protein (*p<0.05, ***p<0.001). **(B)** Increased lipid uptake in M2-derived foam cells**.** Foam cells were stained with Oil Red O (ORO) and the percentages of ORO^+ cells/total cells were quantified. All data are mean ± SEM values of two experiments performed in quadruplicates (***p<0.001). Images show representative examples of ORO stain. Original magnification: 200x. The expression of **(C)** CD36, **(D)** SRA-1 and **(E)** LOX-1 was analyzed by quantitative RT-PCR. Data were normalized to CycB expression and values represent fold increased expression over untreated cells. Data are mean ± SEM of three independent experiments performed in triplicates (*p<0.05, ***p<0.001).

To further test this hypothesis, I performed *in vitro* cholesterol efflux assays using equal amounts of [^{3}H]-cholesterol, which demonstrated a significantly higher HDL-dependent efflux of foam cell cultures derived from IL-13 stimulated macrophages compared to IFN-γ stimulated macrophages (Figure 17A). Moreover, to evaluate the ability of IL-13 to directly increase cholesterol efflux in macrophage foam cells, macrophages were first loaded with CuOx-LDL plus [^{3}H]-cholesterol and then stimulated with IFN-γ and IL-13, respectively. Importantly, HDL-dependent efflux was significantly increased in IL-13 stimulated foam cells using this experimental setup as well (Figure 17B).

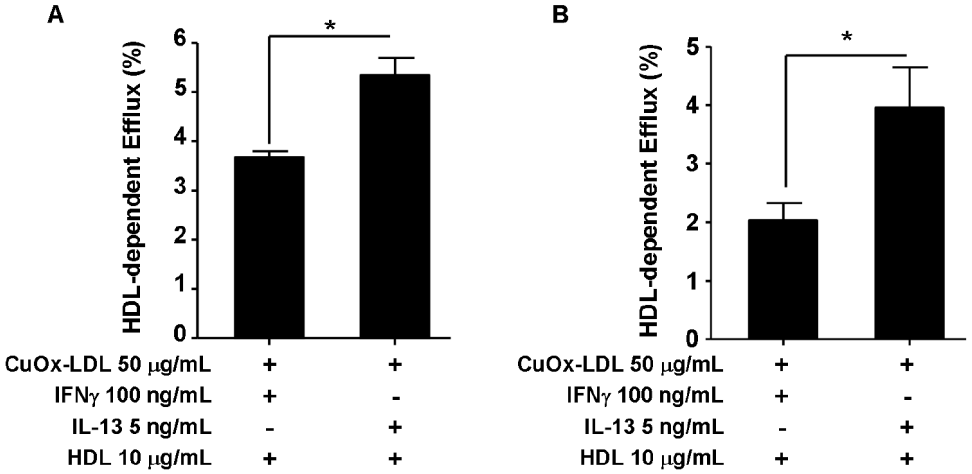

Fig 17: Increased cholesterol efflux by IL-13 stimulation *in vitro*. (A) Increased HDL-dependent cholesterol efflux by M2-derived foam cells. Thioglycollate-elicited macrophages were stimulated with IFN-γ or IL-13 into classically (M1) or alternatively (M2) activated macrophages, respectively, and then incubated with CuOx-LDL plus 1 μCi of [^{3}H]-cholesterol.

(B) Increased HDL-dependent cholesterol efflux by foam cells stimulated with IL-13. Thioglycollate-elicited macrophages were incubated with CuOx-LDL plus 1 μCi of [^{3}H]-cholesterol for 24 hours and then stimulated with IFN-γ or IL-13 into classically (M1) or alternatively (M2) activated macrophage/foam cells, respectively. Subsequently, HDL-dependent efflux was assayed as described in Methods. Data represent percentages of HDL-dependent efflux/total efflux (*$p<0.05$). Data are mean ± SEM of three independent experiments performed in triplicates.

I therefore investigated the expression levels of the two most important receptors responsible for cholesterol efflux in macrophages, ATP-binding cassette A1 (ABCA1) and G1 (ABCG1) by immunoblotting, and found that upon stimulation with CuOx-LDL the expression of both ABC transporters was significantly up-regulated in foam cells derived from IL-13-activated macrophages compared to IFN-γ-activated foam cells (Figure 18A-C) and non-activated foam cells (data not shown). This was also confirmed by quantitative PCR on the mRNA level (Figure 18D and 18E). In contrast, IFN-γ-activated macrophages exhibited only a significant up-regulation of ABCG1 protein following CuOx-LDL stimulation, albeit to a lesser degree than IL-13 activated macrophages (Figure 18C). Consistent with that, IL-13 stimulation also resulted in the increased expression of the nuclear receptor LXRα, which is the main transcription factor controlling ABCA1 and G1 expression (Figure 18F).

To correlate these *in vitro* findings with effects of IL-13 on macrophage function *in vivo*, lesions of cholesterol-fed *LDLR*$^{-/-}$ mice that received either IL-13 or PBS (See Figure 7), were analyzed for ABCA1 expression by immunohistochemistry. Remarkably, atherosclerotic lesions of IL-13- treated mice showed a significantly higher number of ABCA1 expressing cells compared to lesions from control mice (Figure 19).

Taken together, our data demonstrate that macrophages alternatively activated by IL-13 have an overall increased capacity of OxLDL clearance, as they display increased uptake as well as increased cholesterol efflux capacities without enhancing foam cell formation. This should result in a more efficient removal of pro-inflammatory OxLDL and consequently a less inflammatory environment in atherosclerotic lesions.

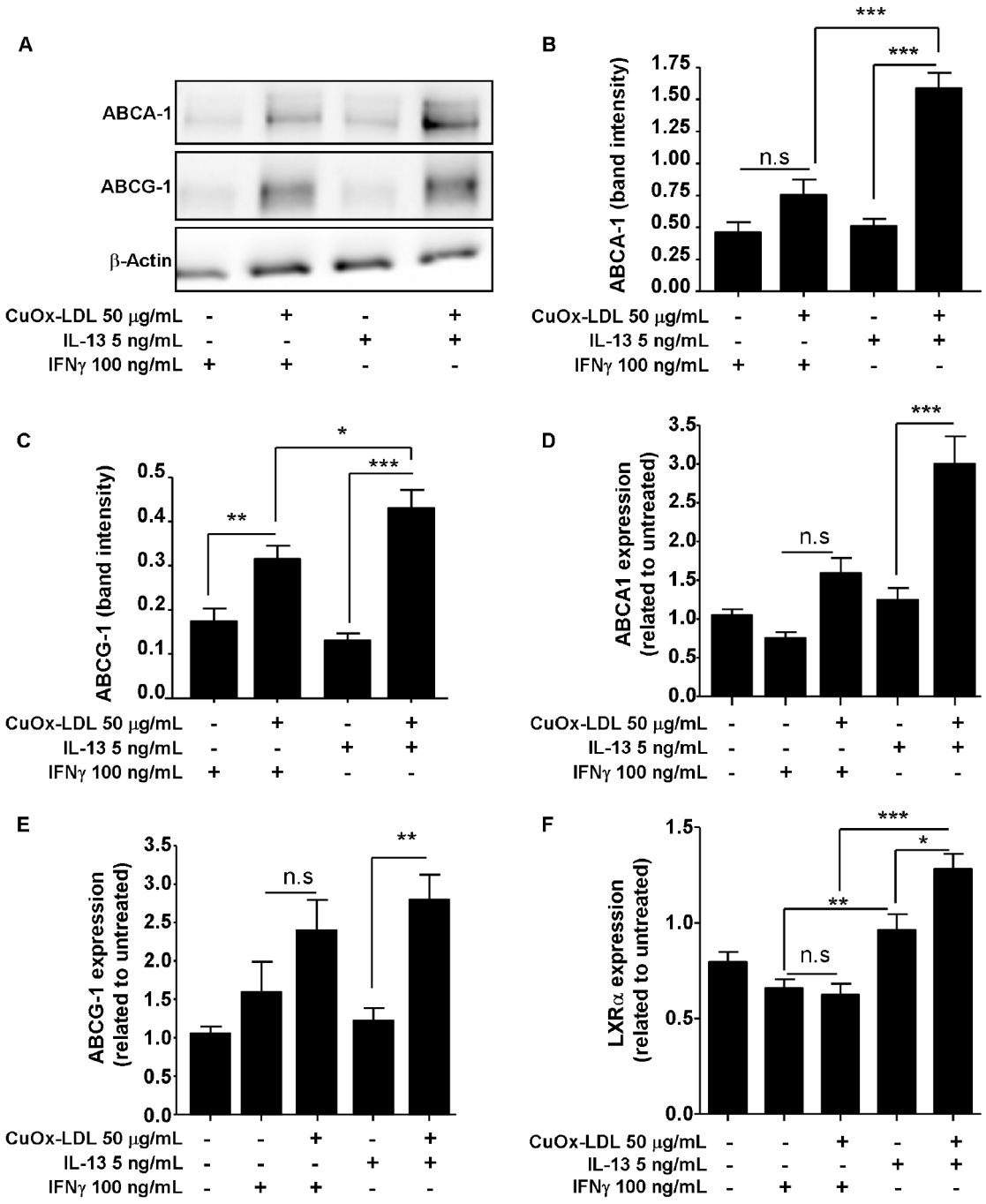

Fig 18: Increased cholesterol efflux machinery in M2-derived foam cells. Thioglycollate-elicited macrophages were differentiated with IFN-γ or IL-13 into classically (M1) or alternatively (M2), respectively, and then incubated with CuOx-LDL for 24h to generate foam cells. **(A-C)** Increased ABCA1 and ABCG1 expression in M2-derived foam cells. **(A)** Shown is a representative Western blot for the presence of ABCA1, ABCG1, and β-actin in lysates of cells that were treated as indicated. **(B-C)**The graphs show the quantification of the band intensity of **(B)** ABCA1 and **(C)** ABCG1 related to β-actin. The expression of **(D)** ABCA1 and **(E)** ABCG1, and **(F)** LXRα was analyzed by quantitative RT-PCR. Data were normalized to CycB expression and values represent fold increased expression over untreated cells. All data are mean ± SEM values of three independent experiments performed in triplicates (*$p<0.05$, **$p<0.01$, ***$p<0.001$).

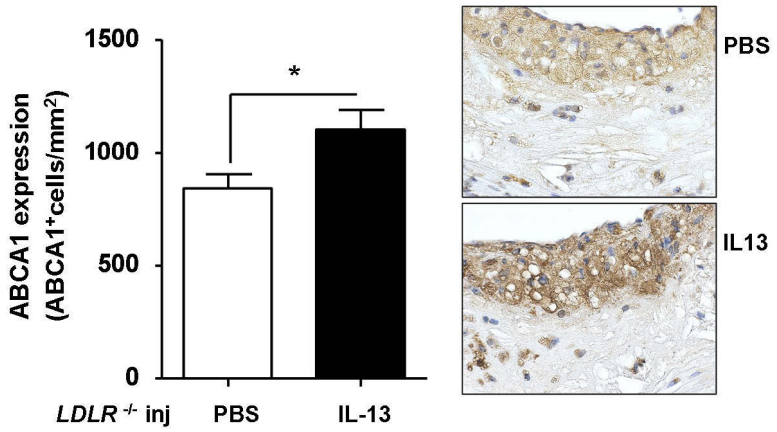

Fig 19: Increased ABCA1 expression in lesions of *LDLR*$^{-/-}$ mice injected with IL-13. *LDLR*$^{-/-}$ mice were fed an atherogenic diet for 16 weeks and received biweekly intraperitoneal injections with PBS (n=11) or IL-13 (n=13) during the last 5 weeks. Sections were stained with an antibody against ABCA1 and values represent the numbers of ABCA1^{+} cells/ mm^2 of total lesion area (*p<0.05). All data are mean ± SEM values of all mice of each group. Images show representative ABCA1 staining. Original magnification: 400x.

5.6. IL-13 deficiency accelerates atherosclerosis.

Finally, to demonstrate the role of IL-13 in the development of atherosclerotic lesions, I transplanted lethally irradiated *LDLR*$^{-/-}$ mice with bone marrow from either *IL-13*$^{+/+}$ or *IL-13*$^{-/-}$ mice. Four weeks after bone marrow transplantation (BMT) and successful replenishment, mice were switched to an atherogenic diet for the subsequent 16 weeks to induce atherosclerosis (Figure 20).

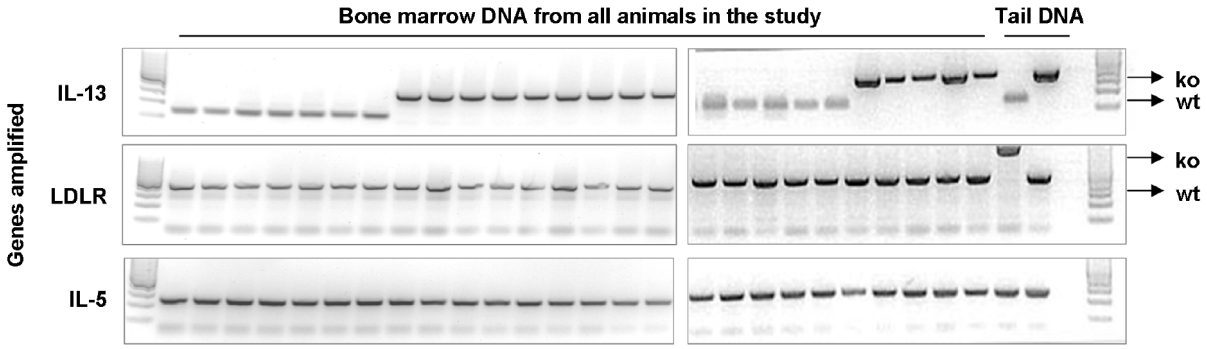

Fig 20: Successful bone marrow reconstitution in IL-13 chimeric mice. *LDLR*$^{-/-}$ mice were reconstituted with bone marrow cells isolated from either *IL-13*$^{+/+}$ mice (n=12) or *IL-13*$^{-/-}$ mice (n=14) and fed an atherogenic diet for 16 weeks. At time of sacrifice bone marrow cells were collected from all mice and genomic DNA extracted and amplified for IL-13, LDLR and IL-5

genes. Tail DNA from a *IL-13*$^{+/+}$, *IL-13*$^{-/-}$ and LDLR$^{-/-}$ mouse were used as positive and negative controls.

At time of sacrifice, the two groups of mice were not different regarding body weight, TC and TG levels (Table IV). Importantly, cross-sectional analyses of lesions in the aortic origin revealed significantly accelerated atherosclerosis with almost two times larger lesions in *IL-13*$^{-/-}$ bone marrow recipients, indicating a protective role of IL-13 in atherogenesis (Figure 21A). In addition, *en face* analyses also showed a trend towards increased lesion formation in recipients of *IL-13*$^{-/-}$ bone marrow (Table IV).

Lesions of *IL-13*$^{-/-}$ bone marrow chimeras displayed increased necrotic core formation, consistent with advanced plaque progression (Figure 21B). Nevertheless, the relative macrophage content was equivalent between the two groups (Figure 21C) with significantly less M2 macrophages in lesions of *IL-13*$^{-/-}$ bone marrow chimeras (Figure 21D). The predominant M1 macrophage areas were similar between the two groups (Figure 21E).

Table IV: Overview of experimental data of the bone marrow transplantation study.

	IL-13$^{+/+}$ → *LDLR*$^{-/-}$ (n=12)	*IL-13*$^{-/-}$ → *LDLR*$^{-/-}$ (n=14)
Atherosclerosis		
Aortic origin (10^4 µm^2/sect.)	11.44 ± 2.03	21.86 ± 2.38**
En face (% of aorta)	4.72 ± 0.78	7.00 ± 1.27
Metabolic parameters		
Weight (g)	29.4 ± 0.78	29.2 ± 0.47
TC (mg/dL)	788.2 ± 85.3	859.8 ± 46.9
TG (mg/dL)	591.2 ± 79.6	606.1 ± 57.4
Serum antibody titers		
Total IgM (mg/mL)	1.64 ± 0.15	1.64 ± 0.11
Total IgG1 (mg/mL)	2.37 ± 0.55	2.00 ± 0.50
Total IgG2c (mg/mL)	1.01 ± 0.14	1.55 ± 0.22*
Splenic cytokines^{A}		
IL-4 (ng/mL)	12.44 ± 2.33	2.20 ± 0.53***
IL-5 (ng/mL)	0.75 ± 0.03	0.91 ± 0.14
IL-10 (ng/mL)	6.66 ± 0.62	2.92 ± 0.35***
IL-13 (ng/mL)	33.68 ± 3.34	2.23 ± 0.12***
IFN-γ (ng/mL)	142.6 ± 4.55	135.0 ± 5.10
Characterization of splenocytes ^{B}		
Total Spleen cells (x10^6)	8.99 ± 0.56	9.89 ± 0.63
CD43$^+$ T-cells (% of total)	22.05 ± 0.51	22.46 ± 0.55
CD220$^+$ B-cells (% of total)	58.14 ± 1.84	55.66 ± 1.61
CD43$^+$IgM$^+$ B1-cells (% of B-cells)	13.53 ± 1.18	14.70 ± 0.97
CD220$^+$IgM$^+$ B2-cells (% of B-cells)	84.47 ± 1.21	83.20 ± 0.93

Atherosclerosis in the aortic origin was analyzed by cross-sections through the aortic origin and values represent the average µm^2/section. *En face* measurements are given in percent lesion area of the aorta. TC, total serum cholesterol; TG, serum triglycerides. ^{A}Cytokine secretion in supernatants of splenocyte cultures following stimulation with anti-CD3/CD28. Cellular populations of ^{B}Splenocytes were analyzed by flow cytometry Values that are statistically different from the control group. ($^{*}p<0.05$; $^{**}p<0.01$; $^{***}p<0.001$). Data are mean ± SEM.

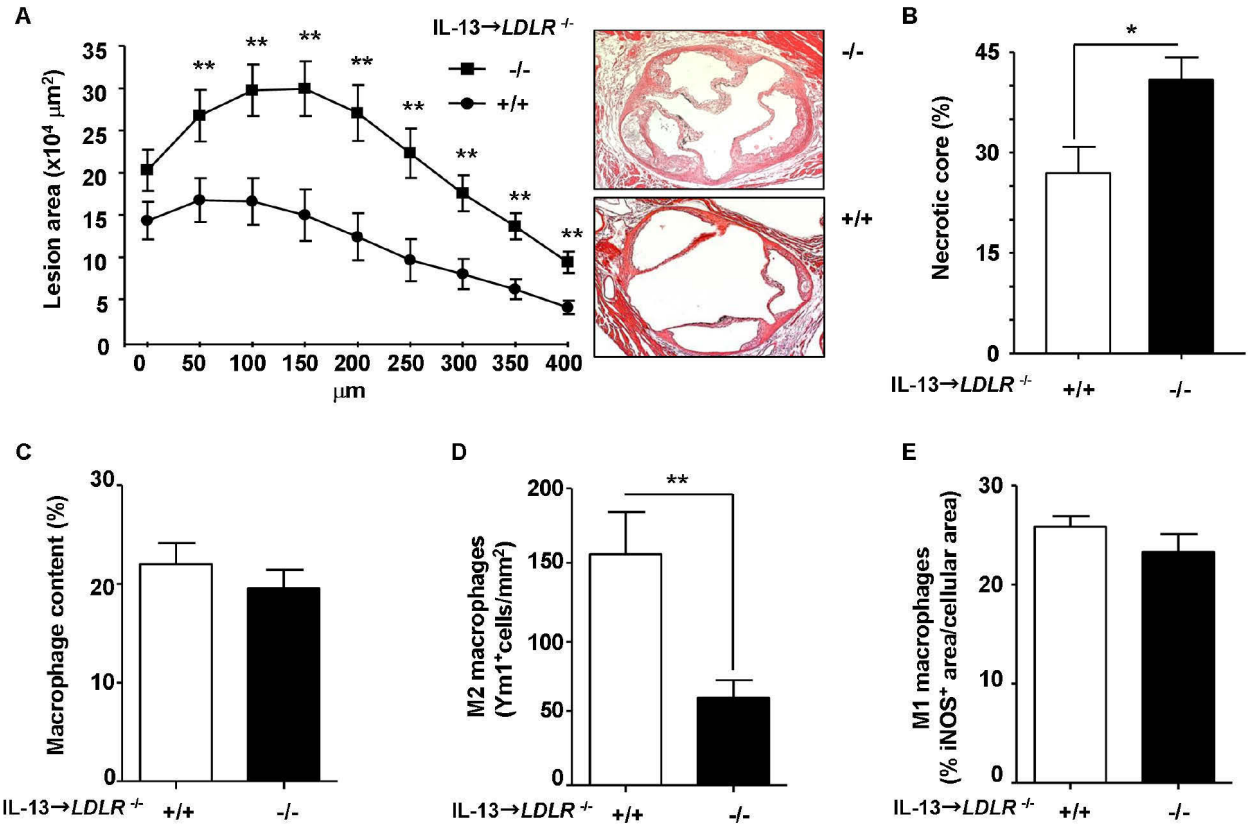

Fig 21: Increased atherosclerosis in *IL-13*-deficient *LDLR*$^{-/-}$ mice. *LDLR*$^{-/-}$ mice were reconstituted with bone marrow from either *IL-13*$^{+/+}$ mice (n=12) or *IL-13*$^{-/-}$ mice (n=14) and fed an atherogenic diet for 16 weeks. **(A)** Increased extent of atherosclerotic lesion size in cross-sections of the aortic origin in mice reconstituted with *IL-13*$^{-/-}$ bone marrow. Values represent µm2/section throughout the entire aortic origin (400µm) (**p<0.01). Images show representative H&E stains. Original magnification: 50x. **(B)** Increased necrotic core area in lesions of recipients of *IL-13*$^{-/-}$ bone marrow. Values represent percentages of necrotic core area/total lesion area (*p<0.05). **(C)** Lesional macrophage content between recipients of *IL-13*$^{-/-}$ or *IL-13*$^{+/+}$ bone marrow. Sections were stained with the macrophage specific anti-mac-3 antibody and values represent the percentages of mac-3^{+} area/cellular lesion area. **(D)** Decreased relative lesional M2 macrophage content in lesions of recipients of *IL-13*$^{-/-}$ bone marrow. Sections were stained with an antibody against Ym-1, which is specifically expressed by M2 macrophages and values represent number of Ym-1^{+}cells/cellular lesion area (**p<0.01). **(E)** Relative lesional M1 macrophage content between recipients of *IL-13*$^{-/-}$ or *IL-13*$^{+/+}$ bone marrow. Sections were stained with an antibody against iNOS, which is specifically expressed by M1 macrophages and values represent the percentages of iNOS^{+} area/cellular lesion area. All data are mean ± SEM values of all mice of each group.

To investigate potential immunological differences paralleling this increased lesion formation, total splenocytes of mice from both groups were stimulated with anti-CD3 and anti-CD28 for 72h to induce maximal T-cell activation *in vitro*. As expected, splenocytes from *IL-13*$^{-/-}$ *LDLR*$^{-/-}$ bone marrow chimeras produced only minimal amounts of IL-13. Moreover, the production of IL-4 and IL-10, but not IL-5 and IFN-γ were significantly diminished in these mice (Figure 22A and Table IV). This selective decrease in Th2 cytokine production was also reflected by a significant increase in Th1 dependent IgG2c antibodies in serum of the *IL-13*$^{-/-}$ *LDLR*$^{-/-}$ bone marrow chimeric mice, while total IgG1 antibody levels were not different (Figure 22B). IgM levels were similar between both groups (Table IV). These changes in T-cell dependent IgG levels resulted in a significantly decreased IgG1:IgG2c ratio indicating an overall Th1-biased response (Figure 22C).

Similar results were obtained for MDA-LDL specific IgG1 and IgG2c titers, respectively (Figure 23A). Importantly, the numbers of splenic T-cells and B-cells (including B1- and B2- cells) were not different between the two groups (Table IV). Consistent with an inherent Th1 bias, non-atherosclerotic *IL-13*-deficient mice that were used as bone marrow donors were also found to display decreased IgG1 and increased IgG2c levels compared to wild-type controls (Figure 23B).

These data indicate that IL-13 deficiency results in an overall pro-inflammatory environment that inhibits alternative activation of lesional macrophages and promotes atherosclerotic lesion development.

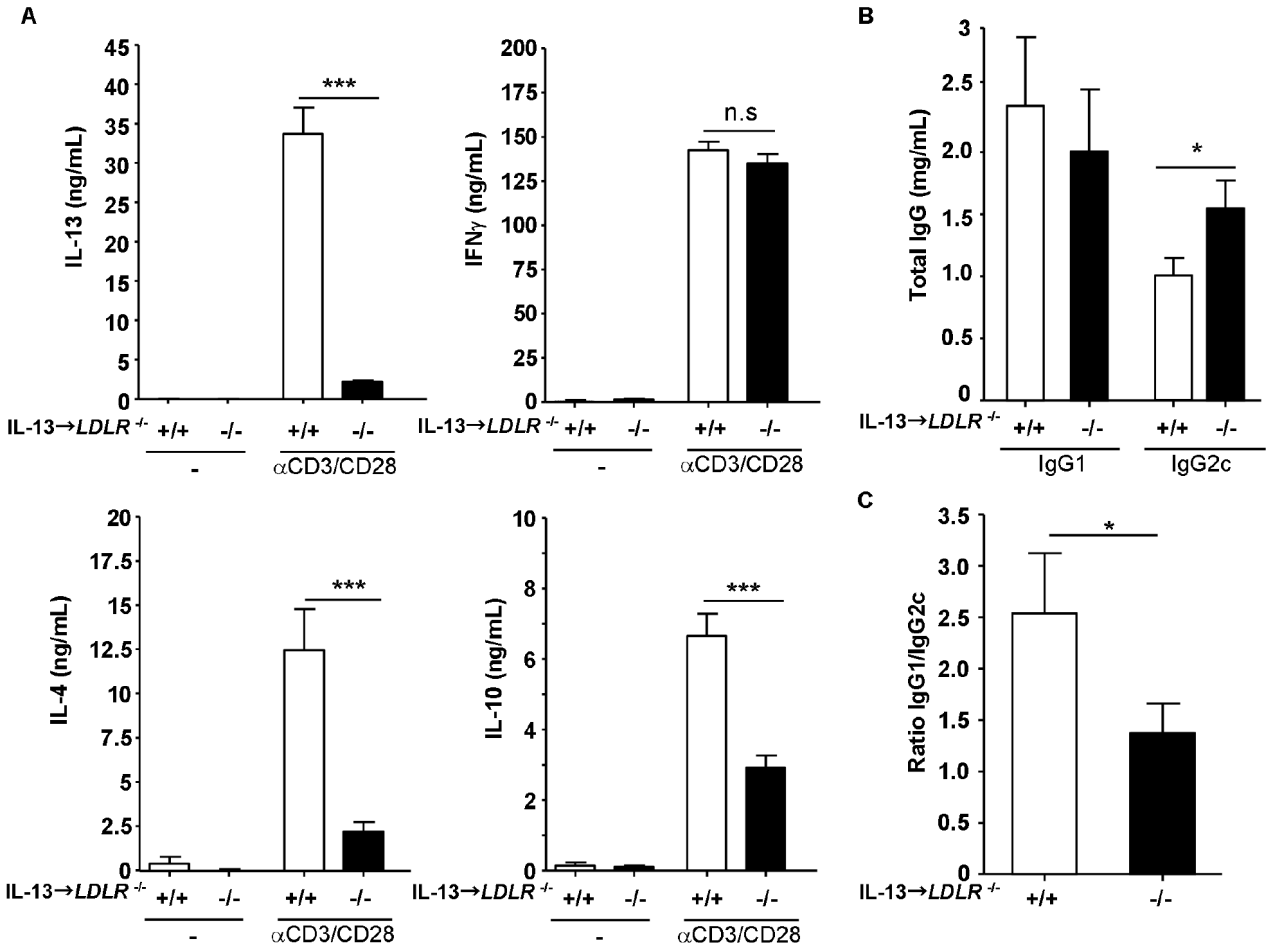

Fig 22: Effect of *IL-13*-deficiency on splenic cytokine production and antibody isotype levels. *LDLR*$^{-/-}$ mice were reconstituted with bone marrow from either *IL-13*$^{+/+}$ mice (n=12) or *IL-13*$^{-/-}$ mice (n=14) and fed an atherogenic diet for 16 weeks. At time of sacrifice spleens and blood were collected from all mice. **(A)** Recipients of *IL-13*-deficient bone marrow show a decreased production of Th2 cytokines (IL-13, IL-4, and IL-10) but not IFN-γ by splenocytes stimulated with anti-CD3/CD28 *in vitro*. Data are presented as ng/ml cytokine of splenocyte cultures (***p<0.001). **(B)** Increased levels of total IgG2c antibodies in sera of *IL-13*-deficient *LDLR*$^{-/-}$ mice. Data are presented as mg/ml of indicated serum IgG isotypes (*p<0.05). **(C)** Decreased ratio of IgG1:IgG2c antibodies in *IL-13*-deficient *LDLR*$^{-/-}$ mice (*p<0.05). All data are mean ± SEM values of all mice of each group.

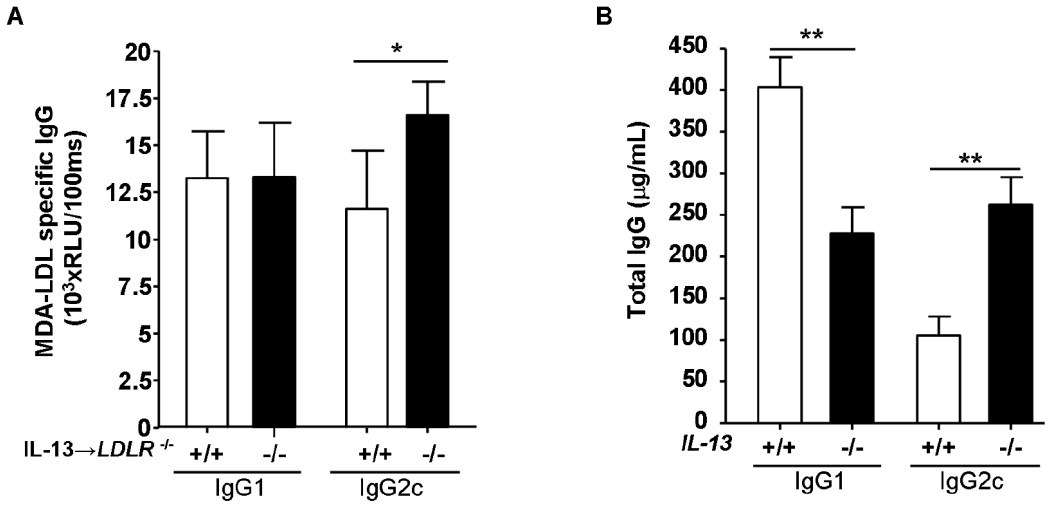

Fig 23: Effect of *IL-13*-deficiency on antibody isotype levels. (A) *LDLR*$^{-/-}$ mice were reconstituted with bone marrow from either *IL-13*$^{+/+}$ mice (n=12) or *IL-13*$^{-/-}$ mice (n=14) and fed an atherogenic diet for 16 weeks. At time of sacrifice blood was collected from all mice, and IgG1 and IgG2c antibodies against MDA-LDL were determined. Values represent relative light units (RLU)/100 ms (*$p<0.05$). **(B)** IL-13$^{-/-}$ mice have increased levels of total IgG2c and decreased levels of total IgG1 antibodies in serum. IgG isotypes in sera of IL-13$^{+/+}$ (n=8) or IL-13$^{-/-}$ mice (n=8) were quantified by ELISA. Data are presented as µg/ml of indicated IgG isotypes (**$p<0.01$). All values are mean ± SEM of all mice of each group.

6. DISCUSSION

In this thesis I demonstrate a previously unrecognized atheroprotective role of IL-13 in murine models of atherogenesis. It was assumed that IL-13 would have a similar pro-atherogenic role in atherosclerosis as IL-4, because both cytokines share similar functions by engaging the same receptor complexes. My data now point to a differential role in atherosclerosis, which can be explained by unique functions of IL-4 and IL-13 as a consequence of the exclusive engagement of the alternative receptors IL-4Rα/γc and IL-13Rα2, respectively, or by differences in ligand affinity for the same IL-4Rα/IL-13Rα1 receptor complex (Kelly-Welch, 2003; LaPorte et al, 2008). This is exemplified by the ability of only IL-4 to differentiate naïve $CD4^+$ T-cells into Th2 cells (Amsen et al, 2009; Seder & Paul, 1994) or the non-redundant role of IL-13 in parasite expulsion, allergic inflammation, and asthma (Bancroft et al, 1998; Grunig et al, 1998; Liang et al, 2011). In support of this, previous reports identified a protective function of IL-13 in models of autoimmune myocarditis (Cihakova et al, 2008) and liver injury induced by ischemia/reperfusion (Kato et al, 2003; Yoshidome et al, 1999) mainly by its capacity to induce an overall anti-inflammatory response and to modulate macrophage activation.

Specifically, I found that cholesterol-fed chimeric *IL-13*$^{-/-}$ *LDLR*$^{-/-}$ mice develop nearly two-fold larger lesions in the aortic origin than *LDLR*$^{-/-}$ mice that were reconstituted with wild type bone marrow. This pro-atherogenic effect of IL-13-deficiency was accompanied by an overall Th1-biased immune phenotype, as judged by cytokine release of stimulated splenocyte cultures and Th1/Th2-dependent IgG isotype levels in sera of these mice. These data are consistent with the known impairment in Th2 cell development by *IL-13*-deficient mouse (McKenzie et al, 1998a). Likely this overall shift in the immune response contributed in part to the pro-atherogenic effect shown. In fact, I observed that *LDLR*$^{-/-}$ mice under a hypercholesterolemic diet gradually increase serum levels of IL-13 from basal levels of 0.67 ng/ml up to 2.28 ng/ml of IL-13 at 12 weeks of atherogenic diet (data not shown). This is consistent with a protective endogenous response that is induced upon diet-feeding and lesion development. Similar responses have been described for other anti-atherogenic cytokines such as IL-10, which is also found to increase during lesion formation (Mallat et al, 1999b). The importance of this endogenous response is underscored by the finding that *IL-13*-deficient *LDLR*$^{-/-}$ mice develop accelerated atherosclerosis, suggesting that not only sustained pro-

inflammatory responses but also the failure of anti-inflammatory control mechanisms may lead to disease progression.

To study the atheroprotective effect of IL-13 directly, I examined the impact of exogenous IL-13 administration on established atherosclerotic lesions in cholesterol-fed *LDLR*$^{-/-}$ mice. To avoid hepatic fibrosis (Wynn, 2008), I chose a rather low dose of IL-13 administration to achieve only three times higher serum levels than found in atherosclerotic mice. Importantly, this interventional strategy did not result in an alteration of the Th1/Th2 phenotype of the immune response. Nevertheless, I discovered that IL-13 administration resulted in significantly increased lesional collagen content, which is consistent with the known strong pro-fibrotic role of IL-13 (Wynn, 2008), as well as significantly decreased lesional macrophage content. These alterations in plaque morphology are strongly reminiscent of changes that were reported to occur as a result of lesion regression induced by lowering serum cholesterol or increasing serum HDL in mice (Reis et al, 2001; Rong et al, 2001; Williams et al, 2008). Of interest, the changes in our model of IL-13 administration occurred without changes in serum cholesterol levels. It remains to be shown whether IL-13 is also mechanistically involved in atherosclerotic lesion stabilization during lipid lowering or active lesion regression.

In this regard it is important to point out that Fisher and colleagues recently reported that regression of atherosclerotic lesions is associated with the up-regulation of markers of alternative macrophage activation (M2) (Feig et al, 2011a; Feig et al, 2011b; Feig et al, 2012; Rayner et al, 2011b). M2 macrophages have been documented in murine and human lesions (Bouhlel et al, 2007; Chinetti-Gbaguidi et al, 2011; El Hadri et al, 2012; Khallou-Laschet et al, 2010). I now show that IL-13 administration also induces relative and absolute increases in M2 macrophages in cholesterol-fed *LDLR*$^{-/-}$ mice, and that the same lesions that show increased collagen and a decreased macrophage content have significantly increased numbers of alternatively activated macrophages and furthermore, concomitantly decreased numbers of classically activated macrophages (M1). Because our quantitative assessment of lesional macrophages suggests the presence of still “uncommitted” macrophages (i.e iNOS^{-} and Ym-1^{-}), it can be assumed that IL-13 primarily acts on this particular population of existing macrophages. In contrast, lesions of cholesterol-fed chimeric *IL-13*$^{-/-}$ *LDLR*$^{-/-}$ mice displayed decreased numbers of M2 macrophages. Although this dual classification pattern of macrophages has been considered overly simplistic, it helped characterizing macrophage heterogeneity and plasticity within atherosclerotic plaques (Mantovani et al,

2009; Stoger et al, 2010). My data show for the first time that the macrophage phenotype in atherosclerotic lesions can be modulated by IL-13 independent of cholesterol-lowering.

I also addressed the functional consequences of increased numbers of M2 macrophages with respect to uptake of OxLDL and cholesterol efflux, rate limiting steps in foam cell formation during atherogenesis (Steinberg & Witztum, 2010). Using murine primary macrophages differentially activated with either IL-13 or IFN-γ, respectively, to model potential extremes of cytokine exposure inside the plaques, I observed an increased capacity of IL-13 stimulated macrophages to take up OxLDL. This is consistent with previous studies showing that M2 macrophages exhibit increased expression of scavenger receptor CD36 and possess higher phagocytic activity (Berry, 2007; Gordon & Martinez, 2010). Previously, IL-4/IL-13 stimulation has been shown to activate PPARγ leading to upregulation of CD36 through the generation of endogenous ligands in murine and human macrophages (Huang et al, 1999; Rey, 1998), which might be predicted to lead to enhanced foam cell formation. Indeed, I could also demonstrate increased expression of CD36, but not SRA-1 or LOX-1, in IL-13-activated macrophage foam cells. Herein, I show for the first time that OxLDL-loaded IL-13 activated macrophages exhibited a higher cholesterol-efflux capacity and had increased expression of ABCA1 and ABCG1 compared to IFN-γ activated macrophages, resulting in no net increase in cholesterol accumulation. My data is further supported by a previous report demonstrating decreased ABCA1 expression and cholesterol-efflux of IFN-γ-treated murine foam cells compared to unstimulated foam cells (Panousis & Zuckerman, 2000). In fact, numerous studies have shown the importance of these two ABC transporters and the reverse cholesterol transport in promoting the regression of atherosclerosis (Cuchel & Rader, 2006; Rayner et al, 2011a; Trogan et al, 2006; Wang et al, 2007; YuZhen Zhang, 2005) or preventing its development (Oram & Vaughan, 2006; Out et al, 2008; Tall et al, 2008; Yvan-Charvet et al, 2007). Both receptors act together to transport free cellular cholesterol to lipid-poor molecules, i.e. ApoAI particles for ABCA1, and to lipidated HDL for ABCG1. Finally, the generation of larger lipid-rich HDL molecules is cleared by the liver in a process called reverse cholesterol transport (Kennedy et al, 2005; Tall et al, 2008). *In vivo* evidence demonstrated that ABCA1 and ABCG1 are primarily involved in mediating net cholesterol efflux from macrophages to HDL molecules (Wang et al, 2004; Yvan-Charvet et al, 2007). Of note, various researchers have characterized the pro-inflammatory capacity of cholesterol loading in

macrophages, and current *in vitro* and *in vivo* studies have shown that cholesterol efflux to HDL/ApoA1 molecules abrogates this inflammation (Feig et al, 2011b; Sun et al, 2009; Yvan-Charvet et al, 2008; Zhu et al, 2008).

If translatable to the *in vivo* situation, my data suggest an enhanced ability of IL-13 stimulated M2 type macrophages to clear OxLDL from the extracellular environment and efficiently promote efflux of free cholesterol via ABCA1/G1 pathways without enhancing foam-cell formation - a protective response that would be desirable in a lesional macrophage. In fact, I did find increased expression of ABCA1 in lesions of IL-13-treated mice. It is noteworthy that Chinetti-Gbaguidi et al. recently reported that IL-4 activated human monocyte-derived macrophages are less prone to foam cell formation, although they found lower efflux capacity and increased cholesterol esterification in these cells compared to untreated cells. This comparison to “neutral” monocytes and differences between IL-4 and IL-13 may explain the discrepancies (Chinetti-Gbaguidi et al, 2011). Furthermore, it has been described that human monocytes respond differentially to IL-4/ IL-13 stimulation compared to macrophages mainly by their reduced capacity to express the IL-2 receptor γ chain - γ_c and the IL-13Rα1 (Hart et al, 1999a; Hart et al, 1999b).

A prominent consequence of IL-13 administration was decreased recruitment of monocytes to carotid arteries of atherosclerotic *ApoE*$^{-/-}$ mice, whereas no effect on lesional macrophage egression was observed. The diminished recruitment seems to be largely a consequence of decreased endothelial VCAM-1 expression, which we observed in atherosclerotic mice treated with IL-13. A mechanistic role for VCAM-1 is further supported by the fact that only recruitment of monocytes, but not neutrophils, was affected by the IL-13 intervention. Furthermore, no difference between the recruitment of nonclassical Ly6C^{lo} or classical Ly6C^{hi} monocytes was observed, which is typically dependent on the expression of specific chemokines (Combadiere et al, 2008; Ingersoll et al, 2011; Tacke et al, 2007). In agreement with that, we did not observe an alteration of CCL2 presentation by endothelial cells in carotid the arteries of atherosclerotic *ApoE*$^{-/-}$ mice injected with IL-13. Finally, in analogy to the parallels with lesion regression discussed above, Potteaux *et al*. recently reported that decreased monocyte recruitment during lesion regression was also associated with decreased endothelial VCAM-1 expression (Potteaux et al, 2011). Endothelial VCAM-1 expression is a key event during atherosclerotic lesion formation (Cybulsky et al, 2001; Dansky et al, 2001). However, it is unlikely that IL-13 administration had a direct effect on VCAM-1 expression, as a

previous study demonstrated that IL-13 in fact promoted the up-regulation of VCAM-1 on activated-endothelial cells *in vitro* (Bochner et al, 1995; Woltmann et al, 2000). It is known that VCAM-1 is strongly induced by OxLDL in endothelial cells *in vitro* and at lesion prone-sites even before the appearance of visible lesions (Cybulsky & Gimbrone, 1991; Khan et al, 1995). Therefore, considering these data, one can speculate that a more likely explanation for the decreased VCAM-1 expression is a reduced intimal content of OxLDL as a consequence of enhanced IL-13-induced M2 macrophage-mediated clearance.

Taken together, I propose a model in which a shift towards an anti-inflammatory state in the local microenvironment of atherosclerotic lesions by exogenous administration of IL-13 (or indirectly by increasing Th2 cell-mediated responses) leads to the alternative activation of macrophages present within the plaque. Once activated, these macrophages show increased expression of membrane scavenger receptor CD36, which is responsible for promoting the uptake of free OxLDL trapped inside the intima, and - at the same time - increased expression of ABC-transporters, which can efficiently efflux the excess of free cholesterol generated to HDL molecules. Consequently, the net foam cell formation is unaffected or even decreased, while OxLDL is rapidly cleared (and detoxified), leading to a reduction in the activation of endothelial cells and its presentation of VCAM-1. As a result of this, monocyte recruitment is reduced, resulting in decreased lesional macrophage content. In parallel, IL-13 induces collagen production, deposition, and promotes overall plaque stabilization, despite no changes in serum cholesterol (Figure 24).

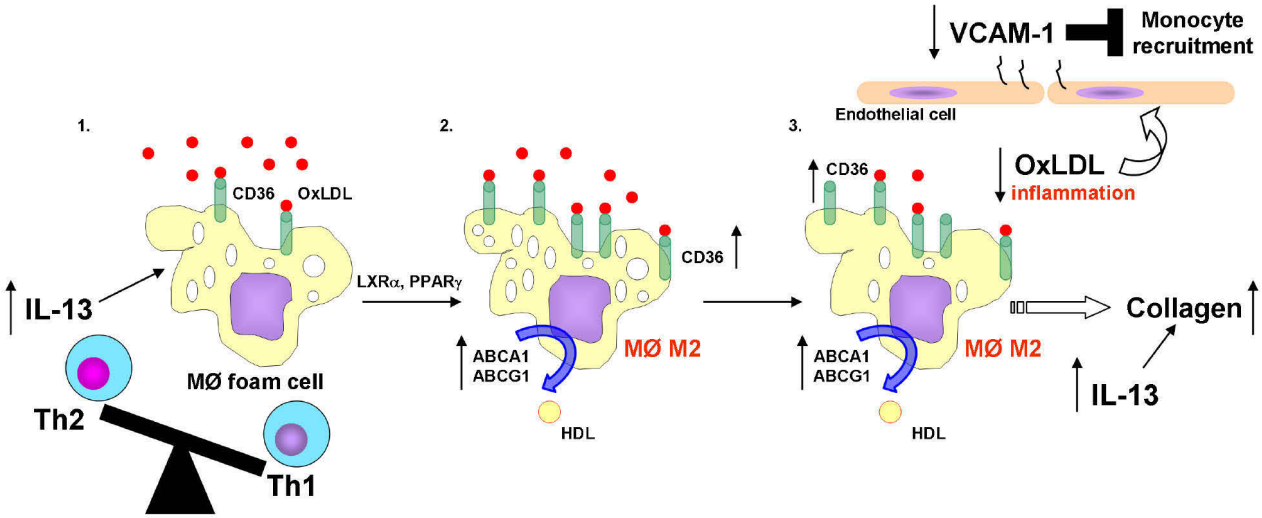

Fig 24: Proposed model for IL-13-induced changes in established atherosclerotic lesions. IL-13-dependent activation of macrophages leads to enhanced OxLDL clearance and an overall anti-inflammatory state within atherosclerotic plaques, which reduces VCAM-1 presentation by endothelial cells and thereby limits monocyte recruitment. As a direct consequence of IL-13 on smooth-muscle cells/fibroblasts or the generation of prolines in alternatively activated macrophages, collagen production and deposition is increased. Over time, this process results in a loss of macrophage content and stabilization of atherosclerotic lesions, promoting plaque regression

In conclusion, my data indicate a key role for IL-13 in halting the progression of atherogenesis and promoting plaque stabilization. I could provide clear evidence that IL-13 leads to decreased VCAM-1 mediated monocyte recruitment to atherosclerotic lesions, enhanced phenotypic modulation towards the reparative and atheroprotective M2 phenotype, and enhanced collagen deposition. Even in the absence of decreased plasma cholesterol levels, the changes induced by IL-13 are strongly reminiscent of effects seen during plaque regression in response to cholesterol lowering. Thus, my findings identify a potential new target for the prevention and treatment of atherosclerosis

7. FUTURE DIRECTIONS

While achieving the aim of this thesis, the results demonstrated here raise at the same time new questions, some of which I will briefly discuss below.

In our model of bone marrow transplantation, mice were unable to produce IL-13, but at the same time displayed an impairment of IL-4 production by activated T-cells. Because, the role of IL-4 in atherosclerosis is controversial (Davenport & Tipping, 2003; King et al, 2007; King et al, 2002), and IL-13 and IL-4 share partially common actions by signalling through the same receptor complex (IL-4Rα/IL-13Rα1), the specific contribution of each of these two cytokines in atherosclerosis development could be further examined. Thus, an intervention study using *IL-13Rα1 vs. IL-13Rα2*-deficient *LDLR*$^{-/-}$ mice would be a possibility to evaluate effects that are exclusive to IL-13. Moreover, the same study of exogenous administration of IL-13 could be performed using atherosclerotic *IL-4*$^{-/-}$ mice, as these mice were shown to develop equal lesions as their respective controls (King et al, 2007). These studies may contribute to our understanding in how these two Th2 cytokines differentially influence atherosclerosis.

Cytokines are known to be present in both mouse and human atherosclerotic lesions (Ait-Oufella et al, 2011), but up to date there are no studies available regarding IL-13 expression within plaques during disease development. It would be of interest to evaluate if IL-13 production is regulated and has a functional role during experimental atherosclerosis regression, because regression studies showed morphologic changes in lesion composition that were similar to the ones observed in this thesis during exogenous administration of IL-13 – namely decreased macrophage content, increased collagen production and alternative activation of macrophages. Moreover, a novel innate lymphoid cell type, termed nuocyte, which is chiefly responsible for the production of IL-13 during parasite infection and sufficient to promote parasite expulsion, has been discovered recently. These cells were shown to be activated by a combination of cytokines (i.e. IL-25, IL-33) and they are present in the small intestine, spleen and mesenteric lymph nodes (Neill et al, 2010). It will be highly important to elucidate the presence and impact of these cells and their relatives (Moro et al, 2010; Price et al, 2010; Saenz et al, 2010) in the adventitial tissue surrounding the plaques (or even inside) as a potential source of IL-13 production in atherosclerotic lesions. Interestingly, IL-33 is produced by activated endothelial cells and plays an important protective role in

atherosclerosis development. In addition, gut activation and IL-25 production due to increased lipids present in the atherogenic diet may represent another pathway for the activation of these new Th2- innate producing cells. Therefore, studies using an IL-13 reporter mouse to determine the activation, distribution, and contribution of IL-13-expressing cells during atherosclerosis may contribute to our understanding of the direct effect of this cytokine in lesion morphology during disease development and regression.

Macrophages are hallmark cells of all stages of atherosclerosis and its importance in disease initiation and progression has been studied extensively. Cellular diversity and plasticity are essential features of macrophages that become a potential and interesting target for disease modulation (Mantovani et al, 2009; Saha et al, 2009). The atherosclerotic plaque microenvironment is a complex source of stimulating signals, which contribute to very diverse pro- and anti-atherogenic programs executed in lesional macrophages. As a result of this, differential macrophage activation can modulate lipid metabolism, inflammatory responses, and plaque stability, and ultimately the progression and outcome of this disease. In this regard a number of unanswered questions exist. For example, the relationship between peripheral blood monocyte subsets and plaque macrophage heterogeneity remains to be elucidated at different stages of lesion formation. Furthermore, inner-plaque polarization requirements and the molecular mechanism underlying it are still unknown. The better characterization of atheroma-associated macrophage profiles with reliable markers and their counterparts in humans is much needed and “omics” approaches could further help understand the heterogeneity and polarization of macrophages during atherosclerosis development (Feig et al, 2012; Hoeksema et al, 2012).

It is known that monocyte recruitment to atherosclerotic lesions leads to plaque progression, thus new approachs to target cell adhesion could prevent not only the initiation of disease but also have an important impact on established and advanced plaques (Saha et al, 2009). In fact, a recent study pointed out the importance of other adhesion molecules in addition of VCAM-1, such as ICAM and osteopontin in the inhibition of monocyte recruitment upon lipid lowering (Potteaux et al, 2011). Moreover, IL-13 has been implicated in promoting P-selectin, but not E-selectin expression in human umbilical veins (Woltmann et al, 2000). Hence, it would be of interest to extend the investigation on other adhesion molecules and their impact on the reduction of monocyte recruitment induced by IL-13 treatment in established and advanced atherosclerosis.

By these means, we aim to further characterize the protective role of IL-13 during atherosclerosis and identify relevant pathways modulated by this cytokine as potential targets for therapeutic interventions.

8. REFERENCES

Ait-Oufella H, Salomon BL, Potteaux S, Robertson AK, Gourdy P, Zoll J, Merval R, Esposito B, Cohen JL, Fisson S, Flavell RA, Hansson GK, Klatzmann D, Tedgui A, Mallat Z (2006) Natural regulatory T cells control the development of atherosclerosis in mice. *Nat Med* 12(2)**:** 178-180

Ait-Oufella H, Taleb S, Mallat Z, Tedgui A (2011) Recent advances on the role of cytokines in atherosclerosis. *Arterioscler Thromb Vasc Biol* 31(5)**:** 969-979

Amsen D, Spilianakis CG, Flavell RA (2009) How are T(H)1 and T(H)2 effector cells made? *Curr Opin Immunol* 21(2)**:** 153-160

Anthony RM, Urban JF, Jr., Alem F, Hamed HA, Rozo CT, Boucher JL, Van Rooijen N, Gause WC (2006) Memory T(H)2 cells induce alternatively activated macrophages to mediate protection against nematode parasites. *Nat Med* 12(8)**:** 955-960

Antoniu SA (2010) Pitrakinra, a dual IL-4/IL-13 antagonist for the potential treatment of asthma and eczema. *Curr Opin Investig Drugs* 11(11)**:** 1286-1294

Arima K, Umeshita-Suyama R, Sakata Y, Akaiwa M, Mao XQ, Enomoto T, Dake Y, Shimazu S, Yamashita T, Sugawara N, Brodeur S, Geha R, Puri RK, Sayegh MH, Adra CN, Hamasaki N, Hopkin JM, Shirakawa T, Izuhara K (2002) Upregulation of IL-13 concentration in vivo by the IL13 variant associated with bronchial asthma. *J Allergy and clin immunol* 109(6)**:** 980-987

Balkwill F, Burke F (1989) The cytokine network. *Immunol Today* 10**:** 299-304

Bancroft AJ, McKenzie AN, Grencis RK (1998) A critical role for IL-13 in resistance to intestinal nematode infection. *J Immunol* 160(7)**:** 3453-3461

Barlow JL, McKenzie AN (2011) Nuocytes: expanding the innate cell repertoire in type-2 immunity. *J Leukoc Biol* 90(5)**:** 867-874

Belperio JA, Dy M, Burdick MD, Xue YY, Li K, Elias JA, Keane MP (2002) Interaction of IL-13 and C10 in the pathogenesis of bleomycin-induced pulmonary fibrosis. *Am J Respir Cell Mol Biol* 27(4)**:** 419-427

Berry A, Balard, P., Coste, A., Olagnier, D., Lagane, C., Authier, H, Benoit-Vical, F., Lepert, J.C., Séguéla, J.P., Magnaval, J.F., Chambon, P., Metzger, D., Desvergne, B., Wahli, W., Auwerx, J. and Pipy, B. (2007) IL-13 induces expression of CD36 in human monocytes through PPArg activation. *Eur J Immunol* 37**:** 1642-1652

Binder CJ, Chang MK, Shaw PX, Miller YI, Hartvigsen K, Dewan A, Witztum JL (2002) Innate and acquired immunity in atherogenesis. *Nat Med* 8(11)**:** 1218-1226

Binder CJ, Hartvigsen K, Chang MK, Miller M, Broide D, Palinski W, Curtiss LK, Corr M, Witztum JL (2004) IL-5 links adaptive and natural immunity specific for epitopes of oxidized LDL and protects from atherosclerosis. *J Clin Invest* 114(3)**:** 427-437

Binder CJ, Horkko S, Dewan A, Chang MK, Kieu EP, Goodyear CS, Shaw PX, Palinski W, Witztum JL, Silverman GJ (2003) Pneumococcal vaccination decreases atherosclerotic lesion formation: molecular mimicry between Streptococcus pneumoniae and oxidized LDL. *Nat Med* 9(6)**:** 736-743

Blease K, Jakubzick C, Westwick J, Lukacs N, Kunkel SL, Hogaboam CM (2001) Therapeutic effect of IL-13 immunoneutralization during chronic experimental fungal asthma. *J Immunol* 166(8)**:** 5219-5224

Bochner BS, Klunk DA, Sterbinsky SA, Coffman RL, Schleimer RP (1995) IL-13 selectively induces vascular cell adhesion molecule-1 expression in human endothelial cells. *J Immunol* 154(2)**:** 799-803

Bottema RW, Nolte IM, Howard TD, Koppelman GH, Dubois AE, de Meer G, Kerkhof M, Bleecker ER, Meyers DA, Postma DS (2010) Interleukin 13 and interleukin 4 receptor-alpha polymorphisms in rhinitis and asthma. *International archives of allergy and immunology* 153(3)**:** 259-267

Bouhlel MA, Derudas B, Rigamonti E, Dievart R, Brozek J, Haulon S, Zawadzki C, Jude B, Torpier G, Marx N, Staels B, Chinetti-Gbaguidi G (2007) PPARgamma activation primes human monocytes into alternative M2 macrophages with anti-inflammatory properties. *Cell Metab* 6(2)**:** 137-143

Brightling CE, Saha S, Hollins F (2010) Interleukin-13: prospects for new treatments. *Clin Exp Allergy* 40(1)**:** 42-49

Brown KD, Zurawski SM, Mosmann TR, Zurawski G (1989) A family of small inducible proteins secreted by leukocytes are members of a new superfamily that includes leukocyte and fibroblast-derived inflammatory agents, growth factors, and indicators of various activation processes. *J Immunol* 142(2)**:** 679-687

Buono C, Binder CJ, Stavrakis G, Witztum JL, Glimcher LH, Lichtman AH (2005) T-bet deficiency reduces atherosclerosis and alters plaque antigen-specific immune responses. *Proc Natl Acad Sci U S A* 102(5)**:** 1596-1601

Buono C, Come CE, Stavrakis G, Maguire GF, Connelly PW, Lichtman AH (2003) Influence of interferon-gamma on the extent and phenotype of diet-induced atherosclerosis in the LDLR-deficient mouse. *Arterioscler Thromb Vasc Biol* 23(3)**:** 454-460

Butcher MJ, Galkina EV (2012) Phenotypic and functional heterogeneity of macrophages and dendritic cell subsets in the healthy and atherosclerosis-prone aorta. *Front Physiol* 3**:** 44

Chiaramonte MG, Cheever AW, Malley JD, Donaldson DD, Wynn TA (2001) Studies of murine schistosomiasis reveal interleukin-13 blockade as a treatment for established and progressive liver fibrosis. *Hepatology* 34(2)**:** 273-282

Chiaramonte MG, Donaldson DD, Cheever AW, Wynn TA (1999a) An IL-13 inhibitor blocks the development of hepatic fibrosis during a T-helper type 2-dominated inflammatory response. *J Clin Invest* 104(6)**:** 777-785

Chiaramonte MG, Schopf LR, Neben TY, Cheever AW, Donaldson DD, Wynn TA (1999b) IL-13 is a key regulatory cytokine for Th2 cell-mediated pulmonary granuloma formation and IgE responses induced by Schistosoma mansoni eggs. *J Immunol* 162(2)**:** 920-930

Chinetti-Gbaguidi G, Baron M, Bouhlel MA, Vanhoutte J, Copin C, Sebti Y, Derudas B, Mayi T, Bories G, Tailleux A, Haulon S, Zawadzki C, Jude B, Staels B (2011) Human atherosclerotic plaque alternative macrophages display low cholesterol handling but high phagocytosis because of distinct activities of the PPARgamma and LXRalpha pathways. *Circ Res* 108(8)**:** 985-995

Chomarat P, Banchereau J (1998) Interleukin-4 and interleukin-13: their similarities and discrepancies. *International reviews of immunology* 17(1-4)**:** 1-52

Cihakova D, Barin JG, Afanasyeva M, Kimura M, Fairweather D, Berg M, Talor MV, Baldeviano GC, Frisancho S, Gabrielson K, Bedja D, Rose NR (2008) Interleukin-13 protects against experimental autoimmune myocarditis by regulating macrophage differentiation. *Am J Pathol* 172(5)**:** 1195-1208

Collins R, Armitage J, Parish S, Sleigh P, Peto R (2003) MRC/BHF Heart Protection Study of cholesterol-lowering with simvastatin in 5963 people with diabetes: a randomised placebo-controlled trial. *Lancet* 361(9374)**:** 2005-2016

Combadiere C, Potteaux S, Rodero M, Simon T, Pezard A, Esposito B, Merval R, Proudfoot A, Tedgui A, Mallat Z (2008) Combined inhibition of CCL2, CX3CR1, and CCR5 abrogates Ly6C(hi) and Ly6C(lo) monocytosis and almost abolishes atherosclerosis in hypercholesterolemic mice. *Circulation* 117(13)**:** 1649-1657

Corren J, Busse W, Meltzer EO, Mansfield L, Bensch G, Fahrenholz J, Wenzel SE, Chon Y, Dunn M, Weng HH, Lin SL (2010) A randomized, controlled, phase 2 study of AMG 317, an IL-4Ralpha antagonist, in patients with asthma. *Am J Respir Crit Care Med* 181(8)**:** 788-796

Corren J, Lemanske RF, Hanania NA, Korenblat PE, Parsey MV, Arron JR, Harris JM, Scheerens H, Wu LC, Su Z, Mosesova S, Eisner MD, Bohen SP, Matthews JG (2011) Lebrikizumab treatment in adults with asthma. *N Engl J Med* 365(12)**:** 1088-1098

Coste A, Dubourdeau M, Linas MD, Cassaing S, Lepert JC, Balard P, Chalmeton S (2003) PPARgamma promotes mannose receptor gene expression in murine macrophages and contributes to the induction of this receptor by IL-13. *Immunity* 19**:** 329-339

Cuchel M, Rader DJ (2006) Macrophage Reverse Cholesterol Transport: Key to the Regression of Atherosclerosis? *Circulation* 113**:** 2548-2555

Cybulsky MI, Gimbrone MA, Jr. (1991) Endothelial expression of a mononuclear leukocyte adhesion molecule during atherogenesis. *Science (New York, NY* 251(4995)**:** 788-791

Cybulsky MI, Iiyama K, Li H, Zhu S, Chen M, Iiyama M, Davis V, Gutierrez-Ramos JC, Connelly PW, Milstone DS (2001) A major role for VCAM-1, but not ICAM-1, in early atherosclerosis. *J Clin Invest* 107(10)**:** 1255-1262

Dansky HM, Barlow CB, Lominska C, Sikes JL, Kao C, Weinsaft J, Cybulsky MI, Smith JD (2001) Adhesion of monocytes to arterial endothelium and initiation of atherosclerosis are critically dependent on vascular cell adhesion molecule-1 gene dosage. *Arterioscler Thromb Vasc Biol* 21(10)**:** 1662-1667

Davenport P, Tipping PG (2003) The role of interleukin-4 and interleukin-12 in the progression of atherosclerosis in apolipoprotein E-deficient mice. *Am J Pathol* 163(3)**:** 1117-1125

de Vries JE (1998) The role of IL-13 and its receptor in allergy and inflammatory responses. *The Journal of allergy and clinical immunology* 102(2)**:** 165-169

Doherty TM, Kastelein R, Menon S, Andrade S, Coffman RL (1993) Modulation of murine macrophage function by IL-13. *J Immunol* 151(12)**:** 7151-7160

Donaldson DD, Whitters MJ, Fitz LJ, Neben TY, Finnerty H, Henderson SL, O'Hara RM, Jr., Beier DR, Turner KJ, Wood CR, Collins M (1998) The murine IL-13 receptor alpha 2: molecular cloning, characterization, and comparison with murine IL-13 receptor alpha 1. *J Immunol* 161(5)**:** 2317-2324

Drechsler M, Megens RT, van Zandvoort M, Weber C, Soehnlein O (2010) Hyperlipidemia-triggered neutrophilia promotes early atherosclerosis. *Circulation* 122(18)**:** 1837-1845

Edwards JP, Zhang X, Frauwirth KA, Mosser DM (2006) Biochemical and functional characterization of three activated macrophage populations. *J Leukoc Biol* 80(6)**:** 1298-1307

El Hadri K, Mahmood DF, Couchie D, Jguirim-Souissi I, Genze F, Diderot V, Syrovets T, Lunov O, Simmet T, Rouis M (2012) Thioredoxin-1 promotes anti-inflammatory macrophages of the M2 phenotype and antagonizes atherosclerosis. *Arterioscler Thromb Vasc Biol* 32(6)**:** 1445-1452

Engel D, Beckers L, Wijnands E, Seijkens T, Lievens D, Drechsler M, Gerdes N, Soehnlein O, Daemen MJ, Stan RV, Biessen EA, Lutgens E (2011) Caveolin-1 deficiency decreases atherosclerosis by hampering leukocyte influx into the arterial wall and generating a regulatory T-cell response. *FASEB J* 25(11)**:** 3838-3848

Erbel C, Chen L, Bea F, Wangler S, Celik S, Lasitschka F, Wang Y, Bockler D, Katus H, Dengler T (2009) Inhibition of IL-17A attenuates atherosclerotic lesion development in apoE-deficient mice. *J Immunol* 183**:** 8167-8175

Fallon PG, Richardson EJ, McKenzie GJ, McKenzie AN (2000) Schistosome infection of transgenic mice defines distinct and contrasting pathogenic roles for IL-4 and IL-13: IL-13 is a profibrotic agent. *J Immunol* 164(5)**:** 2585-2591

Feig JE, Parathath S, Rong JX, Mick SL, Vengrenyuk Y, Grauer L, Young SG, Fisher EA (2011a) Reversal of hyperlipidemia with a genetic switch favorably affects the content and inflammatory state of macrophages in atherosclerotic plaques. *Circulation* 123(9)**:** 989-998

Feig JE, Pineda-Torra I, Sanson M, Bradley MN, Vengrenyuk Y, Bogunovic D, Gautier EL, Rubinstein D, Hong C, Liu J, Wu C, van Rooijen N, Bhardwaj N, Garabedian M, Tontonoz P, Fisher EA (2010) LXR promotes the maximal egress of monocyte-derived cells from mouse aortic plaques during atherosclerosis regression. *J Clin Invest* 120(12)**:** 4415-4424

Feig JE, Quick JS, Fisher EA (2009) The role of a murine transplantation model of atherosclerosis regression in drug discovery. *Curr Opin Investig Drugs* 10(3)**:** 232-238

Feig JE, Rong JX, Shamir R, Sanson M, Vengrenyuk Y, Liu J, Rayner K, Moore K, Garabedian M, Fisher EA (2011b) HDL promotes rapid atherosclerosis regression in mice and alters inflammatory properties of plaque monocyte-derived cells. *Proc Natl Acad Sci U S A* 108(17)**:** 7166-7171

Feig JE, Shang Y, Rotllan N, Vengrenyuk Y, Wu C, Shamir R, Torra IP, Fernandez-Hernando C, Fisher EA, Garabedian MJ (2011c) Statins promote the regression of atherosclerosis via activation of the CCR7-dependent emigration pathway in macrophages. *PLoS One* 6(12)**:** e28534

Feig JE, Vengrenyuk Y, Reiser V, Wu C, Statnikov A, Aliferis CF, Garabedian MJ, Fisher EA, Puig O (2012) Regression of atherosclerosis is characterized by broad changes in the plaque macrophage transcriptome. *PLoS One* 7(6)**:** e39790

Fichtner-Feigl S, Fuss IJ, Young CA, Watanabe T, Geissler EK, Schlitt HJ, Kitani A, Strober W (2007) Induction of IL-13 triggers TGF-beta1-dependent tissue fibrosis in chronic 2,4,6-trinitrobenzene sulfonic acid colitis. *J Immunol* 178(9)**:** 5859-5870

Fichtner-Feigl S, Strober W, Kawakami K, Puri RK, Kitani A (2006) IL-13 signaling through the IL-13alpha2 receptor is involved in induction of TGF-beta1 production and fibrosis. *Nat Med* 12(1)**:** 99-106

Gales A, Conduche A, Bernad J, Lefevre L, Olagnier D, Beraud M, Martin-Blondel G, Linas MD, Auwerx J, Coste A, Pipy B (2010) PPARgamma controls dectin-1 expression required for host antifungal defense against Candida albicans. *PLoS Pathog* 6(1)**:** e1000714

Gautier EL, Jakubzick C, Randolph GJ (2009) Regulation of the migration and survival of monocyte subsets by chemokine receptors and its relevance to atherosclerosis. *Arterioscler Thromb Vasc Biol* 29(10)**:** 1412-1418

Gauvreau GM, Boulet LP, Cockcroft DW, Fitzgerald JM, Carlsten C, Davis BE, Deschesnes F, Duong M, Durn BL, Howie KJ, Hui L, Kasaian MT, Killian KJ, Strinich TX, Watson RM, Y N, Zhou S, Raible D, O'Byrne PM (2011) Effects of interleukin-13 blockade on allergen-induced airway responses in mild atopic asthma. *Am J Respir Crit Care Med* 183(8)**:** 1007-1014

Gleissner CA (2012) Macrophage Phenotype Modulation by CXCL4 in Atherosclerosis. *Front Physiol* 3**:** 1-7

Gleissner CA, Shaked I, Little KM, Ley K (2010) CXC chemokine ligand 4 induces a unique transcriptome in monocyte-derived macrophages. *J Immunol* 184(9)**:** 4810-4818

Gordon S, Martinez FO (2010) Alternative activation of macrophages: mechanism and functions. *Immunity* 32(5)**:** 593-604

Gordon S, Taylor PR (2005) Monocyte and macrophage heterogeneity. *Nat Rev Immunol* 5(12)**:** 953-964

Grunig G, Warnock M, Wakil AE, Venkayya R, Brombacher F, Rennick DM, Sheppard D, Mohrs M, Donaldson DD, Locksley RM, Corry DB (1998) Requirement for IL-13 independently of IL-4 in experimental asthma. *Science (New York, NY* 282(5397)**:** 2261-2263

Gupta S, Pablo AM, Jiang X, Wang N, Tall AR, Schindler C (1997) IFN-gamma potentiates atherosclerosis in ApoE knock-out mice. *J Clin Invest* 99(11)**:** 2752-2761

Hansbro PM, Kaiko GE, Foster PS (2011) Cytokine/anti-cytokine therapy - novel treatments for asthma? *Br J Pharmacol* 163(1)**:** 81-95

Hansson GK, Hermansson A (2011) The immune system in atherosclerosis. *Nature immunology* 12(3)**:** 204-212

Hart PH, Bonder CS, Balogh J, Dickensheets HL, Donnelly RP, Finlay-Jones JJ (1999a) Differential responses of human monocytes and macrophages to IL-4 and IL-13. *J Leukoc Biol* 66(4)**:** 575-578

Hart PH, Bonder CS, Balogh J, Dickensheets HL, Vazquez N, Davies KV, Finlay-Jones JJ, Donnelly RP (1999b) Diminished responses to IL-13 by human monocytes differentiated in vitro: role of the IL-13Ralpha1 chain and STAT6. *Eur J Immunol* 29(7)**:** 2087-2097

Heinzmann A, Mao XQ, Akaiwa M, Kreomer RT, Gao PS, Ohshima K, Umeshita R, Abe Y, Braun S, Yamashita T, Roberts MH, Sugimoto R, Arima K, Arinobu Y, Yu B, Kruse S, Enomoto T, Dake Y, Kawai M, Shimazu S, Sasaki S, Adra CN, Kitaichi M, Inoue H, Yamauchi K, Tomichi N, Kurimoto F, Hamasaki N, Hopkin JM, Izuhara K, Shirakawa T, Deichmann KA (2000) Genetic variants of IL-13 signalling and human asthma and atopy. *Hum Mol Genet* 9(4)**:** 549-559

Hershey GKK (2003) IL-13 receptors and signaling pathways: an evolving web. *The Journal of allergy and clinical immunology* 111(4)**:** 677-690

Hesse M, Modolell M, La Flamme AC, Schito M, Fuentes JM, Cheever AW, Pearce EJ, Wynn TA (2001) Differential regulation of nitric oxide synthase-2 and arginase-1 by type 1/type 2 cytokines in vivo: granulomatous pathology is shaped by the pattern of L-arginine metabolism. *J Immunol* 167(11)**:** 6533-6544

Hickey MJ, Granger DN, Kubes P (1999) Molecular mechanisms underlying IL-4-induced leukocyte recruitment in vivo: a critical role for the alpha 4 integrin. *J Immunol* 163(6)**:** 3441-3448

Hoeksema MA, Stoger JL, de Winther MP (2012) Molecular pathways regulating macrophage polarization: implications for atherosclerosis. *Curr Atheroscler Rep* 14(3)**:** 254-263

Horie S, Okubo Y, Hossain M, Sato E, Nomura H, Koyama S, Suzuki J, Isobe M, Sekiguchi M (1997) Interleukin-13 but not interleukin-4 prolongs eosinophil survival and induces eosinophil chemotaxis. *Intern Med* 36(3)**:** 179-185

Huang JT, Welch JS, Ricote M, Binder CJ, Willson TM, Kelly C, Witztum JL, Funk CD, Conrad D, Glass CK (1999) Interleukin-4-dependent production of PPAR-gamma ligands in macrophages by 12/15-lipoxygenase. *Nature* 400(6742)**:** 378-382

Huber SA, Sakkinen P, David C, Newell MK, Tracy RP (2001) T helper-cell phenotype regulates atherosclerosis in mice under conditions of mild hypercholesterolemia. *Circulation* 103(21)**:** 2610-2616

Ingersoll MA, Platt AM, Potteaux S, Randolph GJ (2011) Monocyte trafficking in acute and chronic inflammation. *Trends in immunology* 32(10)**:** 470-477

Kadl A, Meher AK, Sharma PR, Lee MY, Doran AC, Johnstone SR, Elliott MR, Gruber F, Han J, Chen W, Kensler T, Ravichandran KS, Isakson BE, Wamhoff BR, Leitinger N (2010) Identification of a novel macrophage phenotype that develops in response to atherogenic phospholipids via Nrf2. *Circ Res* 107(6)**:** 737-746

Kasaian MT, Miller DK (2008) IL-13 as a therapeutic target for respiratory disease. *Biochem Pharmacol* 76(2): 147-55

Kato A, Okaya T, Lentsch AB (2003) Endogenous IL-13 protects hepatocytes and vascular endothelial cells during ischemia/reperfusion injury. *Hepatology* 37(2)**:** 304-312

Kawakami K, Taguchi J, Murata T, Puri RK (2001) The interleukin-13 receptor alpha2 chain: an essential component for binding and internalization but not for interleukin-13-induced signal transduction through the STAT6 pathway. *Blood* 97(9)**:** 2673-2679

Kelly-Welch AE, Hanson, E.M., Boothby, M.R., and Keegan, A.D. (2003) Interleukin-4 and interleukin-13 signaling connections maps. *Science (New York, NY* 300**:** 1527-1528

Kennedy MA, Barrera GC, Nakamura K, Baldan A, Tarr P, Fishbein MC, Frank J, Francone OL, Edwards PA (2005) ABCG1 has a critical role in mediating cholesterol efflux to HDL and preventing cellular lipid accumulation. *Cell Metab* 1(2)**:** 121-131

Khallou-Laschet J, Varthaman A, Fornasa G, Compain C, Gaston AT, Clement M, Dussiot M, Levillain O, Graff-Dubois S, Nicoletti A, Caligiuri G (2010) Macrophage plasticity in experimental atherosclerosis. *PLoS One* 5(1)**:** e8852

Khan BV, Parthasarathy SS, Alexander RW, Medford RM (1995) Modified low density lipoprotein and its constituents augment cytokine-activated vascular cell adhesion molecule-1 gene expression in human vascular endothelial cells. *J Clin Invest* 95(3)**:** 1262-1270

King VL, Cassis LA, Daugherty A (2007) Interleukin-4 does not influence development of hypercholesterolemia or angiotensin II-induced atherosclerotic lesions in mice. *Am J Pathol* 171(6)**:** 2040-2047

King VL, Szilvassy SJ, Daugherty A (2002) Interleukin-4 deficiency decreases atherosclerotic lesion formation in a site-specific manner in female LDL receptor-/- mice. *Arterioscler Thromb Vasc Biol* 22(3)**:** 456-461

Koga M, Kai H, Yasukawa H, Yamamoto T, Kawai Y, Kato S, Kusaba K, Kai M, Egashira K, Kataoka Y, Imaizumi T (2007) Inhibition of progression and stabilization of plaques by postnatal interferon-γ function blocking in ApoE-knockout mice. *Cir Res* 101**:** 348-356

Kumar RK, Herbert C, Yang M, Koskinen AM, McKenzie AN, Foster PS (2002) Role of interleukin-13 in eosinophil accumulation and airway remodelling in a mouse model of chronic asthma. *Clin Exp Allergy* 32(7)**:** 1104-1111

Kuperman DA, Schleimer RP (2008) Interleukin-4, interleukin-13, signal transducer and activator of transcription factor 6, and allergic asthma. *Current molecular medicine* 8(5)**:** 384-392

Lanone S, Zheng T, Zhu Z, Liu W, Lee CG, Ma B, Chen Q, Homer RJ, Wang J, Rabach LA, Rabach ME, Shipley JM, Shapiro SD, Senior RM, Elias JA (2002) Overlapping and enzyme-specific contributions of matrix metalloproteinases-9 and -12 in IL-13-induced inflammation and remodeling. *J Clin Invest* 110(4)**:** 463-474

LaPorte SL, Juo ZS, Vaclavikova J, Colf LA, Qi X, Heller NM, Keegan AD, Garcia KC (2008) Molecular and structural basis of cytokine receptor pleiotropy in the interleukin-4/13 system. *Cell* 132(2)**:** 259-272

LaRosa JC, Grundy SM, Waters DD, Shear C, Barter P, Fruchart JC, Gotto AM, Greten H, Kastelein JJ, Shepherd J, Wenger NK (2005) Intensive lipid lowering with atorvastatin in patients with stable coronary disease. *N Engl J Med* 352(14)**:** 1425-1435

Laurat E, Poirier B, Tupin E, Caligiuri G, Hansson GK, Bariety J, Nicoletti A (2001) In vivo downregulation of T helper cell 1 immune responses reduces atherogenesis in apolipoprotein E-knockout mice. *Circulation* 104(2)**:** 197-202

Lee CG, Homer RJ, Zhu Z, Lanone S, Wang X, Koteliansky V, Shipley JM, Gotwals P, Noble P, Chen Q, Senior RM, Elias JA (2001) Interleukin-13 induces tissue fibrosis by selectively stimulating and activating transforming growth factor beta(1). *J Exp Med* 194(6)**:** 809-821

Lentsch AB, Shanley TP, Sarma V, Ward PA (1997) In vivo suppression of NF-kappa B and preservation of I kappa B alpha by interleukin-10 and interleukin-13. *J Clin Invest* 100(10)**:** 2443-2448

Leskinen MJ, Kovanen PT, Lindstedt KA (2003) Regulation of smooth muscle cell growth, function and death in vitro by activated mast cells--a potential mechanism for the weakening and rupture of atherosclerotic plaques. *Biochem Pharmacol* 66(8)**:** 1493-1498

Letterio JJ, Roberts AB (1998) Regulation of immune responses by TGF-beta. *Annu Rev Immunol* 16**:** 137-161

Ley K, Miller YI, Hedrick CC (2011) Monocyte and macrophage dynamics during atherogenesis. *Arterioscler Thromb Vasc Biol* 31(7)**:** 1506-1516

Liang HE, Reinhardt RL, Bando JK, Sullivan BM, Ho IC, Locksley RM (2011) Divergent expression patterns of IL-4 and IL-13 define unique functions in allergic immunity. *Nature immunology* 13(1)**:** 58-66
Libby P, Ridker PM, Hansson GK (2011) Progress and challenges in translating the biology of atherosclerosis. *Nature* 473(7347)**:** 317-325

Liu Y, Munker S, Mullenbach R, Weng HL (2012) IL-13 Signaling in Liver Fibrogenesis. *Front Immunol* 3**:** 116

Llodra J, Angeli V, Liu J, Trogan E, Fisher EA, Randolph GJ (2004) Emigration of monocyte-derived cells from atherosclerotic lesions characterizes regressive, but not progressive, plaques. *Proc Natl Acad Sci U S A* 101(32)**:** 11779-11784

Luttmann W, Knoechel B, Foerster M, Matthys H, Virchow JC, Jr., Kroegel C (1996) Activation of human eosinophils by IL-13. Induction of CD69 surface antigen, its relationship to messenger RNA expression, and promotion of cellular viability. *J Immunol* 157(4)**:** 1678-1683

Mallat Z, Besnard S, Duriez M, Deleuze V, Emmanuel F, Bureau MF, Soubrier F, Esposito B, Duez H, Fievet C, Staels B, Duverger N, Scherman D, Tedgui A (1999a) Protective role of interleukin-10 in atherosclerosis. *Circ Res* 85(8)**:** e17-24

Mallat Z, Heymes C, Ohan J, Faggin E, Leseche G, Tedgui A (1999b) Expression of interleukin-10 in advanced human atherosclerotic plaques: relation to inducible nitric oxide synthase expression and cell death. *Arterioscler Thromb Vasc Biol* 19(3)**:** 611-616

Mantovani A, Garlanda C, Locati M (2009) Macrophage diversity and polarization in atherosclerosis: a question of balance. *Arterioscler Thromb Vasc Biol* 29(10)**:** 1419-1423

Mattes J, Yang M, Siqueira A, Clark K, MacKenzie J, McKenzie AN, Webb DC, Matthaei KI, Foster PS (2001) IL-13 induces airways hyperreactivity independently of the IL-4R alpha chain in the allergic lung. *J Immunol* 167(3)**:** 1683-1692

McKenzie AN, Culpepper JA, de Waal Malefyt R, Briere F, Punnonen J, Aversa G, Sato A, Dang W, Cocks BG, Menon S, et al. (1993) Interleukin 13, a T-cell-derived cytokine that regulates human monocyte and B-cell function. *Proc Natl Acad Sci U S A* 90(8)**:** 3735-3739

McKenzie G, Emson C, Bell S, Anderson S, Fallon P, Zurawski G, Murray R, Grencis Ra, McKenzie N (1998a) Impaired Development of Th2 Cells in IL-13-Deficient Mice. *Immunity* 9**:** 423-432

McKenzie GJ, Bancroft A, Grencis RK, McKenzie AN (1998b) A distinct role for interleukin-13 in Th2-cell-mediated immune responses. *Curr Biol* 8(6)**:** 339-342

Mentink-Kane MM, Wynn TA (2004) Opposing roles for IL-13 and IL-13 receptor alpha 2 in health and disease. *Immunol Rev* 202**:** 191-202

Miller AM, Xu D, Asquith DL, Denby L, Li Y, Sattar N, Baker AH, McInnes IB, Liew FY (2008) IL-33 reduces the development of atherosclerosis. *J Exp Med* 205(2)**:** 339-346

Minty A, Chalon P, Derocq JM, Dumont X, Guillemot JC, Kaghad M, Labit C, Leplatois P, Liauzun P, Miloux B, et al. (1993) Interleukin-13 is a new human lymphokine regulating inflammatory and immune responses. *Nature* 362(6417)**:** 248-250

Mitchell J, Dimov V, Townley RG (2010) IL-13 and the IL-13 receptor as therapeutic targets for asthma and allergic disease. *Curr Opin Investig Drugs* 11(5)**:** 527-534

Moro K, Yamada T, Tanabe M, Takeuchi T, Ikawa T, Kawamoto H, Furusawa J, Ohtani M, Fujii H, Koyasu S (2010) Innate production of T(H)2 cytokines by adipose tissue-associated c-Kit(+)Sca-1(+) lymphoid cells. *Nature* 463(7280)**:** 540-544

Munder M, Eichmann K, Moran JM, Centeno F, Soler G, Modolell M (1999) Th1/Th2-regulated expression of arginase isoforms in murine macrophages and dendritic cells. *J Immunol* 163(7)**:** 3771-3777

Nair MG, Cochrane DW, Allen JE (2003) Macrophages in chronic type 2 inflammation have a novel phenotype characterized by the abundant expression of Ym1 and Fizz1 that can be partly replicated in vitro. *Immunol Lett* 85(2)**:** 173-180
Neill DR, Wong SH, Bellosi A, Flynn RJ, Daly M, Langford TK, Bucks C, Kane CM, Fallon PG, Pannell R, Jolin HE, McKenzie AN (2010) Nuocytes represent a new innate effector leukocyte that mediates type-2 immunity. *Nature* 464(7293)**:** 1367-1370

Nissen SE (2005a) Effect of intensive lipid lowering on progression of coronary atherosclerosis: evidence for an early benefit from the Reversal of Atherosclerosis with Aggressive Lipid Lowering (REVERSAL) trial. *Am J Cardiol* 96(5A)**:** 61F-68F

Nissen SE (2005b) Halting the progression of atherosclerosis with intensive lipid lowering: results from the Reversal of Atherosclerosis with Aggressive Lipid Lowering (REVERSAL) trial. *Am J Med* 118 Suppl 12A**:** 22-27

Nissen SE, Nicholls SJ, Sipahi I, Libby P, Raichlen JS, Ballantyne CM, Davignon J, Erbel R, Fruchart JC, Tardif JC, Schoenhagen P, Crowe T, Cain V, Wolski K, Goormastic M, Tuzcu EM (2006) Effect of very high-intensity statin therapy on regression of coronary atherosclerosis: the ASTEROID trial. *JAMA* 295(13)**:** 1556-1565

O'Connor WJ, Kamanaka M, Booth C, Town T, Nakae S, Iwakura Y, Kolls J, Flavell R (2009) A protective function for interleukin 17A in T cell–mediated intestinal inflammation. *Nature immunology* 10**:** 603– 609

Oliphant CJ, Barlow JL, McKenzie AN (2011) Insights into the initiation of type 2 immune responses. *Immunology* 134(4)**:** 378-385

Oram JF, Vaughan AM (2006) ATP-Binding cassette cholesterol transporters and cardiovascular disease. *Circ Res* 99(10)**:** 1031-1043

Oriente A, Fedarko NS, Pacocha SE, Huang SK, Lichtenstein LM, Essayan DM (2000) Interleukin-13 modulates collagen homeostasis in human skin and keloid fibroblasts. *J Pharmacol Exp Ther* 292(3)**:** 988-994

Out R, Hoekstra M, Habets K, Meurs I, de Waard V, Hildebrand RB, Wang Y, Chimini G, Kuiper J, Van Berkel TJ, Van Eck M (2008) Combined deletion of macrophage ABCA1 and ABCG1 leads to massive lipid accumulation in tissue macrophages and distinct atherosclerosis at relatively low plasma cholesterol levels. *Arterioscler Thromb Vasc Biol* 28(2)**:** 258-264

Panousis CG, Zuckerman SH (2000) Interferon-gamma induces downregulation of Tangier disease gene (ATP-binding-cassette transporter 1) in macrophage-derived foam cells. *Arterioscler Thromb Vasc Biol* 20(6)**:** 1565-1571

Pinderski Oslund LJ, Hedrick CC, Olvera T, Hagenbaugh A, Territo M, Berliner JA, Fyfe AI (1999) Interleukin-10 blocks atherosclerotic events in vitro and in vivo. *Arterioscler Thromb Vasc Biol* 19(12)**:** 2847-2853

Pope SM, Brandt EB, Mishra A, Hogan SP, Zimmermann N, Matthaei KI, Foster PS, Rothenberg ME (2001) IL-13 induces eosinophil recruitment into the lung by an IL-5- and eotaxin-dependent mechanism. *The Journal of allergy and clinical immunology* 108(4)**:** 594-601

Potteaux S, Gautier EL, Hutchison SB, van Rooijen N, Rader DJ, Thomas MJ, Sorci-Thomas MG, Randolph GJ (2011) Suppressed monocyte recruitment drives macrophage removal from atherosclerotic plaques of Apoe-/- mice during disease regression. *J Clin Invest* 121(5)**:** 2025-2036

Price AE, Liang HE, Sullivan BM, Reinhardt RL, Eisley CJ, Erle DJ, Locksley RM (2010) Systemically dispersed innate IL-13-expressing cells in type 2 immunity. *Proc Natl Acad Sci U S A* 107(25)**:** 11489-11494

Punnonen J, Aversa G, Cocks BG, McKenzie AN, Menon S, Zurawski G, de Waal Malefyt R, de Vries JE (1993) Interleukin 13 induces interleukin 4-independent IgG4 and IgE synthesis and CD23 expression by human B cells. *Proc Natl Acad Sci U S A* 90(8)**:** 3730-3734

Raes G, De Baetselier P, Noel W, Beschin A, Brombacher F, Hassanzadeh Gh G (2002a) Differential expression of FIZZ1 and Ym1 in alternatively versus classically activated macrophages. *J Leukoc Biol* 71(4)**:** 597-602

Raes G, Noel W, Beschin A, Brys L, de Baetselier P, Hassanzadeh GH (2002b) FIZZ1 and Ym as tools to discriminate between differentially activated macrophages. *Dev Immunol* 9(3)**:** 151-159

Rayner KJ, Sheedy FJ, Esau CC, Hussain FN, Temel RE, Parathath S, van Gils JM, Rayner AJ, Chang AN, Suarez Y, Fernandez-Hernando C, Fisher EA, Moore KJ (2011a) Antagonism of miR-33 in mice promotes reverse cholesterol transport and regression of atherosclerosis. *Journal of Clinical Investigation* 121(7)**:** 2921-2931

Rayner KJ, Sheedy FJ, Esau CC, Hussain FN, Temel RE, Parathath S, van Gils JM, Rayner AJ, Chang AN, Suarez Y, Fernandez-Hernando C, Fisher EA, Moore KJ (2011b) Antagonism of miR-33 in mice promotes reverse cholesterol transport and regression of atherosclerosis. *J Clin Invest* 121(7)**:** 2921-2931

Reis ED, Li J, Fayad ZA, Rong JX, Hansoty D, Aguinaldo JG, Fallon JT, Fisher EA (2001) Dramatic remodeling of advanced atherosclerotic plaques of the apolipoprotein E-deficient mouse in a novel transplantation model. *J Vasc Surg* 34(3)**:** 541-547

Rey A, M'Rini, C., Sozzani, P., Lamboeuf, Y., Beraud, M., Caput, D., Ferrara, P. and Pipy, B. (1998) IL-13 increases the cPLA2 gene and protein expression and the mobilization of arachidonic acid during inflammatory process in mouse peritoneal macrophages. *Biochem Biophys Acta* 1393**:** 244-252

Robertson AK, Hansson GK (2006) T cells in atherogenesis: for better or for worse? *Arterioscler Thromb Vasc Biol* 26(11)**:** 2421-2432

Rong JX, Li J, Reis ED, Choudhury RP, Dansky HM, Elmalem VI, Fallon JT, Breslow JL, Fisher EA (2001) Elevating high-density lipoprotein cholesterol in apolipoprotein E-deficient mice remodels advanced atherosclerotic lesions by decreasing macrophage and increasing smooth muscle cell content. *Circulation* 104(20)**:** 2447-2452

Saenz SA, Siracusa MC, Perrigoue JG, Spencer SP, Urban JF, Jr., Tocker JE, Budelsky AL, Kleinschek MA, Kastelein RA, Kambayashi T, Bhandoola A, Artis D (2010) IL25 elicits a multipotent progenitor cell population that promotes T(H)2 cytokine responses. *Nature* 464(7293)**:** 1362-1366

Saha P, Modarai B, Humphries J, Mattock K, Waltham M, Burnand KG, Smith A (2009) The monocyte/macrophage as a therapeutic target in atherosclerosis. *Curr Opin Pharmacol* 9**:** 109-118

Sampi M, Ukkola O, Paivansalo M, Kesaniemi YA, Binder CJ, Horkko S (2008) Plasma interleukin-5 levels are related to antibodies binding to oxidized low-density lipoprotein and to decreased subclinical atherosclerosis. *J Am Coll Cardiol* 52(17)**:** 1370-1378

Schiller NK, Kubo N, Boisvert WA, Curtiss LK (2001) Effect of gamma-irradiation and bone marrow transplantation on atherosclerosis in LDL receptor-deficient mice. *Arterioscler Thromb Vasc Biol* 21(10)**:** 1674-1680

Seder R, Paul W (1994) Acquisition of lymphokine-producing phenotype by CD4+ T cells. *Annu Rev Immunol* 12**:** 635-673

Shalhoub J, Falck-Hansen MA, Davies AH, Monaco C (2011) Innate immunity and monocyte-macrophage activation in atherosclerosis. *J Inflamm (Lond)* 8**:** 9

Singh D, Kane B, Molfino NA, Faggioni R, Roskos L, Woodcock A (2010) A phase 1 study evaluating the pharmacokinetics, safety and tolerability of repeat dosing with a human IL-13 antibody (CAT-354) in subjects with asthma. *BMC Pulm Med* 10**:** 3

Smith E, Prasad K, Butcher M, Dobrian A, Kolls J, Ley K, Galkina E (2010) Blockade of interleukin-17A results in reduced atherosclerosis in apolipoprotein E-deficient mice. *Circulation* 121**:** 1746-1755

Steinberg D, Witztum JL (2010) Oxidized low-density lipoprotein and atherosclerosis. *Arterioscler Thromb Vasc Biol* 30(12)**:** 2311-2316

Stoger JL, Goossens P, de Winther MP (2010) Macrophage heterogeneity: relevance and functional implications in atherosclerosis. *Curr Vasc Pharmacol* 8(2)**:** 233-248

Sun Y, Ishibashi M, Seimon T, Lee M, Sharma SM, Fitzgerald KA, Samokhin AO, Wang Y, Sayers S, Aikawa M, Jerome WG, Ostrowski MC, Bromme D, Libby P, Tabas IA, Welch CL, Tall AR (2009) Free cholesterol accumulation in macrophage membranes activates Toll-like receptors and p38 mitogen-activated protein kinase and induces cathepsin K. *Circ Res* 104(4)**:** 455-465

Swirski FK, Pittet MJ, Kircher MF, Aikawa E, Jaffer FA, Libby P, Weissleder R (2006) Monocyte accumulation in mouse atherogenesis is progressive and proportional to extent of disease. *Proc Natl Acad Sci U S A* 103(27)**:** 10340-10345

Tacke F, Alvarez D, Kaplan TJ, Jakubzick C, Spanbroek R, Llodra J, Garin A, Liu J, Mack M, van Rooijen N, Lira SA, Habenicht AJ, Randolph GJ (2007) Monocyte subsets differentially employ CCR2, CCR5, and CX3CR1 to accumulate within atherosclerotic plaques. *J Clin Invest* 117(1)**:** 185-194

Taleb S, Romain M, Ramkhelawon B, Uyttenhove C, Pasterkamp G, Herbin O, Esposito B, Perez N, Yasukawa H, Van Snick J, Yoshimura A, Tedgui A, Mallat Z (2009) Loss of SOCS3 expression in T cells reveals a regulatory role for interleukin-17 in atherosclerosis. *J Exp Med* 206**:** 2067–2077

Taleb S, Tedgui A, Mallat Z (2010) Interleukin-17: friend or foe in atherosclerosis? *Curr Opin Lipidol* 21**:** 404-408

Tall AR, Yvan-Charvet L, Terasaka N, Pagler T, Wang N (2008) HDL, ABC transporters, and cholesterol efflux: implications for the treatment of atherosclerosis. *Cell Metab* 7(5)**:** 365-375

Tedgui A, Mallat Z (2006) Cytokines in atherosclerosis: pathogenic and regulatory pathways. *Physiol Rev* 86(2)**:** 515-581

Tellides G, Tereb DA, Kirkiles-Smith NC, Kim RW, Wilson JH, Schechner JS, Lorber MI, Pober JS (2000) Interferon-gamma elicits arteriosclerosis in the absence of leukocytes. *Nature* 403(6766)**:** 207-211

Townley RG, Sapkota M, Sapkota K (2011) IL-13 and its genetic variants: effect on current asthma treatments. *Discov Med* 12(67)**:** 513-523

Trogan E, Fayad ZA, Itskovich VV, Aguinaldo JG, Mani V, Fallon JT, Chereshnev I, Fisher EA (2004) Serial studies of mouse atherosclerosis by in vivo magnetic resonance imaging detect lesion regression after correction of dyslipidemia. *Arterioscler Thromb Vasc Biol* 24(9)**:** 1714-1719

Trogan E, Feig JE, Dogan S, Rothblat GH, Angeli V, Tacke F, Randolph GJ, Fisher EA (2006) Gene expression changes in foam cells and the role of chemokine receptor CCR7 during atherosclerosis regression in ApoE-deficient mice. *Proc Natl Acad Sci U S A* 103(10)**:** 3781-3786

Walch L, Massade L, Dufilho M, Brunet A, Rendu F (2006) Pro-atherogenic effect of interleukin-4 in endothelial cells: modulation of oxidative stress, nitric oxide and monocyte chemoattractant protein-1 expression. *Atherosclerosis* 187**:** 285-291

Waldo SW, Li Y, Buono C, Zhao B, Billings EM, Chang J, Kruth HS (2008) Heterogeneity of human macrophages in culture and in atherosclerotic plaques. *Am J Pathol* 172(4)**:** 1112-1126

Wang N, Lan D, Chen W, Matsuura F, Tall AR (2004) ATP-binding cassette transporters G1 and G4 mediate cellular cholesterol efflux to high-density lipoproteins. *Proc Natl Acad Sci U S A* 101(26)**:** 9774-9779

Wang X, Collins HL, Ranalletta M, Fuki IV, Billheimer JT, Rothblat GH, Tall AR, Rader DJ (2007) Macrophage ABCA1 and ABCG1, but not SR-BI, promote macrophage reverse cholesterol transport in vivo. *J Clin Invest* 117(8)**:** 2216-2224

Weber C, Zernecke A, Libby P (2008) The multifaceted contributions of leukocyte subsets to atherosclerosis: lessons from mouse models. *Nat Rev Immunol* 8(10)**:** 802-815

Welch JS, Escoubet-Lozach L, Sykes DB, Liddiard K, Greaves DR, Glass CK (2002) TH2 cytokines and allergic challenge induce Ym1 expression in macrophages by a STAT6-dependent mechanism. *J Biol Chem* 277(45)**:** 42821-42829

Wenzel S, Wilbraham D, Fuller R, Getz EB, Longphre M (2007) Effect of an interleukin-4 variant on late phase asthmatic response to allergen challenge in asthmatic patients: results of two phase 2a studies. *Lancet* 370(9596)**:** 1422-1431

Whitman S, Ravisankar P, Elam H, Daugherty A (2000) Exogenous interferon-γ enhances atherosclerosis in apolipoprotein E $^{-/-}$ mice. *Am J Pathol* 157**:** 1819-1824

Williams KJ, Feig JE, Fisher EA (2008) Rapid regression of atherosclerosis: insights from the clinical and experimental literature. *Nature clinical practice Cardiovascular medicine* 5(2)**:** 91-102

Wills-Karp M, Luyimbazi J, Xu X, Schofield B, Neben TY, Karp CL, Donaldson DD (1998) Interleukin-13: central mediator of allergic asthma. *Science (New York, NY* 282(5397)**:** 2258-2261

Wolfs IM, Donners MM, de Winther MP (2011) Differentiation factors and cytokines in the atherosclerotic plaque micro-environment as a trigger for macrophage polarisation. *Thromb Haemost* 106(5)**:** 763-771

Woltmann G, McNulty CA, Dewson G, Symon FA, Wardlaw AJ (2000) Interleukin-13 induces PSGL-1/P-selectin-dependent adhesion of eosinophils, but not neutrophils, to human umbilical vein endothelial cells under flow. *Blood* 95(10)**:** 3146-3152

Wood N, Whitters MJ, Jacobson BA, Witek J, Sypek JP, Kasaian M, Eppihimer MJ, Unger M, Tanaka T, Goldman SJ, Collins M, Donaldson DD, Grusby MJ (2003) Enhanced interleukin (IL)-13 responses in mice lacking IL-13 receptor alpha 2. *J Exp Med* 197(6)**:** 703-709

Wynn TA (2003) IL-13 effector functions. *Ann Rev Immunol* 21**:** 425-456

Wynn TA (2004) Fibrotic disease and the T(H)1/T(H)2 paradigm. *Nat Rev Immunol* 4(8)**:** 583-594

Wynn TA (2008) Cellular and molecular mechanisms of fibrosis. *J Pathol* 214(2)**:** 199-210

Wynn TA (2011) Integrating mechanisms of pulmonary fibrosis. *J Exp Med* 208(7)**:** 1339-1350

Yoshidome H, Kato A, Miyazaki M, Edwards MJ, Lentsch AB (1999) IL-13 activates STAT6 and inhibits liver injury induced by ischemia/reperfusion. *Am J Pathol* 155(4)**:** 1059-1064

YuZhen Zhang JRDS, Muredach Reilly,Jeffrey T. Billheimer,George H. Rothblat and Daniel J. Rader (2005) Hepatic expression of scavenger receptor class B type I (SR-BI) is a positive regulator of macrophage reverse cholesterol transport in vivo. *Journal of Clinical Investigation* 115**:** 2870-2874

Yvan-Charvet L, Ranalletta M, Wang N, Han S, Terasaka N, Li R, Welch C, Tall AR (2007) Combined deficiency of ABCA1 and ABCG1 promotes foam cell accumulation and accelerates atherosclerosis in mice. *J Clin Invest* 117(12)**:** 3900-3908

Yvan-Charvet L, Welch C, Pagler TA, Ranalletta M, Lamkanfi M, Han S, Ishibashi M, Li R, Wang N, Tall AR (2008) Increased inflammatory gene expression in ABC transporter-deficient macrophages: free cholesterol accumulation, increased signaling via toll-like receptors, and neutrophil infiltration of atherosclerotic lesions. *Circulation* 118(18)**:** 1837-1847

Zhang JG, Hilton DJ, Willson TA, McFarlane C, Roberts BA, Moritz RL, Simpson RJ, Alexander WS, Metcalf D, Nicola NA (1997) Identification, purification, and characterization of a soluble interleukin (IL)-13-binding protein. Evidence that it is distinct from the cloned Il-13 receptor and Il-4 receptor alpha-chains. *J Biol Chem* 272(14)**:** 9474-9480

Zhao A, Urban JF, Jr., Anthony RM, Sun R, Stiltz J, van Rooijen N, Wynn TA, Gause WC, Shea-Donohue T (2008) Th2 cytokine-induced alterations in intestinal smooth muscle function depend on alternatively activated macrophages. *Gastroenterology* 135(1)**:** 217-225 e211

Zhou X, Paulsson G, Stemme S, Hansson GK (1998) Hypercholesterolemia is associated with a T helper (Th) 1/Th2 switch of the autoimmune response in atherosclerotic apo E-knockout mice. *J Clin Invest* 101(8)**:** 1717-1725

Zhu X, Lee JY, Timmins JM, Brown JM, Boudyguina E, Mulya A, Gebre AK, Willingham MC, Hiltbold EM, Mishra N, Maeda N, Parks JS (2008) Increased cellular free cholesterol in macrophage-specific Abca1 knock-out mice enhances pro-inflammatory response of macrophages. *J Biol Chem* 283(34)**:** 22930-22941

Zhu Z, Homer RJ, Wang Z, Chen Q, Geba GP, Wang J, Zhang Y, Elias JA (1999) Pulmonary expression of interleukin-13 causes inflammation, mucus hypersecretion, subepithelial fibrosis, physiologic abnormalities, and eotaxin production. *J Clin Invest* 103(6)**:** 779-788

Zurawski G, de Vries JE (1994) Interleukin 13, an interleukin 4-like cytokine that acts on monocytes and B cells, but not on T cells. *Immunol Today* 15(1)**:** 19-26

9. PUBLICATION BASED ON THE THESIS

Cardilo-Reis L, Gruber S, Schreier SM, Drechsler M, Papac-Milicevic N, Weber C, Wagner O, Stangl H, Soehnlein O, and Binder CJ (2012). **Interleukin-13 protects from atherosclerosis and modulates plaque composition by skewing the macrophage phenotype**. *EMBO Mol Med* 4(10): 1072-1086.

10. ACKNOWLEDGEMENTS

First of all, I want to thank my husband David for his constant encouragement, criticism, and principally for his deep belief in my scientific potentials. Thanks for supporting my dreams with such passion! It is needless to thank our masterpiece, Clara, who has enlightened my life since the very first moment.

I personally thank Oswald Wagner, who gave me the opportunity to perform my PhD thesis in his Department, and thereby opened the possibility to accomplish this work.

I thank my supervisor Christoph Binder who has given me this nice project and, importantly, endured together with me the difficult periods. It hasn't been so easy, but we completed it successfully!

I thank all the colleagues in the lab who gave me support over the years. Especially to Sabrina Gruber and Nikolina Papac-Milicevic, I thank you for being "my hands" and joining your efforts during a decisive period of my doctorate. I am grateful to Karsten Hartvigsen for all his scientific advices, and even more so for having brought balance to the group. It is a pity that one year passed so quickly! I thank Laura Göderle for her help in establishing the histological techniques. Finally, I am deeply indebted to Maria Ozsvar Kozma for persistently being the best technician ever and a "mother" to all of us.

I give thanks to the members of my thesis-committee, Sylvia Knapp and Herbert Stangl for stimulating discussions.

I want to acknowledge all my external collaborators, in particular Sabine Schreier, Maik Drechsler, and Oliver Söhnlein for promptly accepting to participate in this work.

My special thanks go to Karin Hagenbichler, who swiftly navigated me through Austrian bureaucracy during these five years – always with a friendly smile.

I thank all "CeMMies", and among them especially my dearest friends Sandrine, Adriana and Ana, for having transformed these years into a shiny and enjoyable time. I had unforgettable moments with you girls!

I would like to thank all my friends in Brazil who, despite being far away; supported me constantly. I'm especially grateful to Lourdes who shared the first Viennese impressions with me and helped me realize how beautiful this city is!

Surely, I owe a great deal of gratitude to the Weismann family for undoubtedly absorbing me as part of the family long before the official "yes".

I couldn't stay without deeply thanking my family – my father, my sister, Marli and Elias for having always supported and believed on me, besides having bravely endured all these years apart. You are my basis - I wouldn't have made it without you!

Last but not least, I thank God for the continuous opportunity of improving myself.

11. FUNDING

This work was supported by grants from the GenAU program (DRAGON), the Austrian Academy of Sciences and the Fondation Leducq.

12. AUTHORS CURRICULUM VITAE

Personal Information

Name	Larissa Cardilo dos Reis Weismann, M.Sc.
Date of Birth	December 23rd, 1982
Nationality	Brazilian
Address	CeMM Center for Molecular Medicine of the Austrian Academy of Sciences Department of Laboratory Medicine Medical University of Vienna Lazarettgasse 14 1090 Vienna Austria
E-mail	larissa.reis@meduniwien.ac.at

Education

Mar 2007 – present	Doctoral studies in the international PhD program N094 "Vascular Biology" of the Medical University of Vienna, Austria. Supervisor: Univ. Prof Christoph J. Binder, M.D. PhD. Thesis project: The role of Th2 cytokines in the development of atherosclerosis
Mar 2004 – Mar 2006	Master of Science in the Institute of Medical Biochemistry at Federal University of Rio de Janeiro, Brazil. ▪ Research visit at University of Sao Paulo, Ribeirao Preto, Sao Paulo, Brazil. Laboratory of Lucia H. Faccioli, PhD (Oct 2005) Supervisor: Univ. Prof. Vera L. Goncalves Koatz, M.D. PhD. Thesis title: "The role of neutrophils in the modulation of the oestrus cycle in mice" Graduation with honours.
2000-2004	Bachelor studies in Biomedicine at Federal University of Rio de Janeiro, Brazil. ▪ Bachelor thesis: "The effect of cigarette smoke exposure in acute pulmonary inflammation". Supervisor: Univ. Prof. Vera L. Goncalves Koatz, M.D. PhD. (Mar 2002 – Mar 2004) ▪ Practical training: "Antithrombotic and anti-inflammatory properties of glycosaminoglicans purified from sea invertebrates". Supervisor: Univ. Prof. Mauro S. G. Pavao, PhD. (Aug 2000 – Mar 2002) Graduation with honours.
1997-1999	High-School at Colégio Miguel Couto, Rio de Janeiro, Brazil.

Languages

Portuguese	mother tongue
English	fluent, written and spoken
German	intermediate

Peer Review Publications

Cardilo-Reis L, Gruber, S, Schreier SM, Drechsler M, Papac-Milicevic N, Weber C, Wagner O, Stangl H, Soehnlein O, and Binder CJ. **Interleukin-13 protects from atherosclerosis and modulates plaque composition by skewing the macrophage phenotype.** EMBO Mol Med.2012 Oct; 4(10):1072-1086.

Cardilo-Reis L, Witztum JL, and Binder CJ. **When monocytes come (too) close to our hearts.** J. Am. Coll. Cardiol. 2010 Apr; 55(15):1639-41.

Castro P, Nasser H, Abraao A, Dos Reis LC, Rica I, Valenca SS, Rezende DC, Quintas LE, Cavalcante MC, Porto LC, and Koatz VL. **Aspirin and indomethacin reduce lung inflammation of mice exposed to cigarette smoke**. Biochem Pharmacol. 2009 Mar; 77(6):1029-39.

Medeiros MM, Peixoto JR, Oliveira AC, Cardilo-Reis L, Koatz VL, Van Kaer L, Previato JO, Medonca-Previato L, Nobrega A, and Bellio M. **Toll-like receptor 4 (TLR4)-dependent proinflammatory and immunomodulatory properties of the glycoinositophospholipid (GILP) from *Trypanosoma cruzi*.** J. Leukocyte. Biol. 2007 Sep; 82(3):488-96.

Borsig L*, Wang L*, Cavalcante MC, Cardilo-Reis L, Ferreira PL, Mourao PA, Esko JD, and Pavao MS. **Selectin blocking activity of a fucosylated chondroitin sulphate glycosaminoglycan from sea cucumber. Effect on tumor metastasis and neutrophil recruitment**. J. Biol. Chem. 2007 May; 282(20):14984-91. *equal contribution

Cardilo-Reis L*, Cavalcante MC*, Silveira CBM, and Pavao MS. ***In vivo* antithrombotic properties of a heparin from oocyte test cells of the sea squirt *Styela plicata* (Chrodata-Tunicata)**. Braz. J. Med. Biol. Res. 2006 Nov; 39:1409-15. *equal contribution

Castro P, Legora-Machado A, Cardilo-Reis L, Valenca S, Porto LC, Walker C, Zuany-Amorin C, and Koatz VL. **Inhibition of interleukin-1β reduces mouse lung inflammation induced by exposure to cigarette smoke**. Eur. J. Pharmacol. 2004 Sep; 498(1-3):279-86.

Conferences

2010	Keystone Symposium “Advances in Molecular Mechanisms of Atherosclerosis (J7)”, Banff, Canada. *Poster presentation.*
2009	Young Scientist Association Conference, Vienna, Austria. *Oral presentation*
2008	European Vascular Genomics Network Summer School, Cracow, Poland. *Poster presentation.*